

2007

# Wet and dry aging of polymer-asphalt blends: chemistry and performance

Ionela Chiparus Glover

*Louisiana State University and Agricultural and Mechanical College, ichiparus2001@yahoo.com*

Follow this and additional works at: [https://digitalcommons.lsu.edu/gradschool\\_dissertations](https://digitalcommons.lsu.edu/gradschool_dissertations)



Part of the [Chemistry Commons](#)

---

## Recommended Citation

Glover, Ionela Chiparus, "Wet and dry aging of polymer-asphalt blends: chemistry and performance" (2007). *LSU Doctoral Dissertations*. 2747.

[https://digitalcommons.lsu.edu/gradschool\\_dissertations/2747](https://digitalcommons.lsu.edu/gradschool_dissertations/2747)

This Dissertation is brought to you for free and open access by the Graduate School at LSU Digital Commons. It has been accepted for inclusion in LSU Doctoral Dissertations by an authorized graduate school editor of LSU Digital Commons. For more information, please contact [gradetd@lsu.edu](mailto:gradetd@lsu.edu).

# **WET AND DRY AGING OF POLYMER-ASPHALT BLENDS: CHEMISTRY AND PERFORMANCE**

A Dissertation  
Submitted to the Graduate Faculty of the  
Louisiana State University and  
Agricultural and Mechanical College  
in partial fulfillment of the  
requirements for the degree of  
Doctor of Philosophy

in

The Department of Chemistry

by  
Ionela Chiparus Glover  
B.S., Technical University "Gheorghe Asachi" Iasi, Romania, 1989  
December 2007

## **ACKNOWLEDGMENTS**

There are many people whom I would like to thank and acknowledge for support and assistance during my doctoral program at LSU. I would especially like to express my gratitude to Drs. William H. Daly and Ioan I. Negulescu for their generous time, commitment and enthusiasm for my education and research. Throughout my doctoral tenure they encouraged me to refine the research skills and analytical abilities necessary to complete my course of studies. Dr. Louay N. Mohammad deserves my special thanks for advising me in the civil engineering part of the project, which was essential for the success of the entire work.

I would like to extend my gratitude to Dr. William E. Crowe and Dr. Michael Blum, the other two members of my exceptional doctoral committee, for their time and encouragement.

I am grateful also to Louisiana Transportation Research Center and to Louisiana Department of Transportation and Development, particularly to Mr. Christopher D. Abadie, P.E., and his staff, for their guidance in asphalt characterization, for providing the asphalt binders and for allowing me to use their laboratory and equipment to conduct my investigations. My gratitude also goes out to Mr. Gaylon Baumgardner, Executive Vice President of Paragon Technical Services, and to Mississippi Department of Transportation for providing the aged asphalt pavement samples without which my field research could not be completed. Last but not least, I would like to thank Louisiana State University for allowing me to be a part of its first class research community.

The invaluable support and encouragement of my family during my doctoral program was essential for completing this step in my education I would especially like to thank my dear son

Christopher and my husband Don for providing balance, love and joy. My mother, Veronica, and my father, Vasile, unselfishly volunteered to help in the care of our son Christopher during my studies and I would like to send my heartfelt thanks to them.

Finally, I would like to thank all of the professors, colleagues, friends and family members who assisted me along the way until this dissertation has been completed and whose contributions are too numerous and diverse to mention in a few short paragraphs.

# TABLE OF CONTENTS

Acknowledgments.....	ii
List of Tables.....	vi
List of Figures.....	viii
List of Abbreviations and Acronyms.....	xviii
Glossary of Terms.....	xix
Abstract.....	xxv
Chapter 1 Introduction.....	1
1.1 Overview.....	1
1.2 Background.....	2
1.3 Objectives.....	14
Chapter 2 Materials, Methods and Procedures.....	15
2.1 Materials.....	15
2.1.1 Asphalt Binder.....	15
2.1.2 Polymer Additive.....	15
2.2 Methods and Procedures.....	16
2.2.1 Atmospheric Extraction.....	16
2.2.2 Aging.....	17
2.2.3 FTIR Spectroscopy.....	21
2.2.4 Non-Aqueous Potentiometric Titration.....	22
2.2.5 GPC Characterization.....	25
2.2.6 Epifluorescence Microscopy.....	28
2.2.7 Induced Decomposition of Asphalt Components.....	28
2.2.8 Rheological Measurements.....	31
Chapter 3 Chemical Alteration by Aging, Results and Discussions.....	36
3.1 FTIR Characterization.....	37
3.1.1 Conclusions.....	43
3.2 Non-Aqueous Potentiometric Titration.....	45
3.2.1 Conclusions.....	53
3.3 Gel Permeation Chromatography.....	54
3.3.1 Conclusions.....	69

Chapter 4 Induced Decomposition of Asphalt Components.....	72
4.1 Conclusions.....	113
Chapter 5 Rheology Analysis.....	117
5.1 Critical Temperature.....	118
5.2 Repeated Creep and Creep-Recovery Test.....	124
5.3 Conclusions.....	129
Chapter 6 Summary and Conclusions.....	131
Chapter 7 Research in Progress and Future Work.....	134
References.....	138
Appendix A: Additional Tables.....	142
Appendix B: Letter of Permission.....	144
Vita.....	146

## LIST OF TABLES

Table 2.2.2-1 Exposure times of samples collected for analysis from the RCAT @90°C.....	20
Table 2.2.2-2 Exposure times of samples collected for analysis from the RCAT @100°C.....	21
Table 2.2.5-1 Elution volume ( $V_e$ ) values for Polystyrene standards.....	27
Table 2.2.5-2 Percentage of insoluble species not passing through 0.2 $\mu$ m filter.....	27
Table 2.2.5-3 Major chemical groups expected to be seen by GPC. ....	28
Table 2.2.7-1 Proportions of Redox pair used.....	30
Table 2.2.8-1 Critical temperatures $T_c$ ( $\tan\delta = 1$ , $G' = G''$ ) field aged asphalt samples.....	32
Table 3.3-1 Concentrations of carboxylic acid, after multiple dry and wet PAVs cycles.....	41
Table 3.1-2 Summary of carboxylic acid concentrations from FTIR measurements.....	41
Table 3.1-3 Time equivalence between PAV and RCAT laboratory aged samples.....	43
Table 3.2-1 Concentration values for PMAC multiple dry PAV samples.....	48
Table 3.2-2 Carboxylic acids concentrations from FTIR and potentiometric titration experiments.....	49
Table 3.2-3 Acid concentration meq/g field samples from PT and FTIR.....	49
Table 3.2-4 Summary of carboxylic acid concentrations, meq acid/g PMAC.....	50
Table 3.2-5 Data collection for carboxylic acid concentrations.....	52
Table 3.3-1 Integrated area values for asphalt binders after dry and wet PAV operations.....	59
Table 3.3-2 Integrated area values for asphalt binders extracted from field samples.....	64

Table 3.3-3 Integrated area changes of PMAC-RCAT aged for HMW polymer chains .....	68
Table 4-1 Comparison of integrated area for field aged asphalt samples and laboratory blend with redox1 and redox5 dry PAV aged.....	110
Table 5.1-1 Critical Temperatures data collection.....	120
Table 5.1-2 Critical temperatures $T_c$ ( $\tan\delta = 1, G' = G''$ ) of aged PMAC samples determined at a frequency of 10 rad/s.....	122
Table 5.2-1 Data collection from creep-recovery test 1/9 25 Pa and 70°C.....	128
Table 5.2-2 Accumulated deformation of laboratory- and field aged binders after 1000 cycles (1 second loading 25 Pa followed by 9 second recovery periods) at 70°C.....	129
Table 7-1 MSCR average percent recovery at 25°C for various asphalt binder samples.....	136



## LIST OF FIGURES

Figure 1.2-1 Typical cross-section of pavements (adapted from reference <sup>4</sup> ).....	2
Figure 1.2-2 Schematic representation of Petroleum (or crude oil) refinery – adapted from chemistry encyclopedia –oil refinery .....	4
Figure 1.2-3 Asphalt components (adapted from reference <sup>6</sup> ).....	4
Figure 1.2-4 Asphaltenes and Maltenes (adapted from V.S.S. Asphalt Technology).....	4
Figure 1.2-5 The chemical structure of SBS tri-block copolymer.....	9
Figure 1.2-6 Adhesion of asphalt on aggregates surface (adapted from V.S.S. Asphalts website).....	12
Figure 1.2-7 Adhesive and Cohesive failure (adapted from straightdope.com).....	12
Figure 2.2.1-1 Picture of Soxhlet apparatus for extraction.....	16
Figure 2.2.1-2 Picture of Rotary evaporator of asphalt using toluene.....	16
Figure 2.2.2-1 RTFOT instrument (adapted from Controls Testing Equipment LTD).....	18
Figure 2.2.2-2 TFOT instrument (adapted from Controls Testing Equipment LTD).....	18
Figure 2.2.2-3 PAV instrument (adapted from reference <sup>21</sup> ).....	18
Figure 2.2.2-4 Rotating Cylinder Aging Test (RCAT) instrument.....	20
Figure 2.2.4-1. Figure 2.2.4-1. Titration curve of KHP standard.....	24
Figure 2.2.4-2. Example of a titration curve for original PMAC.....	24
Figure 2.2.4-3 Titration curve of benzoic acid 0.025M.....	24
Figure 2.2.4-4 First derivative of titration curve for benzoic acid titration.....	24
Figure 2.2.4-5 Titration curve for asphalt cement and 1% wt benzoic acid.....	25

Figure 2.2.4-6 First derivative for asphalt +1% wt benzoic acid.....	25
Figure 2.2.5-1 Elution volumes for GPC column set calibration with PS standards.....	27
Figure 2.2.5-2 Molecular weight vs. elution volume for PS standards.....	27
Figure 2.2.5-3 Linear calibration from PS GPC traces.....	27
Figure 2.2.8-1 AR 2000 instrument.....	32
Figure 2.2.8-2 Setting of the AR 2000 instrument in DSR mode.....	32
Figure 2.2.8-3 Silicon molds for DSR mode DSR (adapted after wsdot.edu/materials).....	32
Figure 2.2.8-4 Asphalt sandwich DSR (adapted after reference <sup>29</sup> ).....	32
Figure 2.2.8-5 Example in recording strains for MSCR(adapted from Asphalt Institute July 2006).....	34
Figure 3.1-1 FTIR spectra showing carbonyl absorbance of reference compounds; 1% wt in PMAC.....	40
Figure 3.1-2 FTIR spectra showing the increasing 1695 cm <sup>-1</sup> peak in PMAC after oxidative aging.....	40
Figure 3.1-3 Calibration curve benzoic acid mixture with PMAC.....	40
Figure 3.1-4 Changes of carboxylic acid of dry and wet PMAC aged samples.....	40
Figure 3.1-5 Carboxylic acids concentrations of asphalt binders field aged .....	41
Figure 3.1-7 Carboxylic acid concentrations of PMAC aged in RCAT conditions, @ 90°C...	42
Figure 3.1-8 Comparison of carboxylic acid concentrations of PMAC PAV aged and RCAT-aged.....	42
Figure 3.1-9 Time equivalence RCAT-PAV after FTIR determination of carboxylic acids concentrations for PMAC lab aged.....	42
Figure 3.2-1 Concentrations values from Potentiometric Titration and FTIR for PMAC samples.....	48
Figure 3.2-2 First derivative of titration curve for PMAC original.....	48

Figure 3.2-3 Carboxylic acid concentration computed from titration data.....	48
Figure 3.2-4 Field samples- comparison potentiometric titration and FTIR.....	49
Figure 3.2-5 Titration curve PMAC original.....	50
Figure 3.2-6 Titration curve PG 64-22 and PEN 150 originals.....	50
Figure 3.2-7 Acids concentration PMAC after RCAT@90°C.....	51
Figure 3.2-8 Acids concentration PMAC after RCAT@100°C.....	51
Figure 3.2-9 Comparison of carboxylic acid concentrations both FTIR and PT measurements of RCAT-aged PMAC samples.....	52
Figure 3.3-1 Regions for a generally asphalt GPC curve, with correspondent in molecular weight values, based on calibration curve.....	55
Figure 3.3-2 GPC traces for the original materials.....	56
Figure 3.3-3 GPC traces for 64-22, original and PAV aged in dry and wet conditions.....	56
Figure 3.3-4 Dynamics of relative changes of integrated area for 64-22 during dry and wet PAV operations.....	57
Figure 3.3-5 Dynamics of relative changes of integrated area for PEN 150 during dry and wet PAV operations.....	57
Figure 3.3-6 GPC traces for PEN 150, original and PAV aged in dry and wet conditions.....	58
Figure 3.3-7 GPC traces for PMAC, original and PAV aged in dry and wet conditions.....	58
Figure 3.3-8 Dynamics of relative changes of integrated area for PMAC during dry and wet PAV operations.....	59
Figure 3.3-9 Comparison PMAC vs. 64-22 after 3 cycles Dry PAV .....	61
Figure 3.3-10 Comparison PMAC vs. 64-22 after 3 cycles Wet PAV .....	61
Figure 3.3-11 Relative changes of integrated area for the asphalt binders analyzed by GPC...	61
Figure 3.3-12 GPC traces for the polymer/decaline aged in dry and wet PAV conditions.....	62
Figure 3.3-13 GPC traces for the polymer/DCM aged in dry and wet PAV conditions.....	62

Figure 3.3-14 GPC traces – details HMW polymer from Figure 3.3-12.....	62
Figure 3.3-15 GPC traces – details HMW polymer from Figure 3.3-13.....	62
Figure 3.3-16 Dynamics of relative changes of integrated area for polymer dissolved in decaline during dry and wet PAV operations.....	63
Figure 3.3-17 Dynamics of relative changes of integrated area for polymer, after DCM volatilization, during dry and wet PAV operations.....	63
Figure 3.3-18 GPC traces for asphalt binder extracted from field sample.....	63
Figure 3.3-19 GPC traces - details HMW from Figure 3.3-18.....	63
Figure 3.3-20 GPC traces – details MMW from Figure 3.3-18.....	64
Figure 3.3-21 GPC traces – details LMW from Figure 3.3-18.....	64
Figure 3.3-22 GPC traces - comparison asphalt binder field aged to PEN 150 lab aged.....	65
Figure 3.3-23 GPC traces - comparison asphalt binder field aged to PMAC lab aged in dry PAV conditions.....	65
Figure 3.3-24 GPC traces - comparison asphalt binder field aged to 64-22/PEN 150 mixture lab aged.....	66
Figure 3.3-25 GPC traces - comparison asphalt binder field aged to asphalts lab aged in wet PAV conditions.....	66
Figure 3.3-26 GPC traces - comparison HMW polymer chains in asphalt binder field aged to HMW polymer chains in PMAC lab aged.....	66
Figure 3.3-27 Epifluorescence microscopy pictures.....	67
Figure 3.3-28 GPC traces for PMAC RCAT aging conditions – changes in HMW polymer region.....	67
Figure 3.3-29 GPC traces for PMAC RCAT aging conditions – changes in MMW polymer and AC region.....	67
Figure 3.3-30 Polymer content changes in PMAC subjected to RCAT aging conditions.....	68
Figure 3.3-31 GPC traces- comparison PMAC original, PMAC aged under RCAT condition and PMAC aged 3 years in field – HMW region.....	69

Figure 3.3-32 GPC traces- comparison PMAC original, PMAC aged under RCAT condition and PMAC aged 3 years in field – MMW region.....	69
Figure 3.3.1-1 Schematic oxidative aging representation of polymer additive.....	69
Figure 3.3.1-2 Schematic representation of asphaltenes association during oxidative aging....	70
Figure 4-1 Generally representation of a free-radical oxidation of an organic molecule catalyzed by metal ions.....	75
Figure 4-2 Cumene hydroperoxide decomposition in the presence of cobalt ion.....	76
Figure 4-3 Reaction scheme.....	76
Figure 4-4 GPC traces for the polymer, polymer-redox1 mixture 1:0.2:20, polymer-redox2 mixture 1:1:20, polymer-redox3 mixture 1:1:100, at room temperature.....	81
Figure 4-5 GPC traces for the polymer, polymer-redox1 mixture 1:0.2:20, polymer-redox2 mixture 1:1:20, after TFOT.....	81
Figure 4-6 GPC traces for the polymer, polymer-redox 1 mixture 1:0.2:20, polymer-redox2 mixture 1:1:20, after dry PAV aging.....	84
Figure 4-7 Changes in molecular weight distribution from GPC traces for polymer and redox1 (1:0.2:20) mixture (original, TFOT, dry PAV).....	84
Figure 4-8 Changes in molecular weight distribution from GPC traces for polymer and redox2 (1:1:20) mixture (original, TFOT, dry PAV).....	84
Figure 4-9 GPC traces for polymer after oxidative aging without redox systems.....	85
Figure 4-10 Relative changes of integrated area in HMW region, before and after dry PAV process, for polymer, polymer and redox1, polymer and redox2 samples.....	85
Figure 4-11 Relative changes of integrated area in MMW region, before and after dry PAV process, for polymer, polymer and redox1, polymer and redox2 samples.....	86
Figure 4-12 GPC traces for the AC 64-22 original, AC with HP (1:0:20), AC-redox2 mixture 1:1:20, at room temperature.....	86
Figure 4-13 GPC traces for the AC 64-22 mixtures with redox1 (1:0.2:20), redox2 (1:1:20), redox3 (1:1:100), redox4 (1:3:20), redox5 (1:1:4) and at room temperature.....	86

Figure 4-14 GPC traces for the AC 64-22 mixtures with redox1 (1:0.2:20), redox2(1:1:20), redox3 (1:1:100), redox4 (1:3:20), redox5 (1:1:4) and at room temperature-details.....	87
Figure 4-15 GPC traces for the AC 64-22 mixtures with redox1 (1:0.2:20), redox2(1:1:20), redox3 (1:1:100), redox4 (1:3:20), redox5 (1:1:4) and at room temperature-details.....	87
Figure 4-16 GPC traces for the AC 64-22, AC 64-22 mixtures with HP (1:0:20), redox2 (1:1:20), after TFOT.....	87
Figure 4-17 GPC traces for the AC 64-22 mixtures with redox1 (1:0.2:20), redox3 (1:1:100), redox4 (1:3:20), redox5 (1:1:4) after TFOT.....	88
Figure 4-18 GPC traces for the AC 64-22, AC 64-22 mixtures with HP (1:0:20), redox2 (1:1:20), after dry PAV aging.....	88
Figure 4-19 GPC traces for the AC 64-22 mixtures with redox1 (1:0.2:20), redox3 (1:1:100), redox4 (1:3:20), redox5 (1:1:4) after PAV.....	88
Figure 4-20 Changes in integrate area from GPC curves for the molecular weight region 50-7K for AC 64-22 original, AC and HP, AC mixtures with redox1, redox2, redox3, redox4, and redox5, at room temperature and after dry PAV.....	89
Figure 4-21 Changes in integrate area from GPC curves for the molecular weight region 7-3K for AC 64-22 original, AC and HP, AC mixtures with redox1, redox2, redox3, redox4, and redox5, at room temperature and after dry PAV.....	89
Figure 4-22 Changes in integrate area from GPC curves for the molecular weight region 50-3K for AC 64-22 original, AC and HP, AC mixtures with redox1, redox2, redox3, redox4, and redox5, at room temperature and after dry PAV.....	89
Figure 4-23 Changes in integrate area from GPC curves for the molecular weight region 3-0.4K for AC 64-22 original, AC and HP, AC mixtures with redox1, redox2, redox3, redox4, and redox5, at room temperature and after dry PAV.....	90
Figure 4-24 Area correlation for blend prepared.....	90
Figure 4-25 GPC traces of the original blend, blend and HP, blend and redox2 (1:1:20), at room temperature.....	91
Figure 4-26 GPC traces-details from Figure 4-25.....	91
Figure 4-27 GPC traces for HMW region original blend with redox1 (1:0.2:20), redox3 (1:1:100), redox5 (1:1:4), room temperature.....	91

Figure 4-28 GPC traces for MMW and LMW region of original blend with redox1 (1:0.2:20), redox3 (1:1:100), redox5 (1:1:4).....	92
Figure 4-29 GPC traces for MMW and LMW region of original blend with redox3 (1:1:100) corrected.....	92
Figure 4-30 Comparison of GPC traces for blend and redox2 and for AC 64-22 and redox2, at room temperature.....	94
Figure 4-31 GPC traces for original blend with redox1 (1:0.2:20), redox2 (1:1:20), redox5 (1:1:4), after TFOT.....	94
Figure 4-32 GPC traces for blend, blend with HP, with redox1 (1:0.2:20), redox2 (1:1:20), redox5 (1:1:4), after TFOT.....	95
Figure 4-33 GPC traces - HMW detail from Figure 4-32.....	95
Figure 4-34 GPC traces – details MMW and LMW from Figure 4-32.....	96
Figure 4-35 GPC traces for blend, blend with HP, blend with redox2 (1:1:20), after PAV.....	96
Figure 4-36 GPC traces – MMW details - for blend, blend with HP, with redox1 (1:0.2:20), redox2 (1:1:20), redox5 (1:1:4), after PAV.....	98
Figure 4-37 GPC traces - HMW details- for blend, blend with HP, with redox1 (1:0.2:20), redox2 (1:1:20), redox5 (1:1:4), after PAV.....	98
Figure 4-38 GPC traces – LMW details- for blend, blend with HP, with redox1 (1:0.2:20), redox2 (1:1:20), redox5 (1:1:4), after PAV.....	99
Figure 4-39 Changes of integrated area in MMW and LMW region, before and after dry PAV process, for blend, blend and redox1, redox2, redox5.....	99
Figure 4-40 Changes of integrated area in HMW region, before and after dry PAV process, for blend, blend and redox1, redox2, redox5.....	100
Figure 4-41 GPC traces –HMW details for blend, blend with HP, blend with redox2, after wet PAV aging.....	102
Figure 4-42 GPC traces for blend with HP, after dry and wet PAV aging.....	102
Figure 4-43 GPC traces –MMW and LMW details for blend, with redox2, after dry and wet PAV aging.....	103

Figure 4-44 GPC traces –MMW details for blend with redox2, after dry and wet PAV aging.....	103
Figure 4-45 Comparison GPC traces for dry and wet PAV aged asphalt cement with and without redox system.....	104
Figure 4-46 GPC traces – MMW details - for dry and wet PAV aged asphalt cement with and without redox system.....	104
Figure 4-47 GPC traces – MMW details - for dry and wet PAV aged asphalt cement without redox system.....	105
Figure 4-48 GPC traces – LMW details - for dry and wet PAV aged asphalt cement without redox system.....	105
Figure 4-49 Changes in integrate area from GPC curves for the molecular weight regions MMW (50-3K)and LMW (3-0.4K) for AC 64-22 dry and wet PAV aged, AC mixture with redox2 (1:1:20) dry and wet PAV aged.....	105
Figure 4-50 GPC traces – MMW details - for original AC, for 3 dry and wet PAV aged asphalt cement, and for AC mixed with redox2 dry and wet aged.....	107
Figure 4-51 GPC traces – MMW details – comparison for wet aged samples contain AC, AC and HP, AC and redox2, blend, blend and HP, blend and redox2.....	107
Figure 4-52 GPC results – integrated area for region MMW of the samples from Figure 4-51.....	107
Figure 4-53 GPC results – integrated area for region LMW of the samples from Figure 4-51.....	108
Figure 4-54 Polymer molecular weight distribution in various blends.....	108
Figure 4-55 PAV aging effect on polymer in different blends.....	111
Figure 4-56 GPC traces for 3 and 5 years old field aged asphalt compared to trace for blend with redox5 dry PAV aged.....	111
Figure 4-57 GPC traces for 3 and 5 years old field aged asphalt compared to trace for blend with redox5 dry PAV aged –details HMW region.....	112
Figure 4-58 GPC traces for 3 and 5 years old field aged asphalt compared to trace for blend with redox1 dry PAV aged.....	112



Figure 4-59 GPC traces for 3 and 5 years old field aged asphalt compared to trace for blend with redox1 dry PAV aged- details HMW region.....	113
Figure 5-1 Principle of visco-elasticity.....	118
Figure 5.1-1 Plot of $G'$ and $G''$ vs. frequency applied to the determination of the cross-over temperature of the AC 64-22 aged without water for 30 hrs (1.5 PAV).....	119
Figure 5.1-2 Variation of critical temperature of multiple PAV dry-aged and wet-aged PMAC samples.....	120
Figure 5.1-3 The correlation between carboxylic acid concentrations determined from FTIR data and $T_c$ of samples aged in dry PAV conditions.....	120
Figure 5.1-4 The correlation between carboxylic acid concentrations determined from PT data and $T_c$ of samples aged in dry PAV conditions.....	120
Figure 5.1-5. The correlation between integrated area from GPC traces and Rheology results for PMAC samples dry PAV.....	123
Figure 5.1-6 Comparison between rheological parameter $T_c$ of laboratory-aged PMAC samples.....	123
Figure 5.1-7 Linear equivalence RCAT-PAV for $T_c$ aged PMAC.....	123
Figure 5.1-8 Non-linear equivalence RCAT-PAV carboxylic acid concentrations for aged PMAC.....	123
Figure 5.2-1 Accumulated deformation (strain) of PMAC during RCRT test at different loads and loading times.....	126
Figure 5.2-2 Output for RCRT test (original PMAC).....	126
Figure 5.2-3 Accumulated deformation (strain) of PAV-aged asphalt binder.....	126
Figure 5.2-4 Accumulated deformations PMAC 10 hours dry PAV aged for three temperatures.....	126
Figure 5.2-5 Wet vs. dry aged samples in different condition test.....	127
Figure 5.2-6 Comparison accumulated strain for PMAC aged in wet and dry conditions.....	127

Figure 5.2-7 The changes in viscosity for PMAC dry and wet PAV aged.....	127
Figure 5.2-8 RCRT- changes of accumulated strain for asphalt field-aged samples.....	127
Figure 5.2-9 RCRT for original PMAC and for RCAT aged PMAC.....	128
Figure 7-1 MSCR results -PMAC average % recovery.....	136
Figure 7-2 MSCR results – average percent recovery for different asphalt binder samples.....	136
Figure 7-3 Exercise for learning how to determine failure point for a certain stress level (The points of area A (for 25°C) and area B (for 40°C) are possible prognoses).....	137

## **LIST OF ABBREVIATIONS AND ACRONYMS**

**AASHTO** – American Association of State Highway and Transportation Officials

**ASTM** – American Society of Testing and Materials

**CRM** - Crumb Rubber Modifier

**ESAL** - Equivalent Single Axle Load

**DOTD** – Department of Transportation and Development

**DSR** - Dynamic Shear Rheometer

**FHWA** – Federal Highway Administration (United States of America)

**HMA** - Hot Mix Asphalt

**PG** - Performance-Graded

**PMAC** – Polymer modified Asphalt Binder

**PAV** - Pressure Aging Vessel

**RCAT** - Rotating Cylinder Aging Test

**RTFOT** - Rolling Thin Film Oven Test

**SUPERPAVE** – Short for "Superior Performing Asphalt Pavement"

**SHRP** - Strategic Highway Research Program

**TFOT** - Thin Films Oven Test

**TGA** - Thermal Gravimetric Analysis

# GLOSSARY OF TERMS

## APPLIED TO ASPHALT PAVING TECHNOLOGY

**Absolute Viscosity** – A measure of the viscosity of asphalt cement with respect to time, measured Pa s, conducted at 60°C (140°F). The test method utilizes a partial vacuum to induce flow in the viscometer.

**Aggregate** – Any hard, mineral material such as gravel, crushed stone, sand, slag, etc.

**Anti-oxidant** – Any material that slows the oxidation reaction (e.g., for asphalt aging).

**Asphalt Binder** – Asphalt cement used in paving applications that has been classified according to the Standard Specification for Performance Graded Asphalt Binder, AASHTO Designation MP1. It can be either unmodified or modified Asphalt Cement, as long as it complies with the specifications.

**Asphalt Cement or Asphalt** – A dark brown to black cementitious material, which occur in nature or are obtained in petroleum processing. Asphalt cement is a constituent in varying proportions of most crude petroleum and is used for paving, roofing, industrial and other special purposes. It is a semi-solid at room temperature and a liquid at hotter temperatures.

**Asphalt Concrete** - A mixture of asphalt binder and aggregate used as a paving material, which is thoroughly mixed and compacted to form a pavement layer.

**Asphalt Content** – The amount of asphalt binder in an asphalt concrete mixture, expressed as a percentage of the weight of the total mix

**Complex Shear Modulus ( $G^*$ )** – A measure of the total resistance to a deformation when exposed to cycles of oscillating shear stress. It consists of a recoverable (elastic) component and a non-recoverable (viscous) component. For Asphalt materials it is highly dependent upon the temperature and frequency of loading.

**Consensus Properties** - Aggregate characteristics that must follow certain criteria to satisfy a SUPERPAVE mix design. Specified test values for these properties are not source specific but widely agreed upon.

**Creep** - Gradual deflection of a material under a constant load. With respect to the Bending Beam Rheometer test for asphalt binder, creep loading simulates the thermal stresses that gradually build up in a pavement when temperature drops.

**Crumb Rubber Modifier (CRM)** - Ground waste tire rubber used in Hot Mix Asphalt and other paving applications.

**Deformation** – Any change of a pavement surface from its original shape.

**Density** – The ratio of the mass of a material compared to its volume (mass per unit volume), often expressed in pounds-per-cubic-foot (pcf), grams-per-cubic-centimeter (g/cc) or grams-per-milliliter (g/ml). In the context of asphalt concrete pavement, density is increased by reducing the amount of air in the pavement layer through compaction processes.

**Design ESAL** - The total number of Equivalent 80-kN (18,000-lb.) Single Axle Load (ESAL) applications expected throughout the Design Period.

**Detachment** - Separation of an asphalt film from an aggregate surface by a thin film of water without an obvious break in the film

**Disintegration** - The breaking up of a pavement into small, loose fragments caused by traffic or weathering.

**Displacement** - involves displacement of asphalt at the aggregate surface through a break

**Ductility** - The ability to be drawn out or stretched thin without breaking. While Ductility is considered an important characteristic of Asphalt Cements in many applications; the presence or absence of Ductility is usually considered more significant than the actual degree of Ductility.

**Durability** - Ability to resist disintegration by weathering and traffic.

**Dynamic Shear Rheometer (DSR)** – Laboratory equipment used to perform the AASHTO TP5 procedure on un-aged, RTFO-aged, and PAV-aged Asphalt Binders. In the DSR, a small disc-shaped sample of Asphalt Binder is sandwiched between two plates, one of which is fixed, and the other of which is oscillating. The DSR measures the Complex Shear Modulus and Phase Angle at intermediate and high temperatures, which can be used to predict resistance to Rutting and Fatigue Cracking in Asphalt Concrete pavements made with the Asphalt Binder being tested.

**Equivalent Single Axle Load (ESAL)** – The effect on pavement performance of any combination of axle loads of varying magnitude equated to the number of 80-kN (18,000-lb.) single-axle loads that are required to produce an equivalent effect.

**Fatigue Cracking** – A crack caused by repeated flexure.

**Fine Aggregate** – Aggregate entirely passing the 4.75 mm (No. 4) sieve and mostly retained on the 75µm (No. 200) sieve.

**Flexibility** – The ability of a pavement to conform to settlement of the foundation without fracturing. Generally, high asphalt binder content or the use of rubber-modified asphalt Binder enhances the flexibility of Asphalt paving mixtures.

**Hot Mix Asphalt (HMA)** - A form of asphalt concrete that is mixed at a contractor's Hot Mix Plant, transported to the roadway in dump trucks, placed using a paver, and compacted with steel-wheel or rubber-tired rollers.

**Kinematic Viscosity** - A measure of the Viscosity of Asphalt Cement, measured in centistokes, conducted at a temperature of 135°C (275°F).

**Load Equivalency Factor** - The number of 80-kN (18,000-lb.) single-axle load applications (ESAL) contributed by one passage of an axle.

**Moisture Susceptibility** – Refers to susceptibility of an asphalt concrete mixture to Stripping. This property is tested during mix design with the ITS test procedure.

**Penetration** – classic measure of estimating the type of asphalts. It is measured using a penetration test where a standard needle is allowed to fall freely in the asphalt cement at a certain temperature; according to the penetration of the needle the asphalt type is decided.

**Performance-Graded (PG)** - Asphalt Binder grade designation used in SUPERPAVE. It is based on the binder's mechanical performance at critical temperatures and aging conditions.

**Permeability** – A measure of the ability of a pavement to allow the passage of air and water into or through it.

**Phase Angle (delta)** – Indicator of the relative amounts of recoverable (elastic) and non-recoverable (viscous) deformation in a material when it is exposed to repeated pulses of Shear Stress; it is highly dependent upon the temperature and frequency of loading.

**Polymer**—a material with a long-chained molecular structure, including natural rubber, synthetic rubber, plastics, etc.

**Polymer Modified Asphalt Binder**— Asphalt Binder that has been blended with a Polymer

**Portland Cement** – A gray, powdery material that meets ASTM Standard C 150 and is composed primarily of tricalcium silicate, dicalcium silicate, tricalcium aluminate, and tetracalcium aluminoferrite. When combined with water, Portland Cement reacts with the water to form a paste, which then becomes rigid as the reaction between the cement and water progresses.

**Portland Cement Concrete (PCC)** – A mixture of Portland Cement, Aggregate, water, and other admixtures that is placed in forms and becomes rigid as it cures. It is a commonly used construction material in both highway and building construction.

**PAV - Pressure Aging Vessel** – A piece of laboratory equipment used to perform AASHTO PP1 procedure on samples of Asphalt Binder after they have been aged in the RTFO. The PAV further ages these binder samples by exposing them to high pressure and temperature for 20 hours to simulate the effects of long-term aging. PAV-aged binders are tested with the DSR, the BBR, and the DTT.

**Raveling** - The progressive separation of Aggregate particles in a pavement from the surface downward or from the edges inward.

**Rotational Viscometer** – equipment used to measure the Viscosity of un-aged modified and unmodified Asphalt Binders using the ASTM D4402 procedure. This test may be performed at a variety of test temperatures to gain insight into the Workability of Asphalt Concrete mixtures containing that particular Asphalt Binder or to develop Temperature-Viscosity Charts for the binder being tested.

**Rutting** - Channelized depressions that develop in the wheel tracks of Asphalt pavements resulting from consolidation under traffic loading in one or more of the underlying pavement layers. Rutting is not a surface problem, and usually begins in the lowest pavement layer. It is a structural problem of insufficient pavement strength caused by either insufficient design pavement thickness or the weakening of an underlying pavement layer due to moisture damage.

**Sand** - fine aggregate resulting from natural disintegration and abrasion of rock.

**Shear Stress** – the stress resulting from the application of forces parallel to each other, but in opposite directions. A Shear failure is one in which the material rips or tears as a result of the applied Shear Stress.

**Slag** - The nonmetallic material, consisting essentially of silicates and alumino-silicates of lime and other compounds, developed simultaneously with iron in a blast furnace. It is a byproduct of the iron manufacturing process.

**Specific Gravity** – The ratio of the weight of a material compared to its volume at the standard temperature.

**Stability** - The ability of an Asphalt Concrete mixture to resist Deformation from imposed loads. Stability is dependent upon both internal friction and cohesion.

**Stiffness** –It is basically reflected by the relationship between stress and strain as a function of loading time at a certain temperature.

**Strain** – Deformation of a physical body under the action of applied forces relative to the initial dimension

**Stress** – Applied loading (force) relative to the unit area of the object subjected to it (force per unit area)

**Stripping** – term applied to hot mix asphalt (HMA) mixtures that generally exhibit separation and removal of asphalt binder film from aggregate surfaces due primarily to the action of moisture and/or moisture vapor.

**Sub-base** - The course in the pavement structure immediately below the base course. If the Subgrade soil has adequate support, it may serve as the sub-base.

**Subgrade** - The soil prepared to support a Pavement Structure or system. It is the foundation of the Pavement Structure.

**SUPERPAVE** – Short for "Superior Performing Asphalt Pavement", a performance-based system for selecting and specifying Asphalt Binders and for designing HMA mixtures that utilizes a Gyrotory Compactor for Compaction of laboratory specimens (“pills”). It integrates the selection of materials (Asphalt Binder and Aggregate) and Volumetric proportioning with the project's climate and design of the traffic loading.

**Temperature susceptibility** - change of the consistency of an asphalt with a change in temperature.

**Viscosity** – A measure of the resistance of a fluid to flow caused by internal friction

**Wearing Course** – The uppermost pavement layer forming the surface of the pavement that is exposed to traffic and environmental conditions

## **GLOSSARY OF POLYMER TERMS**

**Amorphous** - having no ordered arrangement.

**Complex** - two or more molecules which are associated together by some type of interaction, other than a covalent bond.

**Copolymer** - a polymer made from more than one kind of monomer.

**Covalent Bond** - a joining of two atoms when the two share a pair of electrons.

**Crosslinking** – linking of polymer chains in a network architecture



**Crystal** – arrangement of consistent molecules in a neat and orderly fashion.

**Elastomer** - A material that can be stretched many times its original length without breaking which will come back to its original size when the applied force is released.

**Free Radical** - an atom or set of atoms (molecule) which has at least one unpaired electron

**Gel** - a crosslinked polymer which has absorbed a large amount of solvent.

**Hydrodynamic Volume** - the volume of a polymer coil when it is in solution. It can vary depending on the molecular weight and interaction with the solvent

**Hydrogen Bond** - a strong attraction between a hydrogen atom which is attached to an electronegative atom (oxygen, nitrogen), and an electronegative atom usually from another molecule.

**Ion** - an atom or set of atoms (molecule) which has a positive or a negative electrical charge.

**Living Polymerization** - a polymerization reaction in which there is no termination, and the polymer chains continue to grow as long as in the system there are monomer molecules to add to the growing chains.

**Secondary Interaction** - interaction between two atoms or molecules other than a covalent bond. Secondary interactions include hydrogen bonding, ionic interaction, and dispersion forces.

**Strength** - the amount of stress at which the sample is subjected

**Thermoplastic** - a material that can be molded and shaped when heated.

**Thermoset** - a hard and stiff crosslinked material that does not soften or become moldable when heated.

## ABSTRACT

A PG 76-22 Polymer Modified Asphalt Cement composition was subjected in the laboratory to accelerated aging using both a standard Thin Film Oven Test and a Pressure Aging Vessel. Conditions simulating wet atmospheres (PAV in saturated water vapors) as well as very long service terms (multiple dry and wet PAV operations) were studied. A Rotating Cylinder Aging Test has been employed as an alternate asphalt aging technique using the same PMAC composition in order to observe the initial phases of the oxidative aging process. The data provided by this technique was correlated with the actual aging in the field of asphalt pavements. The extent of oxidation and changes in the molecular mass of the asphalt cement components of aged samples were estimated using Fourier Transform Infrared Spectroscopy data, Potentiometric Titrations and Gel Permeation Chromatography analyses. FTIR data show that multiple PAV and RCAT aging introduced polar carboxylic acid oxygen species. PT analysis identified the presence of sulfonic acids in commercial PMACs, apparently derived from sulfur used in preparing the blends. GPC data show that even after extensive RCAT aging the polymer did not degrade significantly. In contrast, the polymer is rapidly crosslinked or degraded by PAV or field aging.

In order to obtain a better understanding of the role of radicals during oxidative processes both under dry and wet conditions, the chemical impact of aging of PMAC components has been modeled using a cobalt naphthenate/cumene hydroperoxide redox system to generate free radicals. Under these conditions, the polymer served as a sacrificial antioxidant and protected the asphalt components from oxidation.

Viscoelastic properties of asphalts were determined from dynamic shear measurements using a high torque instrument. The cross-over temperature at which  $G''$  equals  $G'$  as temperature increases was considered as the critical temperature and chosen as a criterion to assess the advancement of hardening (aging). The oxidative aging in the presence of water promoted an increase in the carbonyl content of aged samples, primarily as acid groups. Aging in the wet atmosphere had also a retarding effect on asphalt hardening.

# **CHAPTER 1**

## **INTRODUCTION**

### **1.1 OVERVIEW**

Healthy economies require a good transportation system, of which roadways are an essential part. Nationally there are more than 2.3 million miles of roads that are surfaced with asphalt or concrete. Annually, approximately \$68 billion is spent on U.S. roadways; half for capital outlays and half for maintenance activities. The production of hot mix asphalt (HMA) is estimated at approximately 500 millions tons annually and employs approximately 900,000 workers in the manufacture and use of HMA. Therefore, the construction and maintenance of asphalt-surfaced roads has a long term and significant impact on the economic vitality of the nation.<sup>1</sup>

Lately, a large percentage of U.S. roads have been reported to be in poor condition. The primary reasons for the deteriorating conditions of our roads include increases in overall traffic, poor asphalt binder quality coming from high-tech refining processes, and changes in climate. Better construction processes are needed to face these challenges. It is necessary to understand the fundamental behavior and properties of the roads before beginning to develop advanced construction processes.

The use of polymer modified asphalt cements in pavement construction was an important step in increasing the life and durability of asphalt roads. Forty states, including Louisiana, began using polymer modified asphalt cements in the 1980's. Some of these roads required rehabilitation and reconstruction sooner than was predicted. More than 85 percent of new asphalt paving in Louisiana is required to use polymer modified asphalt binders, whose usable life may vary significantly.<sup>2</sup> The focus of this research is to characterize asphalt binder

properties. Binder typically represents 3 to 5% by weight of the surface course which comprises the very top of the pavement.<sup>3</sup>

## 1.2 BACKGROUND

Pavements are engineered structures containing layers of compacted material that are designed to withstand the stresses applied by vehicle or other traffic types and provide a smooth riding surface (Figure 1.2-1).

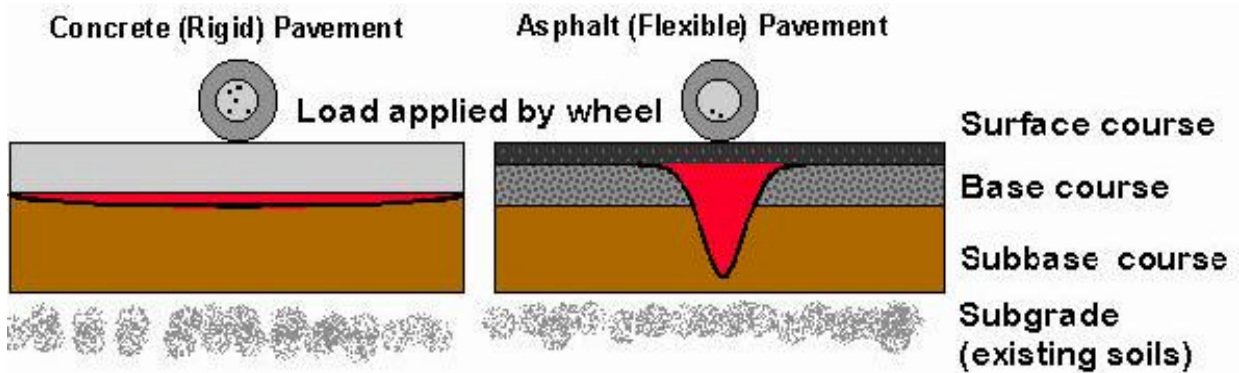


**Figure 1.2-1 Typical cross-section of pavements (adapted from reference<sup>4</sup>)**

A pavement's structure can be divided into three main components: foundation, base and surface layer. Each component plays an important role in the overall performance of a pavement. The foundation is comprised of the subgrade and, in some cases, the sub-base. The foundation carries the loads created by construction traffic. Structurally, it is the final layer to which stress is transferred. The base layer is a main structural element of the design and can consist of several layers. The purpose of the base layer is to spread the wheel load so that the foundation is not over-stressed. Its stiffness and its fatigue resistance (if stabilized) characterize its behavior in the pavement structure. The surface layer is provided to ensure adequate skid resistance and act as a protective layer for the underlying materials. Surface layers are characterized by their stiffness, creep resistance, moisture resistance. Other characteristics of

surface layers are their resistance to low temperature cracking, fatigue resistance and skid resistance. Hard surfaced pavements are typically categorized as flexible or rigid pavements:

- Flexible pavements are those which are surfaced with asphalt materials, referred to them as Hot Mix Asphalt. These types of pavements are called "flexible" since the total pavement structure "bends" or "deflects" due to traffic loads. A flexible pavement structure is generally composed of several layers of materials which can accommodate this "flexing".

- Rigid pavements are those which are surfaced with Portland cement concrete (PCC). These types of pavements are called "rigid" because they are substantially stiffer than flexible pavements due to PCC's high stiffness.

The two main components of Hot Mix Asphalt (HMA) are asphalt cement binder and aggregates.

Asphalt cement is a dark brown-to-black cement-like material obtained mainly by petroleum refining (Figure 1.2-2). Asphalt is used primarily construction of roads and as a major component in roofing materials due to its remarkable binding and waterproofing properties. Asphalts are highly complex and not well characterized materials containing saturated and unsaturated aliphatic and aromatic compounds with molecular weights from 500 to 2000 and carbon numbers higher than C<sub>25</sub> (Figure 1.2-3).<sup>5</sup> Asphalt typically contains about: 80 wt% carbon; 10 wt% hydrogen; up to 6 wt% sulfur; 6.5 wt% asphaltenes; 0.51 wt% small amounts of oxygen and nitrogen; and metals such as iron 33 ppm, nickel 18 ppm, vanadium 39 ppm, copper < 1 ppm.<sup>5</sup> The compounds are classified as asphaltenes or maltenes according to their solubility in hexane or heptane (Figure 1.2-4). Asphaltenes are high-molecular weight species that are insoluble in these solvents, whereas maltenes have lower molecular weights and are soluble. Asphalts normally contain between 5% and 25% by weight of asphaltenes and may be regarded as colloids of asphaltene micelles dispersed in maltenes.

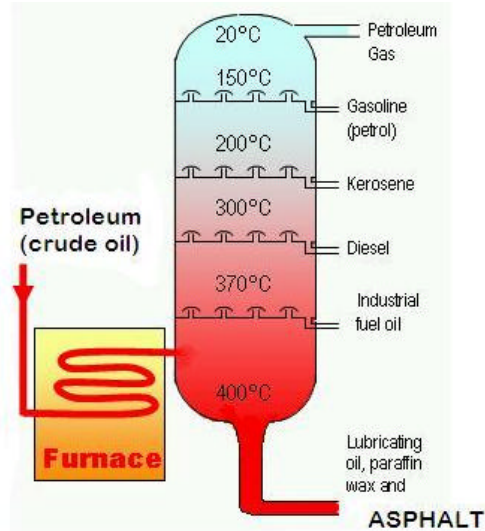


Figure 1.2-2 Schematic representation of Petroleum (or crude oil) refinery – adapted from chemistry encyclopedia –oil refinery.

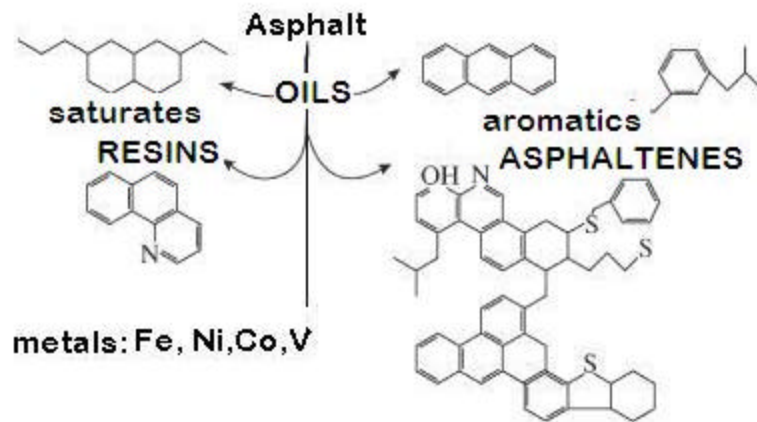


Figure 1.2-3 Asphalt components – (adapted from reference<sup>6</sup>)

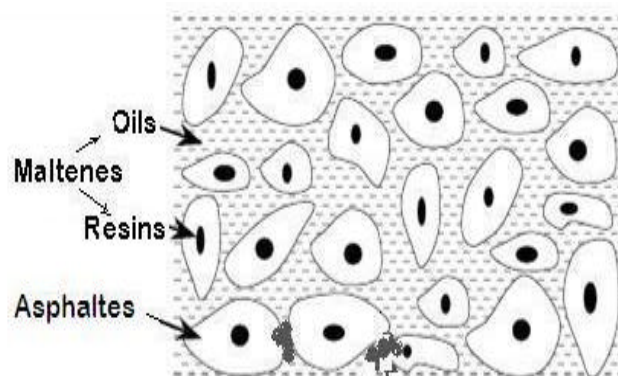


Figure 1.2-4 Asphaltenes and maltenes (adapted from V.S.S. Asphalt Technology)

Asphaltenes consist of highly condensed groups, aromatic ring systems and large amounts of hetero-atoms. Asphaltenes, the product of resin development by geological or processing

effects, are agglomerations of the most polar molecules in the asphalt. The polarity is derived by the presence of hetero-atoms such as sulfur, nitrogen and oxygen attached to carbon atoms in asphalt molecules in different configurations and in the form of different compounds such as:

- oxygen compounds: carboxylic acids, naphthenic acids, phenols, ketones, esters, ethers, anhydrides;
- sulfur compounds: sulfonic acids, sulfoxides, polysulfides, sulfides, thiols, thiophenes;
- nitrogen compounds: pyridinic, pyrrole, indole, carbazole, porphyrins.<sup>7</sup>

Asphaltenes have a strong tendency to associate in conglomerates playing a major role as the “viscosity-building” component and behave as a thickening agent or structuring agent.

Maltenes (Petrolenes) consist of two fractions, oils and resins. Oils are the liquid part of the asphalt and consist of n-, iso- and cyclo-paraffins and condensed naphthenes with some alkyl aromatics. The aromatic portion is mostly naphtho-aromatic hydrocarbons with three or four naphthenic rings per molecule. The oil fraction is non-polar.

Resins are chemically very similar to the asphaltenes as they are a transition from oils to asphaltenes. The resins mainly consist of poly-cyclic molecules containing saturated aromatic and hetero-aromatic rings and hetero-atoms in various functional groups. The resins are not as polar as the asphaltenes and hence are not as interactive.

Asphalt can be classified by its chemical composition and physical properties. The pavement industry typically relies on physical properties of asphalt for the characterization of performance, although the physical properties of asphalt are a direct result of its chemical composition. Typically, the most important physical properties of asphalt are:

- Consistency describes the changes in viscosity of asphalt cement due to changes in temperature since asphalt is a thermoplastic material. Consistency is defined by the following



tests: penetration, viscosity (absolute and kinematic), softening point and ductility. The results provide information about aging, compatibility of blends and low temperature cracking potential.

- Durability is a measure of how the physical properties of asphalt binder change with age (age hardening). In general, as an asphalt binder ages, its viscosity increases and it becomes more stiff and brittle. Asphalts go through two stages of aging. There is short-term aging in an HMA facility (approximated by two tests in the laboratory: TFOT and RTFOT) and long-term aging during while the asphalt is in service (laboratory simulated by using the PAV method).

- Rheology is the study of flow of matter and deformation of matter. Deformation and flow of the asphalt binder is important in HMA pavement performance. HMA pavements that deform and flow too much may be susceptible to rutting and bleeding, while those that are too stiff may be susceptible to fatigue cracking.

- Safety and Purity. Asphalt cement, like most other materials, volatilizes (gives off vapor) when heated. For safety reasons, the flash point of asphalt cement is tested and controlled. Asphalt cement, as used in HMA paving, should consist of almost pure bitumen. Impurities are not active cementing constituents and may be detrimental to asphalt performance (the requirement is 99% purity).<sup>1</sup>

The modification of asphalt cement by mixing it with polymers has been practiced for over 50 years but has received added attention in the past decade or so. Asphalt cement should be modified to achieve the following types of improvements<sup>1</sup>:

- Lower stiffness (or viscosity) at the high temperatures associated with construction. This facilitates pumping of the liquid asphalt binder as well as mixing and compaction of HMA.
- Higher stiffness at high service temperatures. This will reduce the incidence of rutting and shoving.

- Lower stiffness and faster relaxation properties at low service temperatures. This will reduce thermal cracking.

- Increased adhesion between the asphalt binder and the aggregate in the presence of moisture. This will reduce stripping .<sup>1</sup>

Some asphalt cements require modification in order to meet specifications. The required SUPERPAVE specification for the asphalts used in this work is presented in Appendix A-1.

Examples of polymers commonly used in asphalt mixtures and a few of their advantages and disadvantages are presented below:

- Styrene Butadiene Copolymer (radial and linear SBS) – good fatigue resistance, high creep rate, but oxidation susceptibility

- Polyethylene (PE) - high thermal extension but low stiffness

- Styrene Butadiene Rubber (SBR) – very good aging and weather resistance but low tear strength, low ozone resistance, oxidation susceptibility

- Polybutadiene (PB) – excellent wear resistance, impact resilience, but low strength

- Ethylene Vinyl Acetate copolymer (EVA) - storage stability, reducing binder run-off, high temperature viscosity, but may be susceptible to crosslink and low creep resistance. EVA is very good for low temperature zones but presents differential cooling areas along the chain and tearing phenomena is commonly observed. Also due to reduced initial stiffness of the material “chipping loss” is often experienced.

- Ethylene Methyl Acrylate copolymer (EMA)

- Atactic Polypropylene (PP) - good chemical resistance, good fatigue resistance but oxidative degradation, high mould shrinkage and thermal expansion was observed

- Epoxies and Urethanes, Tire Rubber (Crumb) - Polymers can be classified as: elastomeric, with a high level of elastic recovery (i.e. SBS, SBR, Crumb rubber); and plastomeric, with high stiffness and deformation resistance (i.e. EVA, EMA, Urethanes, and PP).

Many types of manufacturing configurations exist to make polymer-modified asphalts. Important steps in the manufacturing process are dispersion and reaction. This is what determines the structure (i.e., morphology) of the final binder and hence its properties. These steps also determine the level of polymer required to achieve the desired results and have an effect on the production cost. Compatible asphalt-polymer systems are desirable because they have superior rheological and stability properties to those of incompatible systems at the same polymer level. Using additives makes improvements in compatibility. A mixture with properties, which allows for ease of storage and transportation, is desirable. To improve these properties, sulfur is added under conditions by which a compatible and homogeneous polymer-asphalt blend is formed. A few methods are suitable to obtain compatibility between asphalt and SBS. One method is to use a high-shear continuous mixing of the asphalt-polymer mixture. However, this method does not solve the problem of compatible blends because, once the high shear mixing stops, the phases begin to separate. Another method is the addition of an inorganic acid to enhance the storage stability of the asphalt-polymer mixture; however, the storage stability can still be further improved without the use of corrosive acid. The use of sulfur is more cost efficient and is a process which prepares asphalt-polymer blends that are phase stable over a broader concentration range of sulfur and polymer and are easier to work with than current blends, while still maintaining the desired creep and rutting resistance. For a 3% polymer used in asphalt it takes a 5%-8 % (of the polymer weight) addition of sulfur to obtain a gel structure.<sup>8</sup> SBS has the tendency to crosslink and to form a gel. Sulfur acts as an accelerator-gel additive by increasing crosslinkage with new sulfur bridges (vulcanization). A high crosslinked polymer

will absorb a large amount of asphaltic components and form a permanent stable gel. It has been reported that the sulfur vulcanization in an SBS copolymer takes place around 170°C temperature and is influenced only by PS structure not PB stereochemistry (lower rate of vulcanization and higher temperature for linear structure).<sup>9</sup>

The polymer modifier used in this research is a poly-(styrene-b-butadiene)-triblock copolymer (SBS). It is synthesized through a living anionic polymerization process, and the resulting block copolymer has the following structure (Figure 1.2-5):

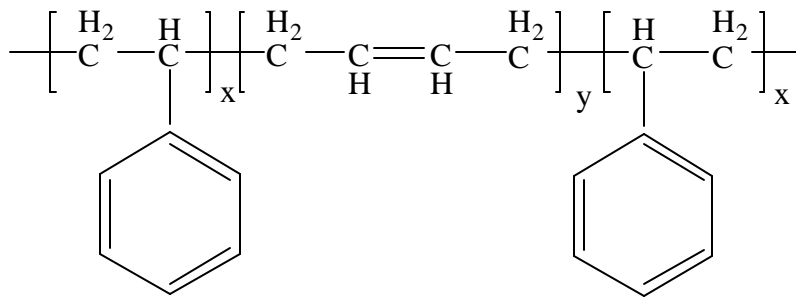


**Figure 1.2-5 The chemical structure of SBS tri-block copolymer**

SBS was chosen for the following reasons: it is suitable for high Louisiana temperatures, it has very good compatibility with asphalts, it has good storage properties, and it requires a low percentage added to asphalt (2-3% wt), it has higher than 90% reliability, and costs are moderate. It is easy to find roads in Louisiana that were built using SBS polymer modified asphalts to for samples for laboratory work.

One of the effects causing polymer failure is the thermal effect. Autoxidation, defined as the thermal oxidation that takes place between room temperature and around 150°C, proceeds by a typical free-radical chain mechanism. Thermal energy, ultraviolet radiation, mechanical stress, metal catalysts, and the addition of initiators form radicals that initiate autoxidation in polymers. It has been suggested that traces of hydroperoxides introduced into the polymer during processing are the source of initiating radicals. Various catalysts, notably the transition metals

and derivatives of these, induce the decomposition of hydroperoxides. Termination of chain reactions takes place slowly, usually through a complex series of reactions because of the combination of propagating radicals and/or through disproportionation reactions.<sup>10</sup>

The thermo-oxidative degradation of an SBS copolymer at 130°C was shown by the appearance in the IR spectra of bands corresponding to hydroxyl and carbonyl groups. As a consequence of the crosslinking, reaction bands typical of gel formation were found in the IR spectra. The degradation mechanism was suggested to be at 1,4 and 1,2 groups by oxygen to peroxides, which leads to the formation of carbonyl or carboxylic groups.<sup>11</sup>

The degradation of the PB block proceeds mainly by  $\alpha$  and  $\beta$  chain scissions whose fragments may consequently stabilize by cyclization reaction. The IR spectra of the copolymer, after being treated thermally, showed a visible decrease for double bonds and vinyl in PB units due to the crosslinking/degradation reaction and an increase in area for carbonyl units. A complex structure of bands appeared at 1000 – 1400  $\text{cm}^{-1}$  which can be connected with gel formation (verified by insolubility in toluene of degraded SBS). From analysis of these spectra the conclusion was that the 1,4 PB groups were more easily degraded than the 1,2 PB units. The products resulting from the thermal degradation have been classified into: gases (6.5% wt.), oils (64% wt.) and residues (29.8% wt.). The analysis of gases showed the presence of light hydrocarbons and alkenes with 1 to 4 carbons. The main compound found in oils is biphenyl propane and a mixture of compounds with 9 to 14 carbons, which suggests a high interaction between the styrene and butadiene units.<sup>12</sup>

Aggregates are the major building material for pavements. The role of the aggregate is to form the matrix of strength in a mix; as such their properties are critical to the success of a mix. Local sources are generally used but some other materials such as expanded clay (light weight aggregate) or slag may be used if they meet the required specification (size and gradation,

mechanical strength, durability, chemical stability, surface texture, crushed shape, absorption and affinity to asphalt, impurities). Aggregates can be classified based on their mineralogy:

- Igneous rocks are volcanic rocks formed from molten rock. Examples of igneous rocks are granite and basalt. Igneous rocks can be classified as either acidic or basic.

- Sedimentary rocks are rocks formed by the laying down of layers of material that is then compressed. Classification is based on the predominant mineral present such as calcareous (limestones, chalks, etc.), siliceous (sandstone) or argillaceous (shale, etc.). Quartzite aggregates are known to exhibit the least adsorption to asphalt and are also known to exhibit the highest catalytic effect in asphalt oxidation. Limestone exhibits the smallest catalytic effect.

- Gravel is formed from the breakdown of any natural rock. Gravel is usually found in rivers or waterways. River gravel is an example of a common type.

- Sands are formed from the deterioration of any natural rock. These often contain clay or silt and should be washed.

- Slag is a by-product of metallurgical processing. Slag can be made from the processing of tin, steel, or copper. Slag is generally hard but absorbent. <sup>1</sup>

For Louisiana, a design asphalt mixture using 4.7% PMAC 76-22 might have the following aggregate gradations by size (usually 80% of aggregate is limestone): 10% stones of 25 mm, 15% chip of 19 mm, 30% chip of 12.5 mm, 31% manufactured sand of 4.75 mm, 14% screen sand of 2.36 mm. Aggregates are selected to have fractional faces, non flat or elongated.

The main property that affects asphalt applications is aggregate absorption (the permeability of aggregate pores) and/or adsorption (adhesion on the surface) of asphalt components. Asphalt must wet the surface of the aggregate and adhere to it. The polar functionalities described above, as well as organo-metallic constituents that contain metals such as nickel, vanadium, and iron, play important roles in asphalt - aggregate interaction.

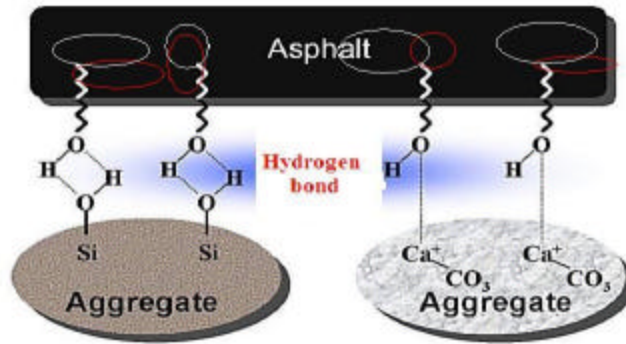


**Figure 1.2-6 Adhesion of asphalt on aggregates surface (adapted from V.S.S. Asphalts website)**

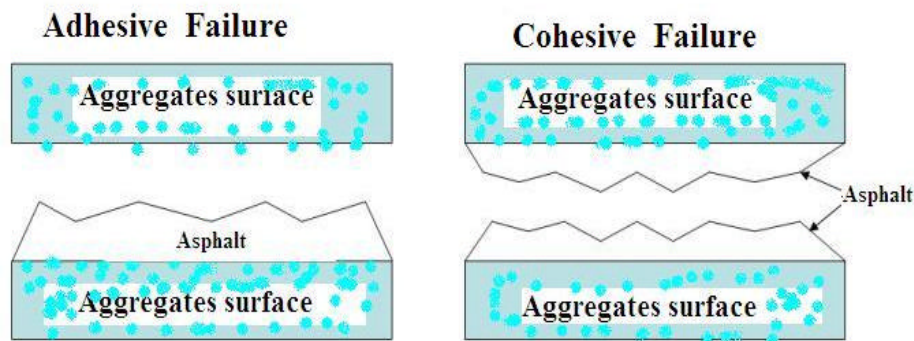


**Figure 1.2-7 Adhesive and Cohesive failure (adapted from straightdope.com)**

When asphalts are contacted with aggregates (Figure 1.2-6), polar groups from asphaltenes are preferentially adsorbed on the aggregate surface leading to an adhesive bonding.<sup>13</sup> Failure of this interaction (Figure 1.2-7) in time can occur between the binder and aggregate (i.e., a failure of adhesion) and a failure within the binder itself (i.e., a failure of cohesion). The loss of bond between aggregates and asphalt is defined as stripping distress. Other types of distress observed in asphalt pavements are: fatigue cracking (repetitive passes associated with overloaded traffic); low temperature cracking; rutting (changes in pavement shape); shoving (slippage between layers); raveling (disintegration of pavement layer); and wear loss (after asphalt cement has oxidized and is eroded).<sup>1</sup>

The role played by time and environmental factors on asphalt pavement distress is a subject of continuous interest.<sup>14</sup> Earlier studies carried out on the effect of temperature and relative humidity on the oxidation of air-blown asphalts, as a function of exposure time, showed that the rate of oxidation is dependent on both of these environmental factors.<sup>15</sup> Hardening is due to chemical reactions, including oxidation, polymerization, and condensation and/or due to physical processes, including loss of volatiles and structural morphological change. However, reaction with oxygen (oxidative hardening) has been shown to be the principal factor responsible for a more brittle structure and an increase in susceptibility to cracking. Oxidative hardening happens at a relatively slow rate and varies seasonally; it occurs faster at higher temperature as diffusion of oxygen increases. Therefore, aging is considered as a chemical as well as a physical problem. Voids and aggregate porosity were also found to be contributing factors but were dependent upon the type of asphalt and average temperature.<sup>16</sup>

Laboratory protocols were recently developed under the Strategic Highway Research Program (SHRP) to simulate the field hardening of asphalt binder and mixes in which the mean annual air temperatures prevalent during field aging have been taken into account but the influence of atmospheric humidity has not been considered.<sup>3</sup> The question is whether the laboratory protocols for aging asphalt binders should consider the exposure to water as a mechanism of the aging atmosphere. Aging in the presence of water of several SHRP core asphalts and of two different polymer modified asphalt cements is currently under investigation at the Western Research Institute (Laramie, WY<sup>17</sup>) and in our laboratory. It is the aim of the present research to address the potential influence of water on the aging of road pavements containing polymer modified asphalt cements. The chemical and physical changes in asphalt properties after oxidative aging under dry and humid conditions will be correlated to appropriate aged field samples.



### **1.3 OBJECTIVES**

The objectives of this research are:

- To analyze chemical alteration, morphology and hardening of a PMAC during laboratory simulated aging (PAV and RCAT)
- To investigate the role of humidity on asphalt aging
- To understand the aging mechanism in the presence of metal ions
- To learn how the new aging technique (RCAT) correlates with the actual field aging of PMAC pavements.
- To determine rheological parameters of asphalts at different stages of aging.

## **CHAPTER 2**

### **MATERIALS, METHODS AND PROCEDURES**

#### **2.1 MATERIALS**

##### **2.1.1 ASPHALT BINDER**

A standard Ergon SBS (styrene-butadiene-styrene) elastomeric polymer modified asphalt cement (PMAC) meeting Louisiana DOTD specifications was obtained from Paragon Technical Service of Jackson, Mississippi. The PMAC (PG 76-22) was prepared by the supplier by blending asphalt cement (AC) PG grade 64-22 with SBS dissolved in soft asphalt cement (PEN 150). Besides PMAC the base components: SBS polymer (Calprene 411) and the asphalts PG 64-22 and PEN 150 were provided by the same supplier.

Three and five-year-old full core HMA wearing course samples (from interstate I-55 near Granada, Mississippi), originally of a similar composition as that of the PMAC listed above, were supplied for comparison. The asphalt from these samples was extracted in our laboratory. The procedure for that extraction process is presented below.

##### **2.1.2 POLYMER ADDITIVE**

SBS tri-block elastomeric copolymer was used, with a commercial name of Calprene 411 dry. A Dynasol product (butadiene/styrene 70/30 %) in crumb form was received from the same service. The characteristics of the SBS tri-block elastomeric copolymer are as follows: radial; 30% weight PS, 70% weight PB, molecular weight from GPC measurement around 650,000 which means estimated 8,500 polybutadiene units and 1,800 polystyrene units (900 PS units each side of PB chain)

## 2.2 METHODS AND PROCEDURES

### 2.2.1 ATMOSPHERIC EXTRACTION

The atmospheric extraction method was used to separate asphalt and aggregates for the field samples received. The apparatus used for extraction was a Soxhlet extractor (Figure 2.2.1-1).



**Figure 2.2.1-1 Picture of Soxhlet apparatus for extraction**

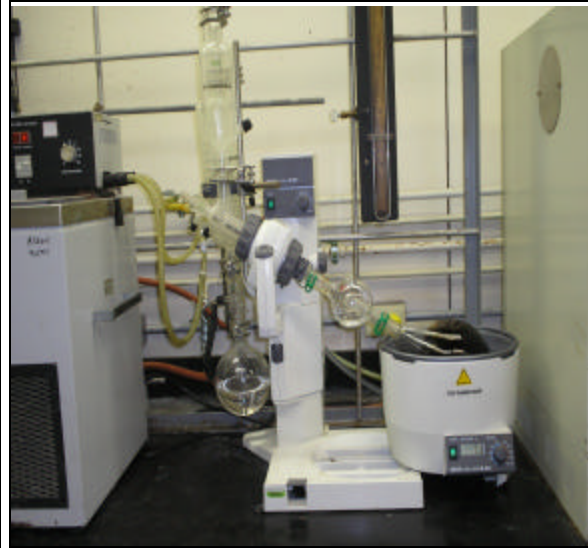


**Figure 2.2.1-2 Picture of Rotary evaporator of asphalt using toluene**

The cores were cut into small pieces to an appropriate dimension to fit inside the extractor and were kept under hot toluene reflux for 24 hours. A nitrogen blanket was applied in order to avoid oxidation. The asphalt cement solution in toluene was cooled and allowed to sit at room temperature at least 12 hours. It was then filtered to remove the fine particles of sand. The filtrate was allowed to stand over night to permit ultra-fine particles to settle and the solution was decanted. The solution was concentrated under vacuum at 0.1 mm Hg and 50°C to 95°C with a Büchi Rotavapor R200 rotary evaporator (Figure 2.2.1-2). The residue was dried for 48 hours in a vacuum oven (Lab-line vacuum oven) first at room temperature for 24 hours, then at 50°C for 12 hours and finally at 115-120°C for another 12 hours. A thermo-gravimetric analysis (TGA)

test was performed on each batch to assure that all the toluene was removed (less than 0.1 percent of the sample evaporated at temperatures below 180°C).<sup>18</sup>

### **2.2.2 AGING**

The original materials were subjected to aging using the Rolling Thin Film Oven Test (RTFOT), Thin Film Oven Test (TFOT), Pressure Aging Vessel (PAV) and Rotating Cylinder Aging Test (RCAT aging). To simulate short time aging during production and handling, RTFOT and TFOT tests has been used in the laboratory. The RTFO test (Figure 2.2.2-1) has been used to perform AASHTO T240 and ASTM D 2872 <sup>19</sup> procedures to simulate aging in asphalt binder samples representative of the aging that occurs during mixing and construction of HMA pavement. The RTFO procedure can be done to provide samples for use in further testing or to determine the mass lost (from lost volatiles) or gained (from the formation of oxidation reaction products) by the binder samples during the aging process. The RTFO aged binder samples by continually exposing them to heat and air flow to promote an oxidation reaction. This reaction is an accelerated version of the aging occurring naturally in Asphalt Binders in pavements. RTFO-aged binders have been tested with the DSR or aged further with the PAV. A total of 35± 0.5 g of material was loaded in an open metal bottle at 163°C for 75 minutes under an air jet with 4 L/min flow rate positioned to blow air into each bottle at its lowest travel position while being circulated in the carriage with a rotation rate of 15°/min. The bottles were held in a horizontal position while the carriage rotated vertically. Because PMAC blends tend to foam excessively, RTFO test was replaced with TFOT. For TFO test (Figure 2.2.2-2) the standard procedures AASHTO T 179 and ASTM D1754 were followed.<sup>20</sup> The pans, loaded with 50±5g of asphalt, were kept on a horizontal carriage for 5 hours under continuous airflow at 163°C. All the samples were weighed before and after TFOT and the calculations indicate a gain

in weight: an average of 0.02% for PEN 150; 0.06% for PG 64-22 and 0.06% for PMAC 76-22. The gain in weight is due to the formation of oxidation reaction products. Materials subjected to TFOT were stirred every hour to avoid skin formation and an inhomogeneous aging.



**Figure 2.2.2-1 RTFOT instrument (adapted from Controls Testing Equipment LTD)**



**Figure 2.2.2-2 TFOT instrument (adapted from Controls Testing Equipment LTD)**

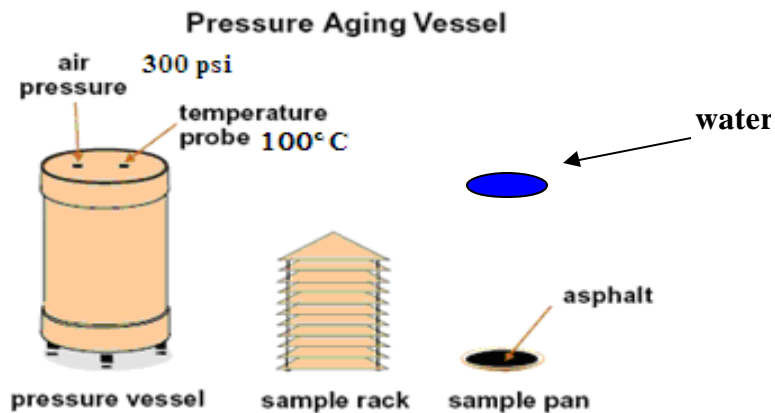


**Figure 2.2.2-3 PAV instrument (adapted from reference<sup>21</sup>)**

After TFOT, the samples were subjected to PAV (Figure 2.2.2-3) (standard procedures ASTM D454 and ASTM D572<sup>22</sup>) aging at 100°C, 2070 kPa (300psi) for 10, 20, 30, 40, 50, 60, 80 and 100 hours in dry and wet conditions. Samples in the following were classified as PAV

DRY and PAV WET as a function of aging conditions used. Wet condition means that one pan was filled with water and placed on the same rack with asphalt samples. After PAV the samples were weighed again, and the results showed an average increase in mass of 0.2% for PEN 150, 0.1% for PG 64-22 and 0.6% for PMAC related to original materials weight.

The suggested pre-heating temperatures, for easier sample pouring into the pans, bottles, or cylinder, are  $150 \pm 5^\circ\text{C}$  for normal asphalts (PG 64-22 and PEN 150) and  $160 \pm 5^\circ\text{C}$  for polymer modified asphalts. The polymer aging process was done using the same TFOT and PAV procedures. Polymer samples preparation involved preparation of solutions. Two solvents were used: decaline (25% weight concentration) for a set of samples and DCM (12% weight concentration) for another set. Polymer samples showed loss of mass when weighed due to solvent removal during the heating process.

The RCAT instrument (Belgian Road Research Center, Brussels, Belgium) used in the present work is presented in Figure 2.2.2-4. It was developed in Belgium by Verhasselt A.F and alt. (starting in 1991) to simulate mainly long-term aging<sup>23</sup> and presented in Project NCHRP 9-36 January 2004 as a good candidate for aging tests. The main components of the device are the cylindrical vessel for aging the asphalts (which can accommodate up to 550 g of material) and the temperature-controlled oven. The manufacturer Normalab Analis, Namur Belgium, provided standard procedures and an operations manual. During rotation, a solid steel roller makes a gravity-induced rotating movement about its axis in the cylinder. Using this roller, the binder in the cylinder is constantly pressed and distributed against the inner wall of the cylinder. As a result, the asphalt surface exposed to air or oxygen is constantly renewed and remixed with the bulk of the material.<sup>23</sup> This test provides the ability to follow the kinetic aspects of aging because it allows small portions of material to be taken at predetermined intervals during the test. The test was run in open atmospheric contact and no excess water was added. The mass of

PMAC tested was 520 g at 90°C under continuous air flowing (between 6 and 7 psi) for 10 days. The oven, as well as the cylinder, was heated and rolled at 90°C on the day before the test. On the day of the test, the binder was heated for 75 min at 163°C. At the same time, while the sample was still hot, a portion was taken to perform the identification tests at an exposure time of  $T_0 = 0$  hours. The material was poured into the hot cylinder and was held for 60 minutes, without rotation or inflow of air, to enable the binder to reach the test temperature. The rotation of the cylinder about its axis was set up at 15 revolutions per minute (for air). To prevent oxidation reactions from occurring mainly at the surface the samples, an inner steel roller constantly renewed the surface. The collection of the samples (10-15 g each) continued according to the program described in Table 2.2.2-1.

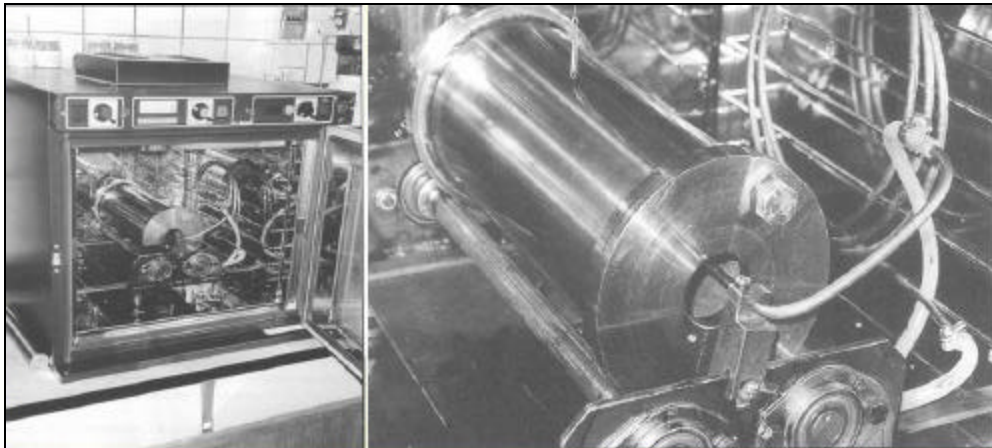


**Figure 2.2.2-4. Rotating Cylinder Aging Test (RCAT) instrument (pictures provided by the manufacturer)<sup>23</sup>**

**Table 2.2.2-1 Exposure times of samples collected for analysis from the RCAT @ 90°C<sup>24</sup>**

RCAT Sample	RCAT Time (hrs)	RCAT Sample	RCAT Time (hrs)
T1	2	T6	73
T2	6	T7	143
T3	19	T8	169
T4	24	T9	193
T5	48	T10	227

As will be seen in the results presented in Chapter 3, no conclusion could be gathered from the first approach and another set of samples was run. With the second set of samples the cylinder was loaded twice with 300 g PMAC material each time. The procedure was the same but the test temperature was changed to 100°C. The temperature of 100°C was chosen for comparison with dry PAV and to see the differences with RCAT at 90°C. The collection of the samples (10-15 g each) was made according to the program described in Table 2.2.2-2.

**Table 2.2.2-2 Exposure times of samples collected for analysis from the RCAT @ 100°C**

RCAT sample 100°C	Aging time hours	RCAT sample 100°C	Aging time hours
R1	70	R5	23
R2	104	R6	48
R3	128	R7	240
R4	152		

### 2.2.3 FTIR SPECTROSCOPY

Quantification of the oxygen uptake during aging is a direct measure of the advancement of the aging process.<sup>25</sup> Spectroscopic determinations using FTIR was chosen for quantification of carboxylic acid concentrations during the oxidative aging of asphalts. All of the asphalt samples (originals, laboratory aged and field extracted) were first dissolved in toluene, concentration of 10% by weight. Using a thin glass pipette, a 0.8 ml solution was poured on a NaCl plate. The time necessary for toluene to totally evaporate from the sample poured on the plate was determined in two ways. The FTIR spectra were recorded every five minutes, and compared with the toluene spectra. When the peaks for toluene disappeared, the samples were subjected to TGA measurements, which showed no solvent presence. After the asphalt film was formed, the FTIR spectra were recorded using a blank plate as a background, baseline correction and smooth coefficient of 25. Samples spectra were run three to five times each. The transmittance files were converted with the software to absorbance spectra. Data were saved in Excel format files



and the graphs were analyzed using Origin 6 software. The data reported represents the average value. In order to build a calibration curve for the peaks observed on the FTIR asphalt sample, a series of organic compounds with potentially similar carbonyl peaks were tested: stearic acid, lauroyl peroxide, benzaldehyde, benzoic acid, 2-decanone, and trans-cinnamaldehyde. From each of those organic compounds was prepared a 1%, 2%, 3%, 5% and 8% weight concentration in asphalt and then the FTIR spectra of each was recorded as described above. The calibration curves are presented in the results-discussion section. The samples studied in this chapter were: PMAC original, aged in dry and wet PAV process, aged using RCAT methodology and asphalt extracted from field samples for comparison.

#### **2.2.4 NON-AQUEOUS POTENTIOMETRIC TITRATION**

To confirm data from FTIR measurements, a determination of acid groups in asphalts was made by nonaqueous potentiometric titration (PT) as described by Buell<sup>26</sup> and Dutta and Holland<sup>27</sup> and adapted by investigators at the Western Research institute in Laramie, WY<sup>17</sup>. The endpoint was determined using an Orion Aplus pH-meter with glass ion-selective indicator electrode. Samples subjected to potentiometric titration were: PMAC unaged and aged under dry PAV and RCAT; PG 64-22 and PEN 150 neat; and field samples. The following organic compounds were necessary to run the test:

- Potassium hydrogen phthalate (KHP) with molecular weight (Mw) =204.23 as standard calibration compound for instrument (oven dried for two hours 100°C);
- Benzoic acid as model compound, Mw=122.12 (oven dried for two hours 100°C);
- Tetra butyl-ammonium hydroxide as base, Mw =799.96;
- Solvents: toluene, isopropyl alcohol, chlorobenzene, and ethanol.

Three grams of asphalt was weighed in an Erlenmeyer and dissolved in a 50 ml mixture of chlorobenzene and ethanol mixture 9/1 v/v. Fifty ml was chosen to be enough to cover the electrode sensor for an accurate reading. The Erlenmeyer was then tightly capped and sealed under argon. The asphalt was totally dissolved under continuous stirring for two hours. The base concentration was 0.025 M tetra-butyl-ammonium hydroxide in a mixture of toluene/isopropyl alcohol 8/2 v/v. The literature recommended a ratio of 8.6/1.4 v/v for this mixture but this ratio did not dissolve the base so the ratio was changed to 8/2 v/v, which dissolved the base instantaneously. The burette was well sealed and filled up with argon. Standard model compounds used were potassium hydrogen phthalate and benzoic acid (dried 2 hours at 100°C). For both solutions 0.025 M concentrations were prepared by dissolving in chlorobenzene/ethanol 9/1 v/v (solutions were also kept under argon).

Before starting the titration in the flask with the asphalt solution, the pH meter electrode and a magnet for continuous stirring were immersed in the solution. The burette and argon tube were placed in the top of the flask and were sealed to keep the argon in the flask. The pH-meter was first calibrated (apparatus manual procedure) and then set up for the millivolts mode. The readings for each point of titration curves were made after the systems were allowed enough time to achieve equilibrium which was indicated by a stable value for potential on the pH-meter screen. The titrations were replicated five to ten times.

The instrument calibration was made as required by the operations manual provided by the manufacturer (Figure 2.2.4-1).

Milliliters of titrant (mL base) added were recorded in table format and then plotted versus mV using Origin software (Figure 2.2.4-2). To quantify titration inputs, a calibration curve (x-axis mV, y-axis ml base) was built using the same benzoic acid as a reference (Figure 2.2.4-5).

From the first derivative curve (Figure 2.2.4-6) the end point was obtained and then concentration per gram of asphalt was computed using the following equation<sup>28</sup>:

$$\frac{\text{meq}}{\text{g}} = \frac{\text{volume of titrant (mL)} * \text{normality of titrant}}{\text{grams of sample}}$$

$$\text{Normality} = \text{Molarity} * n$$

$n = \text{number of protons exchanged in reaction}$

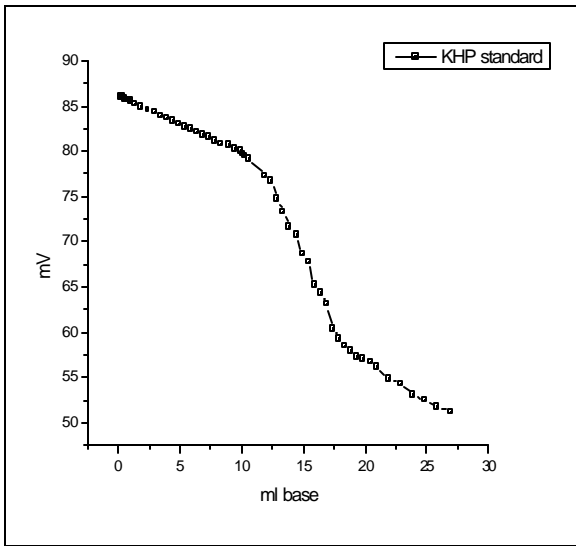


**Figure 2.2.4-1. Titration curve of KHP standard**

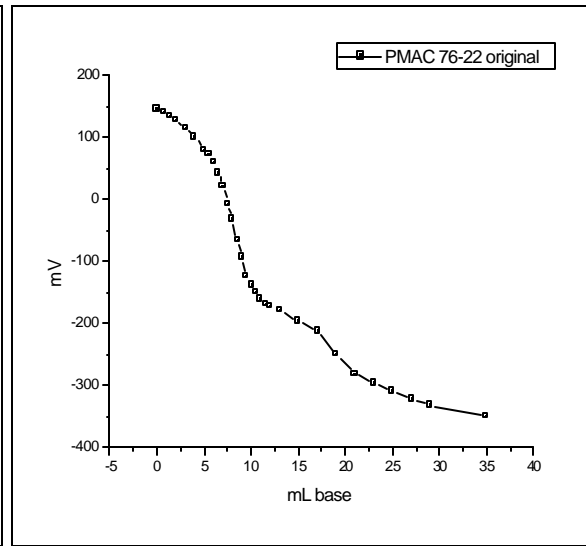


**Figure 2.2.4-2. Example of a titration curve for original PMAC**

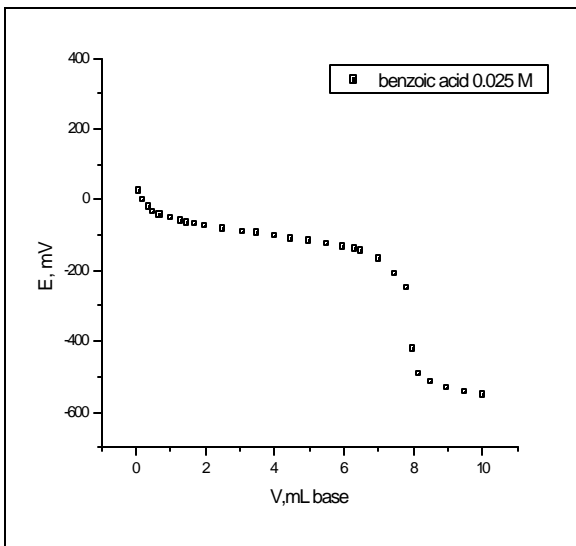


**Figure 2.2.4-3 Titration curve of benzoic acid 0.025M**

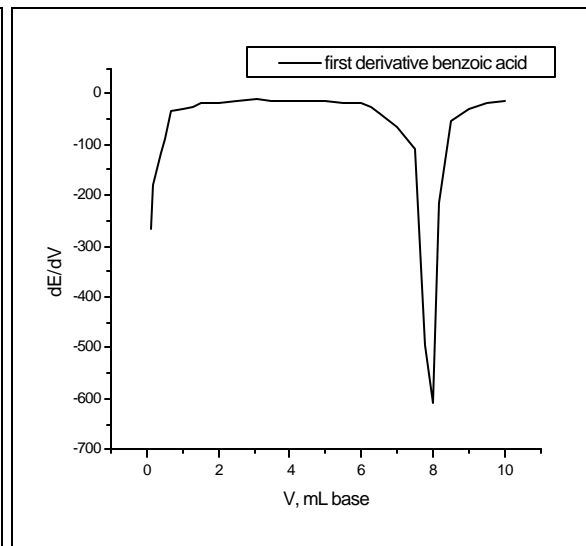


**Figure 2.2.4-4 First derivative of titration curve for benzoic acid titration**

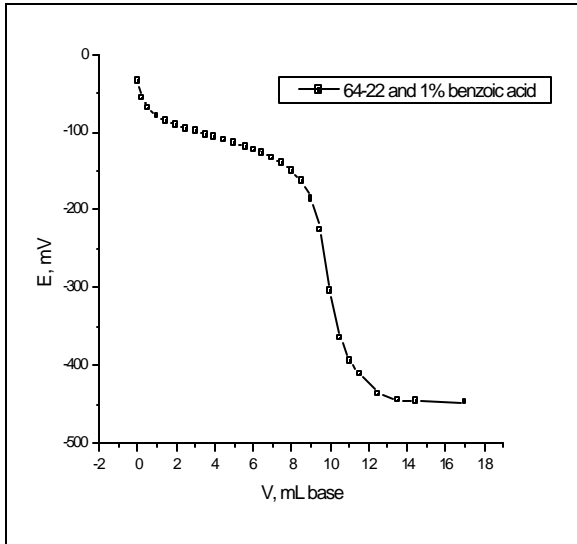


**Figure 2.2.4-5 Titration curve for asphalt cement and 1% wt benzoic acid**

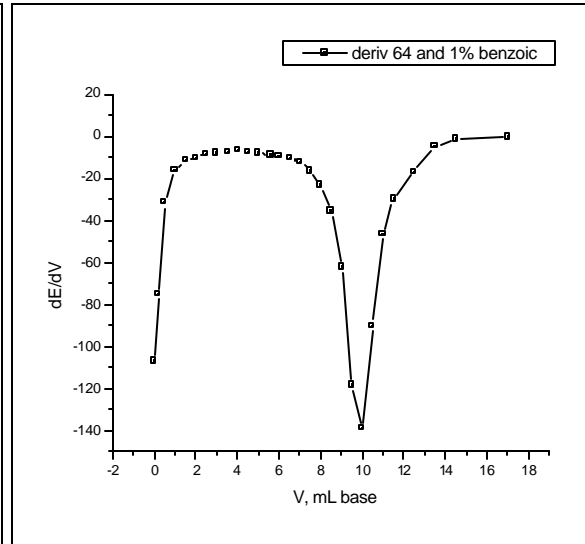


**Figure 2.2.4-6 First derivative for asphalt +1% wt benzoic acid**

To make sure that the end point was an accurate reading, the results were verified by adding benzoic acid (1% and 2% wt.) to the samples and the end point was read by subtraction (Figure 2.2.4-5 and 2.2.4-6).

## 2.2.5 GPC CHARACTERIZATION

The use of gel permeation chromatography is a fast and reliable new method to determine molecular weight and molecular weight distribution of asphalt binders. The polymer content in asphalt can also be analyzed. Since unaged polymer molecules typically weigh 50 times more than asphalt molecules, they can be easily identified using this method. The gel permeation chromatograph used was equipped with a Waters 590 pump and a Waters model 410 differential refractive index detector. The separation of the polymer from the asphalt components was effected with two Phenogel 10  $\mu$ , 300 x 7.8 mm columns (Phenomenex, Torrance, CA), connected in series (1) 10-5 Å (10-1,000 K); (2) MXM (5-500 K). This set of columns was chosen to cover, as much as possible, the molecular weight distribution expected to be seen in asphalt binder GPC curves.<sup>3</sup> The column set was calibrated with narrow molecular weight

polystyrene (PS) standards 3% wt. concentration in tetrahydrofuran (THF) (Table 2.2.5-1 and Figure 2.2.5-1). The molecular weight distribution function of the elution volume for polystyrene standards (Figure 2.2.5-2) was used to build the linear dependency expressed in the log/log scale calibration graph (Figure 2.2.5-3). All asphalt and polymer samples were prepared at a concentration of 2% in THF, injected through 0.2- $\mu$ m filters into 150  $\mu$ L vials. Samples were eluted with THF at 1 mL/min at room temperature and the species concentration in the eluent was recorded using a differential refractometer. The Gel Permeation Chromatography (GPC) method was used to analyze the impact on asphalt cement, polymer and polymer modified asphalt of the wet and dry PAV process. Data were compared to field extracted asphalt blends. The samples run contained:

- Asphalt cement PG 64-22 and PEN 150
- Polymer modified asphalt (PMAC) 76-22
- SBS block copolymer, dissolved in decaline and DCM
- Asphalt extracted from field cores 3 and 5 years old,
- Mixture of asphalt cements (Mix) prepared in laboratory 85% 64-22 with 15% PEN 150

After aging, some samples have insoluble components. To find how much can be insoluble in THF a quick test was run by dissolving a known quantity of materials in THF, and passing the solution through a 0.2 $\mu$ m filter. From the difference in weight of the filter before and after passing the solution (the filter was dried under vacuum for total evaporation of THF) plus the quantities remained in the vial (not going into a syringe) the percentage of insoluble species can be evaluated as shown in Table 2.2.5-2. For consistency, a baseline was drawn and the relative areas were computed by integration. For a given sample, the relative area value was related to the GPC curve of the original material (polymer original with A=1.19531 and PG 64-22 original

with A=11.67349). Table 2.2.5-3 presents major chemical groups, which may be detected by GPC measurements and also describes how they are to be referred to in this analysis.

**Table 2.2.5-1 Elution volume (Ve) values for Polystyrene standards**

Mw polystyrene standards	Ve, mL
523,000	16.92
218,800	17.65
96,000	18.48
66,350	19.13
52,400	19.57
19,880	21.82
9,920	23.50
4,920	25.24
1,940	27.40
1,060	28.83

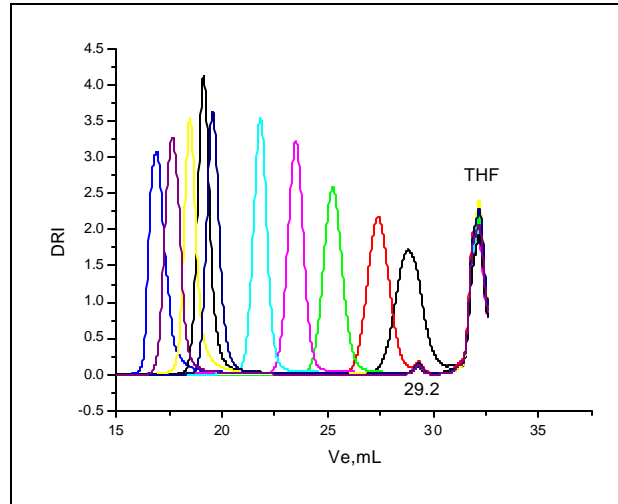


**Figure 2.2.5-1 Elution volumes for GPC column set calibration with PS standards**

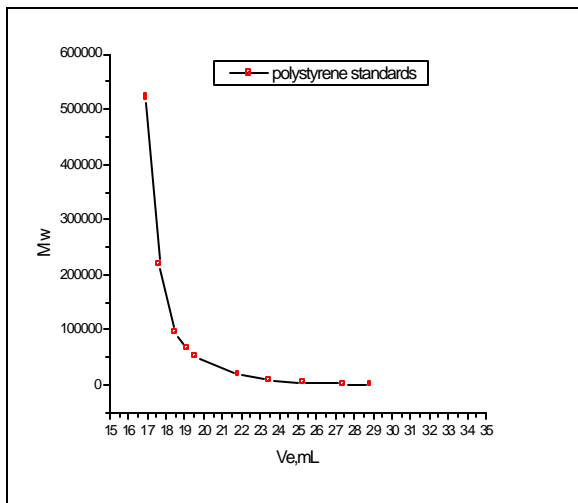


**Figure 2.2.5-2 Molecular weight vs. elution volume for PS standards**

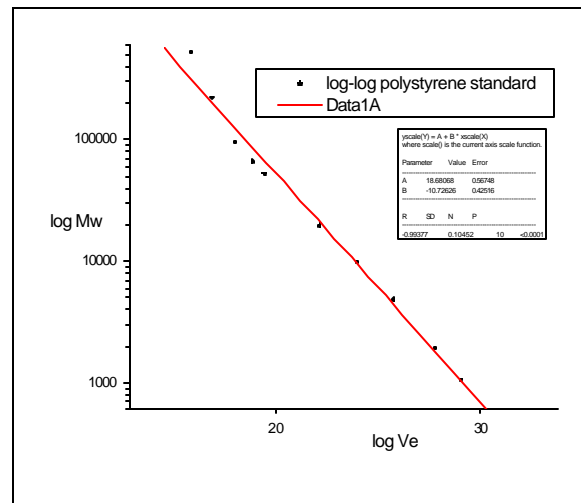


**Figure 2.2.5-3 Linear calibration from PS GPC traces**

**Table 2.2.5-2 Percentage of insoluble species not passing through 0.2mm filter**

PMAC 76-22 original	~7%
Polymer SBS Calprene after PAV	~99%
Blend 64-22 and 3% SBS after PAV	~5%
PMAC 76-22 after PAV	~6%

**Table 2.2.5-3 Major chemical groups expected to be seen by GPC**

	Molecular weight	% of weight of asphalt	Ve, mL	Referred in this work as
asphaltenes	2000 – 5000	5-25	21.2 -26.5	asphaltenes area MMW
resins	800 – 2000	15-25	27.2 -29.2	low molecular weight asphalt area LMW
aromatic oil	500 – 900	45-60	28.6 -29.5	
saturated oil	500 - 1000	5-20	28.8 -29.5	
Calprene SBS original	~650,000	~ 3	~16.78-16.9	high molecular weigh polymer area HMW

### **2.2.6 EPIFLUORESCENCE MICROSCOPY**

To visualize the asphalt blends, the morphology fluorescence microscopy method was used. The technique applies to specimens that can be made to fluoresce, as is the case with asphalt materials. The samples chose for this test were PMAC original material and PMAC dry PAV aged for 50 hours (2.5 PAV cycles).

The asphalt samples were melted first at 150°C for 20 minutes than poured in a bar form. The field mixture was cut in a bar form also. The samples were immersed in liquid nitrogen to obtain a fresh cut without using any mechanical force. The pieces with the most even new surface were placed on the testing surface and at least 3 pictures of each sample were taken. The pictures were adjusted and layered out using Adobe Photoshop.

### **2.2.7 INDUCED DECOMPOSITION OF ASPHALT COMPONENTS**

There is a lack of practical laboratory aging that simulates long-term aging of asphalt at in-service conditions. The aim of this test is to simulate an oxidative aging process catalyzed by metal ions. To accelerate the autoxidation process this test used induced decomposition of a hydroperoxide via a redox mechanism. A typical example of a redox pair used in induced oxidation is a mixture of cobalt salts (acetate or naphthenates) and hydroperoxides (ROOH).

- Cumene hydroperoxide was chosen because its half-time is 10 hours at 125°C (this doesn't apply when cobalt naphthenate is present too).

- Cobalt naphthenate 6% concentration dissolved in mineral oils.

- Solvents: DCM, Decaline, THF

It was not possible to run this test on the commercial PMAC 76-22 (polymer modified) received from the supplier because of the presence of sulfur. Because it was necessary to avoid the effect that sulfur has on metal ions (is poisoning the catalyst), polymer modified asphalt was prepared in the laboratory. This was made by mixing 388 grams of PG 64-22 dissolved with 100 mL dichloromethane (DCM) with 12 grams polymer (SBS, commercial name Calprene 411) and also dissolved in DCM to obtain a concentration of 3% polymer in asphalt. Another 400 grams of PG 64-22 was dissolved in 100 mL DCM and was prepared for samples without polymer (asphalt only). PMAC 76-22 was tested just for comparison. PMAC of 150 grams dissolved in 50 mL DCM was used. To meet the standard requirements of 50 grams materials per pan for TFOT and PAV, empty pans were weighed, and then aliquots were made. After three days under the hood and at room temperature the samples were ready to be mixed with various concentrations of cobalt and hydroperoxide. Having FTIR data for orientation, the first samples were prepared by adding 5 mL hydroperoxide ( $d=1.03 \text{ g/mL}$ ) and 1.65 g cobalt naphthenate to 50 g of asphalt materials. A typical example of a ratio expression for each mixture of cobalt naphthenates and hydroperoxide follows the equations:

a) For  $M_1$  grams of cobalt naphthenates with a 6% cobalt concentration it will be  $6\% \times M_1$  grams of cobalt with atomic mass of 58.933 which give  $6\% \times M_1/58.933$  moles of cobalt used; this quantity is added to 50 grams of asphalt, by dividing by 50, moles per 1 gram asphalt can be computed  $[(6\% \times M_1)/(58.933 \times 50)]$



b) For L1 milliliters of hydroperoxide used with a density of 1.03 g/ml and Mw of 152.19 added to 50 grams asphalt, the moles used for 1 gram asphalt are computed  $[(L1 \times d)/(Mw \times 50)]$

c) Samples were labeled as a function of various concentrations of redox systems used, such as 1: a: b where 1 means 1 gram asphalt; a is moles ratio of cobalt used with respect to redox2 as reference sample; b refers to how much more or less hydroperoxide was used than cobalt with respect also to the redox2 sample as a reference sample (Table 2.2.7-1).

There is a slight difference in sample preparation using various redox systems. Redox2 was added to the asphalt or polymer-modified asphalt before pouring the asphalt materials into pans for the aging process. The rest of the redox systems were added after the asphalts were in the pans. A lower concentration in asphalt due the dilution with redox compounds can be noticed on the GPC curves. Some asphalt samples were mixed only with 5 mL HP, in these cases the ratio was expressed as **1:0:20**. The induced oxidation starts in a short time.

**Table 2.2.7-1 Proportions of Redox pair used**

	Mass cobalt naphthenates (g) M1	Volume hydroperoxide (mL) L1	Moles Cobalt (Co) /1 g asphalt	Cumene hydroperoxide (HP) / 1 g asphalt	RATIO 1-g asphalt a-ratio Co b-ratio HP <b>1:a:b</b>
Redox1	0.33	5	0.00000672	0.000676	<b>1:0.2:20</b>
Redox2	1.65	5	0.00003360	0.000676	<b>1:1:20</b>
Redox3	1.65	25	0.00003360	0.003380	<b>1:1:100</b>
Redox4	4.61	5	0.00009380	0.000676	<b>1:3:20</b>
Redox5	1.65	1	0.00003360	0.000135	<b>1:1:4</b>
	0.00	5	0	0.000676	<b>1:0:20</b>

The samples had to wait 24 hours before injection in the GPC instrument, which allowed the redox systems to react. GPC curves for original materials show the oxidation already working

and because the data sets were cached in different stages these curves have only informational value and do not provide a useful reference for comparison. Samples for the GPC pulled out from pans before aging are referred to as Original, and after aging are named TFOT, dry PAV and wet PAV.

## **2.2.8 RHEOLOGICAL MEASUREMENTS**

Rheology, the study of deformation and flow of matter, can provide important information of Hot Mix Asphalt (HMA) pavement performance.

- Critical temperature.

To discern the changes in rheological characteristics of polymer modified asphalts brought about by aging critical temperature changes with age were measured. The critical temperature  $T_c$  was determined using a dynamic mechanical analyzer known as the AR2000 rheometer (figure 2.2.8-1) which was set up to work in Dynamic Shear mode (Figure 2.2.8-2). This instrument is specially designed for characterization of soft materials (TA Instruments Inc. Waters Corp., New Castle, DE) was used. The basic DSR test uses a thin asphalt binder sample sandwiched between two plates. The lower plate is fixed while the upper plate oscillates back and forth across the sample at 1.59 Hz to create a shearing action. These oscillations at 1.59 Hz (10 radians/sec) are meant to simulate the shearing action corresponding to a traffic speed of about 90 km/hr (55 mph) (Roberts et al., 1996). The steel plates have circle geometry with diameter of 25 mm (used for original materials) and 8 mm (for aged materials) with a test gap between them of 1 and 2 mm respectively. A disk of asphalt with equal diameter to the plates was prepared by pouring in a standard silicon mold (Figure 2.2.8-3) and then placed between the oscillating and fixed plate of the rheometer (Figure 2.2.8-4). The excess asphalt was removed by trimming with a hot spatula. Regardless of the standard procedure (AASHTO TP5) a trimming gap was first set up at 50 microns higher than the test gap, and then the upper plate was set for

the testing gap. An environmental temperature control (ETC) oven allowed a precise control of temperature within 0.1°C.

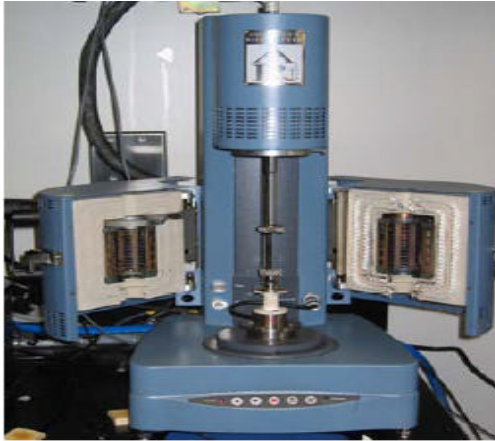


Figure 2.2.8-1 AR 2000 instrument

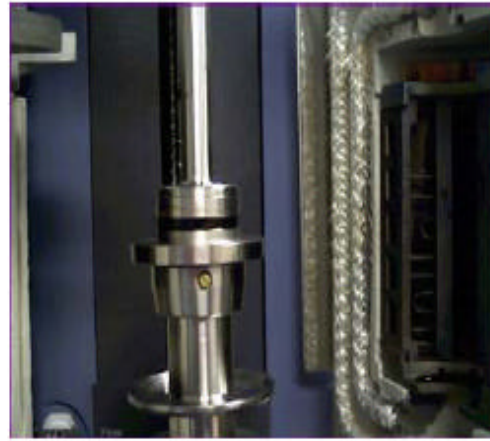


Figure 2.2.8-2 Setting of the AR 2000 instrument in DSR mode

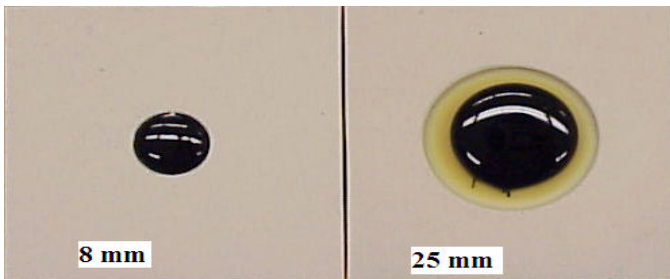


Figure 2.2.8-3 Silicon molds for DSR mode DSR (adapted after [wsdot.edu/materials](http://wsdot.edu/materials))

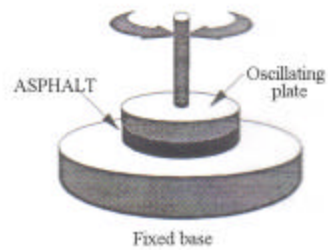


Figure 2.2.8-4 Asphalt sandwich (adapted after reference<sup>29</sup>)

For the same field materials the T<sub>c</sub> were done before in our group (Table 2.2.8-1)<sup>3</sup>:

Table 2.2.8-1 Critical temperatures T<sub>c</sub> (tanδ = 1, G' = G'') field aged asphalt samples

Asphalt Sample	Aging Time	T <sub>c</sub> Road Aged, °C
I-55 Extract	3 yrs	<b>21.0</b>
I-55 Extract	5 yrs	<b>27.3</b>
I-55 Extract	7 yrs	<b>29.4</b>

Test procedures included a 30 minutes temperature equilibration time; dynamic temperature ramp determinations, low cooling rates (1°C/min) and a controlled strain of 1% at constant 10

rad/s frequency. The geometry used was 8 mm. The following equations are then used to determine a complex shearing modulus,  $G^*$  and a phase angle,  $\delta$  (Appendix Table A-2)<sup>30</sup>:

- Repeated Creep and Creep-Recovery test (RCRB). The presence of a macro-network is also confirmed by stress relaxation tests. Repeated creep and recovery tests for binders (RCRB) is suggested (Bahia et al., 1999) as a possible means to estimate the rate of accumulation of permanent strain in the binders. Samples of asphalt binder were tested using the same AR 2000 rheometer and the same sample preparation, 8 mm geometry with a testing gap of 2 mm. The sample was subjected to a repeat sequence of shear loading and unloading. The strain response, as a function of time, was measured and expressed by accumulated strain (displacement). Consistent with the test protocol, two creep loads were chosen at 25 and 300 Pa. The loading time was 1, 2 or 3 seconds with a recovery (unloading) time of 9, 18 or 27 seconds, respectively. The total number of repeated cycles was selected to be 100 and three test temperatures were selected. The test temperatures were 10°C, the critical temperature and a high temperature of 70°C. From displacement and strain data, using the Excel function “vlookup”, the values at the end of each cycle were picked up and plotted as a function of time.

- Effect of Stress Level on Asphalt Binders (MSCR). The current study showed that using only a 300 Pa stress level is not relevant for asphalt blends. Another test was developed, Multiple Stress Creep Recovery (MSCR), by raising the stress level from 25 Pa (0.0036 psi) to 25,600 Pa (3.713 psi) and computing the percentage of recovery.<sup>31</sup> The test protocol followed the same standard sample preparation for dynamic shear rheometer and the instrument used was the same AR 2000. The test procedure was repeated creep recovery with 1-second load and 9 seconds unload, 10 cycles for each stress level at PG temperature (example for 64-22 PG temperature is 64°C). A 30 minutes equilibration time at test temperature was chosen. Differing from the tests presented in literature, the test was run at 25°C, 40°C and PG temperature instead

of only PG temperature, as we considered low temperature behavior for PMACs more critical. Stress levels used were 25, 50, 100, 200, 400, 800, 1600, 3200, 6400, 12800, 25600. The average percentage recovery for each stress level was computed using the equation presented below, where:

$i$  = number of cycle;

$E_c - E_o$  = total strain accumulate ? total

$E_c - E_r$  = final (permanent) strain ? final (Figure 2.2.8-5)

$$\frac{\sum_{i=1}^{i=10} \frac{(E_c - E_o)_i - (E_c - E_r)_i}{(E_c - E_o)_i}}{10} \times 100$$

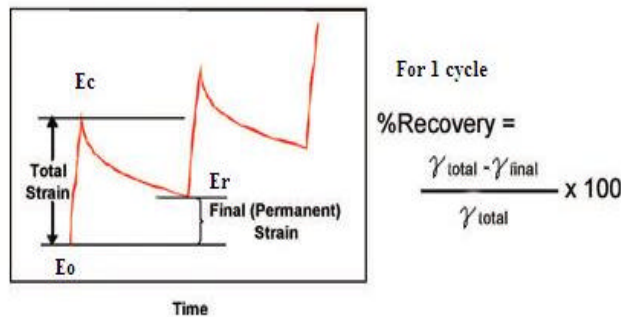


**Figure 2.2.8-5 Example in recording strains for MSCR (adapted from Asphalt Institute July 2006)**

- Failure endpoint – Fatigue test. Correlations can be found to develop a protocol to estimate fatigue life using stress sweep. If stress sweep and time sweep tests failed at the same stress level, the failure endpoint for asphalt materials can be found by plotting complex shear modulus changes in time using the following equation<sup>32</sup>, where

$$N = \text{numbers of cycles} = \text{test time(s)} \times 1.592 \text{ cycle/s}$$

$G^*n$  = complex modulus at cycle  $N$

$G^*o$  = complex modulus at time = 0 sec.

$$N \frac{G^*n}{G^*o}$$

The sample preparation is identical as that for standard DSR measurements. The equilibration time at test temperature was 30 minutes. The procedure used was a time sweep at

constant shear stress of 50,000 Pa as a first trial. The test temperatures range was chosen to be 25°C, 40°C and PG temperature.

### CHAPTER 3

## CHEMICAL ALTERATION BY AGING

## RESULTS AND DISCUSSIONS

The chemical composition of asphalt determines its physical properties. However, the chemical composition of asphalts changes during both the short term (handling and pumping) and long term (field service). One reason for the deterioration of asphalt concrete is aging, mainly oxidative hardening, of asphalt in service. Asphalt aggregate de-bonding (adhesion failure) and / or asphalt phase separation (cohesion failure) is a result of oxidative hardening.

An important indicator of asphalt structure is the content of asphaltenes. A large concentration of asphaltenes will bring the asphalts to a “gel” type behavior (non-Newtonian flow characteristics) which is different from asphalts with a few asphaltenes, designated as “sol” type (Newtonian flow). It has been established that asphaltenes are not stable, can form a separate phase, and can aggregate as a result of chemical alteration.<sup>7</sup> Polar groups created by oxidative aging stabilize this aggregation. The heteroatoms in un-aged bitumen may be polar or non-polar; for example, aliphatic sulfur is non-polar, but becomes a sulfoxide group when oxidized. This is weakly basic and can participate in polar associations. Similarly, hydrocarbon chains are non-polar but become polar when oxidized. The asphalt chemical components have multiple available sites for oxidation such as benzylic and allylic positions (which are especially susceptible to oxidation); alkyl-aromatic sites; and benzylic positions, including tetralin compounds (which lead to hydroperoxides formation). The functionalities formed contain mainly carbonyl groups such as ketones, aldehydes, carboxylic acids, anhydrides as well as a small number of alcohols, sulfur and nitrogen compounds. The presence of polymer in asphalt blends creates new sites available for autoxidation (polybutadiene). Transitional metal ions (in asphalt

composition or carried by aggregates) are the perfect initiators for free radical oxidative decomposition and their presence will enhance the oxy-degradation process. In acidic conditions the water can undergo polar addition to alkene bonds resulting in new alcohol functions.

Two of the most fundamental properties of any organic substance are molecular weight and chemical functionality. In theory, many physical properties, particularly rheological properties, are a function of molecular weight and molecular weight distribution. Chemical functionality determines the extent of intermolecular association, influencing aging and stripping behavior. A number of analytical techniques can be applied to study the changes in asphalt materials during the oxidation process. For the measurements of polar functionalities we can use FTIR; determination of acid content using non-aqueous potentiometric titration (PT); and molecular weight distribution and molecular size determination using gel permeation chromatography (GPC).<sup>7</sup>

### **3.1 FTIR CHARACTERIZATION**

A major factor leading to the hardening and embrittlement of asphalt pavements is the reaction of asphalt with atmospheric oxygen. As proposed by Petersen<sup>33</sup>, the hardening phenomenon is primarily a result of the formation in asphalt of polar oxygen containing functional groups that increase asphalt consistency through strong molecular interaction forces. Therefore, quantification of the oxygen uptake during aging is a direct measure of the advancement of the aging process.<sup>25</sup> Spectroscopic determinations (FTIR) and “wet chemistry” analysis (direct titration of functional groups) are the most commonly used methods. The formation of carbonyl groups was observed, coupled with increased absorption at a frequency of  $1695\text{ cm}^{-1}$ , relating C = O stretching from unsaturated or aromatic carboxylic acids as a result of oxidation. The absorption at the frequency  $1760\text{ cm}^{-1}$  was attributed to anhydride groups also



formed after oxidation. A small number of sulfoxide groups, characterized by the band at the  $1030\text{ cm}^{-1}$  frequency (S = O stretching), were also noted. The bands that appeared at 911 to  $699\text{ cm}^{-1}$  were attributed to the butadiene and styrene part of the SBS co-polymer.<sup>34</sup> An increase was also observed in the intensity of the band at  $3400\text{ cm}^{-1}$  (OH stretching) which was related to oxidation of the polybutadiene portion in the copolymer.<sup>6</sup>

This work concentrated on quantifying the oxygen uptake by measuring changes in carbonyl content based on a calibration curve. Inspection of FTIR spectra for our samples showed weak bands for OH at  $3400\text{ cm}^{-1}$  and aromatic C-H at  $3070\text{ cm}^{-1}$ ; strong bands for CH methylene at  $2923\text{ cm}^{-1}$ ; aromatic C=C bands at  $1456$  and  $1601\text{ cm}^{-1}$ ; bands attributed to PB and PS parts of the polymer at  $966\text{ cm}^{-1}$  and  $730\text{ cm}^{-1}$  (verified by increasing polymer concentration in asphalt with result of increasing intensity for these bands); clear peaks at  $1695\text{ cm}^{-1}$  for unsaturated or aromatic carboxylic acids correlated with bands from C-O around  $1300\text{ cm}^{-1}$ ; weak stretches of sulfur compounds as esters S-OR  $733\text{ cm}^{-1}$  and sulfoxides  $1030\text{ cm}^{-1}$ ; and weak signals for  $1725$  and  $1750\text{ cm}^{-1}$  in dry PAV spectra coming from aldehydes and/or ketones. In addition, the field sample spectra showed a weak peak at  $1735\text{-}1746\text{ cm}^{-1}$  which can be esters and cyclic esters (lactones type), and at  $1785\text{ cm}^{-1}$  for anhydrides. The first step was to choose a reference peak. The  $1456\text{ cm}^{-1}$  peak (aromatic C=C bonds) was the best choice as the reference peak because the aging process didn't affect these bonds. From all the spectra of potential organic reference compounds mixed with PMAC, as shown in Figure 3.1-1, only the spectra of the mixture PMAC-benzoic acid spectra matched the aged asphalt material closely (Figure 3.1-2). Therefore the calibration curve was built using the peak ratio  $1695\text{ cm}^{-1}$  (the stretch of C=O from unsaturated carboxylic acids) to  $1456\text{ cm}^{-1}$  reference peak for benzoic acid with concentrations ranging from 0.05 to 0.7 miliequivalents per gram PMAC (Figure 3.1-3).

A polynomial correlation between the absorbance ratios and carboxylic acid content was observed for concentrations between 0.05 up to 0.18 meq/g followed by a linear relationship from 0.18 to 0.7 meq/g. Based on the calibration curve, the acid concentration dependency on aging under dry and wet PAV conditions was computed (Table 3.1-1). The aging process was run up to 100 hours (5 cycles of PAV) with the idea of reaching a saturation stage of oxidation. The carboxylic acids concentration was higher when the aging occurred in humid conditions as can be visualized in graphic representation Figure 3.1-4. During the PAV dry and wet aging processes the concentration of carboxylic acid increases rapidly in the first 20 hours. Starting with the second PAV (40 hours) the impact of oxygen is still elevated but the changes are not as pronounced as in the first PAV cycle. Acid concentrations in wet conditions almost doubled compared to dry conditions showing that water helped the formation of acids. The same procedure to determine the concentration of carboxylic acids was followed for the field sample (results are presented in Figure 3.1-5 and Table 3.1-2) for comparison with laboratory-aged samples.

In the field a similar increase in carboxylic acids formation is seen. The 3 and 5 years old samples were full core HMA with less water contact. As shown by summary Table 3.1-3, the content of carboxyl groups of field aged asphalt samples after 3 years on the road was similar to, but less than 10 hours dry or wet PAV. The 5-year-old samples correlated with 20 hours dry PAV but less than the equivalent wet PAV.

The FTIR results for dry and wet PAV aged PMAC showed that the thermal oxidation has two reaction rates, a rapid increase in carboxylic acids concentration between 0 and 20 hours PAV followed by a slower process after 20 hours. As there is not enough information in the 0-20 hours aging range, nothing can be concluded about the reaction rate in this range.

To study this process in detail another aging technique, RCAT, which allows for the collection of more samples, was used. The concentrations in carboxylic acids were obtained by the same procedure (Figure 3.1.7) and time equivalence between dry PAV and dry RCAT PMAC asphalt laboratory aged samples are presented in Figure 3.1-8 and Table 3.1-3.

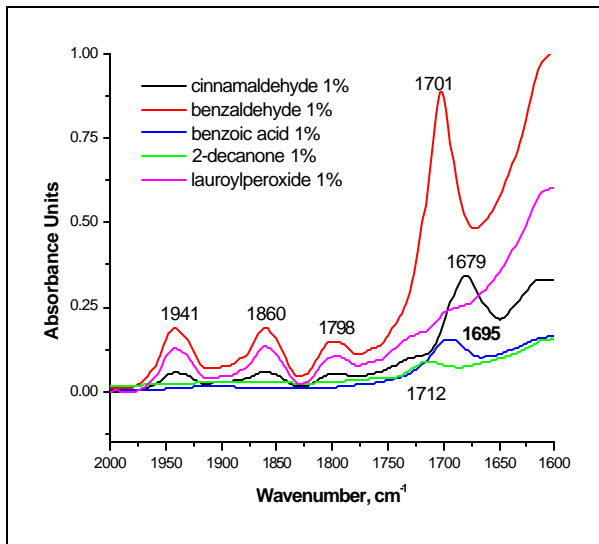


**Figure 3.1-1 FTIR spectra showing carbonyl absorbance of reference compounds; 1%wt in PMAC**

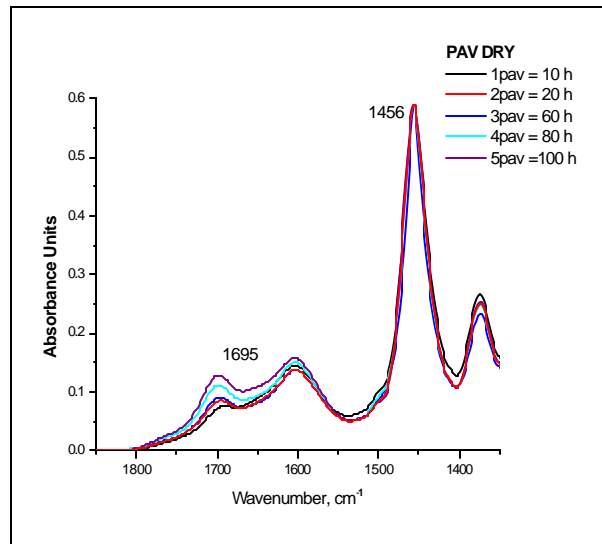


**Figure 3.1-2 FTIR spectra showing the increasing 1695 cm<sup>-1</sup> peak in PMAC after oxidative aging**

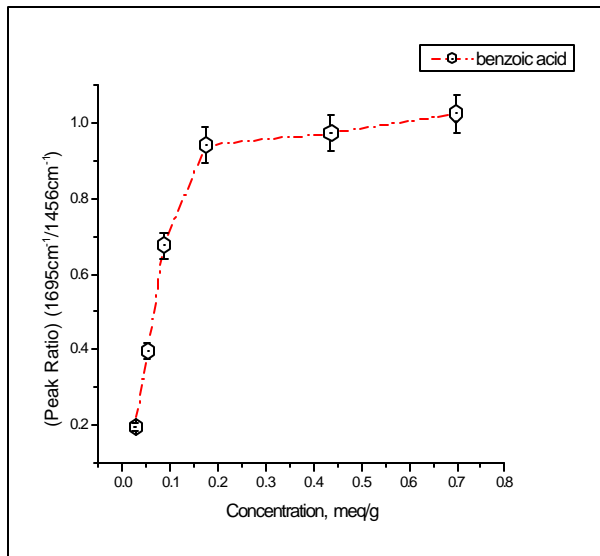


**Figure 3.1-3 Calibration curve benzoic acid mixture with PMAC**

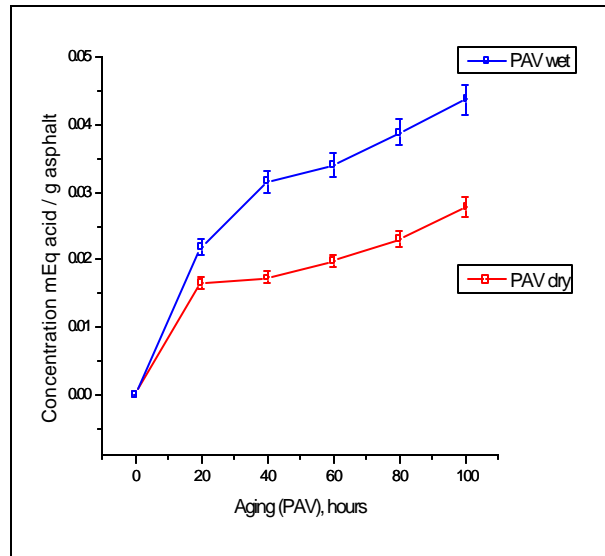


**Figure 3.1-4 Changes of carboxylic acid of dry and wet PMAC aged samples**

**Table 3.3-1 Concentrations of carboxylic acids, after multiple dry and wet PAV's cycles**

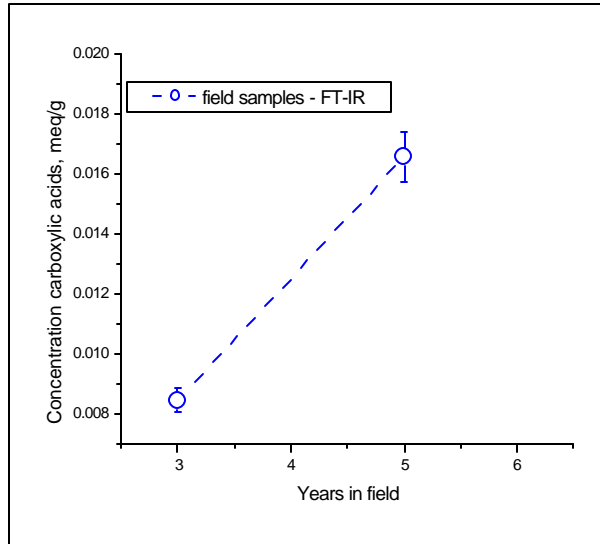


**Figure 3.1-5 Carboxylic acids concentrations of asphalt binders field aged**

Hours PAV	DRY meq/g	WET meq/g
0	0	0
20	0.01656	0.02192
40	0.01732	0.0316
60	0.01979	0.03407
80	0.02302	0.03881
100	0.02782	0.04375

**Table 3.1-2 Summary of carboxylic acid concentrations from FTIR measurements**

HOURS	FTIR	FTIR	YEARS	FTIR
PAV	DRY	WET	FIELD	
	meq/g	meq/g		meq/g
0	0	0		
<b>10</b>	<b>0.0097</b>	<b>0.0098</b>	<b>3</b>	<b>0.0084</b>
<b>20</b>	<b>0.0165</b>	0.0219	<b>5</b>	<b>0.0165</b>
30	0.0169			
40	0.0173	0.0316		
60	0.0197	0.0341		
80	0.0231	0.0388		
100	0.0278	0.0437		

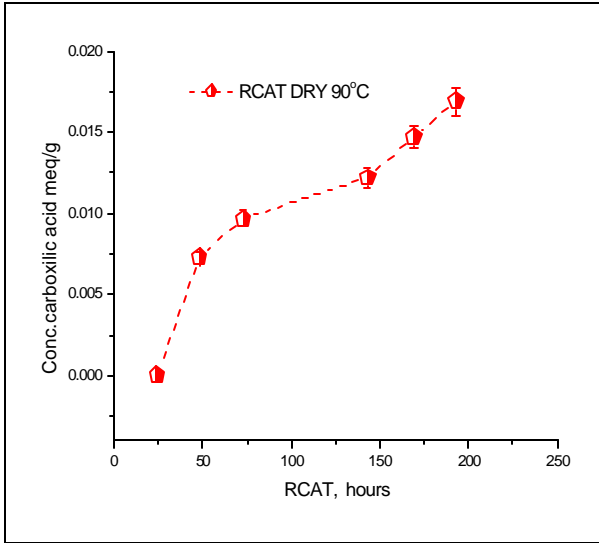


**Figure 3.1-7 Carboxylic acid concentrations of PMAC aged in RCAT conditions, @ 90°C**

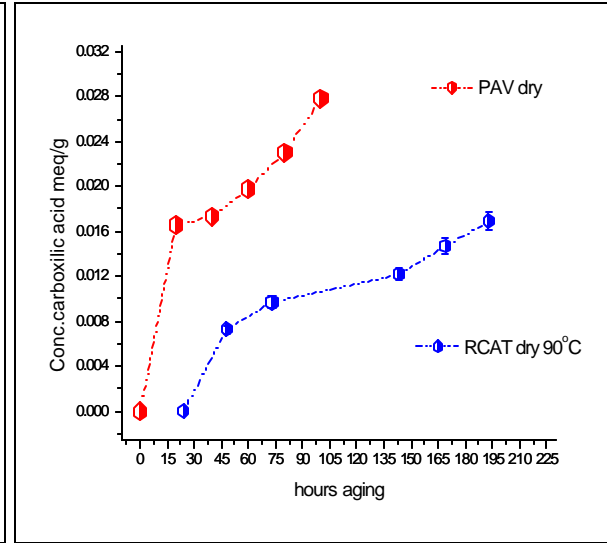


**Figure 3.1-8 Comparison of carboxylic acid concentrations of PMAC PAV aged and RCAT-aged**

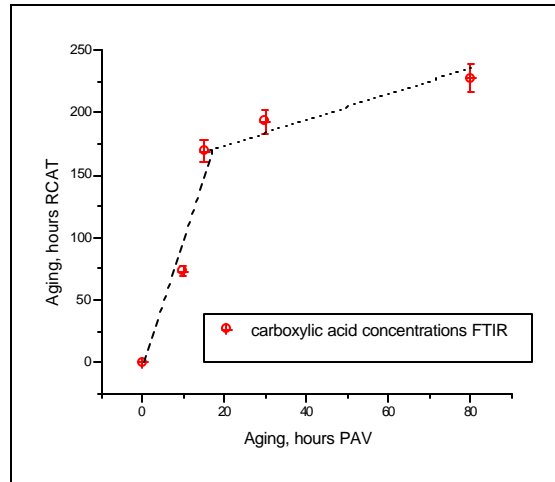


**Figure 3.1-9 Time equivalence RCAT-PAV after FTIR determination of carboxylic acids concentrations for PMAC lab aged**

According to data accentuated by colors in Table 3.1-3 and the graph presented in Figure 3.1-8, the PMAC treatment for 73 RCAT hours @ 90°C was equivalent to laboratory aging for 10 PAV hours at 100°C (half of 1 PAV cycle); 193 hours RCAT are equivalent to 30 hours PAV and the last sample, after 227 hours RCAT aging, is equal to 40 hours wet PAV or more than 100 hours dry PAV. The last RCAT sample (227 hours) is still under verification. During the

collection process the asphalt layer became very thin and excessive oxidation occurred. This indicated a need for better handling of the next sample collections for RCAT. However, to achieve the extent of oxidation equivalent to 20 hours PAV required almost 193 hours of RCAT. Consequently, we can see in more detail that the oxidation process accelerates more rapidly up to 73 hours RCAT (respectively 10 hours PAV) and steadier thereafter. The 3-year-old sample is close to 73 hours and the 5-year-old sample is less than 193 hours RCAT.

**Table 3.1-3 Time equivalence between PAV and RCAT laboratory aged samples**

Hours	FTIR	FTIR	Hours	RCAT 90C	Years	FTIR
PAV	dry	wet	Rcat	dry	Field	
0	0	0	0 - 24	0		
			48	0.0073		
<b>10</b>	<b>0.0097</b>	0.0098	<b>73</b>	<b>0.0097</b>	<b>3</b>	<b>0.0084</b>
			143	0.0122		
			169	0.0147		
<b>20</b>	<b>0.0165</b>	0.0219			<b>5</b>	<b>0.0165</b>
<b>30</b>	<b>0.0169</b>		<b>193</b>	<b>0.0169</b>		
<b>40</b>	0.0173	<b>0.0316</b>				
60	0.0197	0.0341				
80	0.0231	0.0388				
100	0.0278	0.0437				
			<b>227</b>	<b>0.0316</b>		

### 3.1.1 CONCLUSIONS

The FTIR data indicate that multiple PAV aging introduced polar carboxylic acid oxygen species. The concentration of acid groups increased with the aging time. It was higher when the aging operation was carried out in the presence of water. One reason might be that water had a solvation effect on samples during PAV and more available sites were oxidized. As only the dry

PAV's spectra showed aldehydes and ketones present, and no sign in wet PAV results, we might believe that water accelerated the formation of the final product, carboxylic acids. The water may have had a surfactant contribution in carboxylic acids formation. In the dry aging condition, besides carboxylic, other carbonyl groups are formed. The water may have allowed for further oxidation of the aldehydes and ketones by solvation or by hydrate formation. More tests besides FTIR are needed in order to understand the influence of water in oxidation aging.

The field samples indicate an increase in concentration of carboxylic acids with age. Compared to laboratory simulations there is a difference in the field FTIR spectra due to the presence of cyclic esters and anhydrides. Ring formation can take place if functional groups in the same molecule react intramolecular (a hydroxyl acid will form a lactone). The peaks for cyclic esters were observed for 3 and 5-year-old field aged asphalt (core samples). These samples were not in contact with much water but they were in contact with many aggregates. Aggregates can be charged and also carry metal ions. It is possible that positive charges are present around hydroxyl acids and form temporary chelates with a high probability of closing lactone ring. Anhydrides are products of intermolecular reaction between two carboxylic acids groups.

The field data was correlated with laboratory findings. Dry PAV samples are more similar to field samples which were extracted deeper in the surface layer and where, in this case, water didn't have the chance to penetrate. The 3-year-field aged asphalt has a concentration of carboxylic acids less than 10 hours aged PMAC under dry or wet PAV conditions while the 5-year-old asphalt from the field samples shows a very good correlation to 20 hours dry PAV aged PMAC. Generation of acid carboxylic groups may improve the adhesion to aggregates from asphalt pavement. At the same time, the acid polar groups could lead to aggregation of asphaltene components from the base AC.

Dry PAV is a static procedure and a skin formation was noticed. The inner steel mixing rod in the RCAT continuously refreshed the asphalt surface exposed to oxidative aging, so this is not an “ad literam” comparison. RCAT aging was applied in order to better understand the oxidation kinetics and was a useful tool to follow the evolution of carboxylic acids during aging in the 0 to 20 hours PAV range. There is no linear correlation between RCAT-aged samples and PAV-aged samples (Figure 3.1-9). The very first 24 hours RCAT samples didn’t show any oxidation in FTIR spectra (a possibly erroneous results), and for verification the acids concentration can be measured using non-aqueous potentiometric titration.

### **3.2 NON-AQUEOUS POTENTIOMETRIC TITRATION**

Infrared analysis measures an important number of functional groups in asphalt, especially those produced in oxidation. However, the FTIR did not adequately quantify low carboxyl group concentrations (i.e. within 24 hours RCAT aging). One method that can be used for direct quantification of all acids in asphalt is non-aqueous potentiometric titration (PT), which was developed <sup>17</sup> for asphalt analysis based on the work of Dutta, Holland <sup>27</sup> and Buell<sup>7</sup>. Peterson et al describe the method in detail. <sup>7</sup>

Potentiometric methods are based on the difference in potential between 2 electrodes in an electrochemical cell. One of these electrodes is the indicator electrode and the other a reference. In a properly designed system both the reference potential and the liquid junction potential are constant so the indicator potential gives information on the activity of the species in the solution. Indicator electrodes should be chosen to interact with the analyte in question so that the potential measured is directly related to the activity of the species in solution. The most essential component of a pH electrode is a special, sensitive glass membrane that permits the passage of



hydrogen ions, but no other ionic species. When the electrode is immersed in a test solution containing hydrogen ions the external ions diffuse through the membrane until equilibrium is reached between the external and internal concentrations. Thus there is a buildup of charge on the inside of the membrane, which is proportional to the number of hydrogen ions in the external solution. The most common, and simplest, reference system for non-aqueous potentiometric titration is the silver / silver chloride single junction reference electrode.

Potentiometry is generally valuable as a technique for detecting the end-point of titrations, which usually is very close to the equivalence point. The equivalence point (stoichiometric point) occurs when the amount of titrant is equivalent, or equal, to the amount of analyte present in the sample. In some cases there are multiple equivalence points which are multiples of the first equivalent point, such as in the titration of a di- or tri-protic acid. A graph of the titration curve exhibits an inflection point at the equivalence point. The end point is identified by the first derivative  $dE/dV$  peak.

In this work the base and solvents were chosen to be compatible with the potentiometric titration principle and with asphalts. Very often, in organic acid titration, tetrabutylammonium hydroxide, a strong organic base, is used because it is soluble in water, alcohols and organic solvents. The solvent systems were chosen so that components of the asphalt would not precipitate during titration. Asphalts are not soluble in water; therefore, a much less polar solvent must be used. These solvents have a lower dielectric constant than water with the consequence of an end point, which is less sharply defined. Based on previous work done in asphalt titration<sup>27</sup>, this base was our choice to be dissolved in a mixture of toluene, which a good solvent for asphalt and base, and isopropanol, which usually permits the observation of stoichiometric curves when used in titration. For asphalt samples the solvent mixture used was chlorobenzene and ethanol. Chlorobenzene is a good solvent for asphalt and the base and might

not disrupt asphaltene associations. Ethanol is less polar than water, and is miscible with most organic liquids including non-polar liquids such as aliphatic hydrocarbons. To make sure that the end point was accurately read, the results were verified by adding benzoic acid (1% and 2% wt.) to the samples and the end point was based upon the incremental change observed. Based on calibration data presented in Chapter 2, acid concentrations were calculated for PMAC dry PAV samples and compared with FTIR results (Figure 3.2-1 and Table 3.2-1). The acid concentrations from PT results were different than FTIR. The measurements revealed that the PMAC sample contained stronger acids, moderate weak carboxylic acids and weak acids (Figure 3.2-2). If the concentration was computed for carboxylic acids only the data indicates that concentrations of carboxylic acids do correlate with our FTIR data as presented in Table 3.2-2 and Figure 3.2-3. Analysis of field samples by potentiometric titration indicated higher acid concentrations than observed by FTIR (Figure 3.2-4 and Table 3.2-3) because of the strong acids presence. A summary of the carboxylic acids concentrations (meq/g) obtained from various samples by running FTIR and potentiometric titration is presented in Table 3.2-4.

Potentiometric titration of oxidative aged PMAC showed that aging caused a significant buildup of acidic species. Inspection of titration curves showed the presence of strong acids, moderate weak corresponding to carboxylic acids and weak which may be phenols. Earlier studies showed that sulfur compounds were present at negligible concentrations in the asphalts, such as thiols, sulfones and sulfonic acids, as well as sulfoxides, sulfides and thiophenes.<sup>35</sup> The potential values observed for sulfonic acids present in asphalt range from +300 to +200 mV that was well above the range for carboxylic acids (-50 to -150 mV).<sup>35</sup> Our titration curves showed the presence of strong acids and positive values for potential only for the PMAC sample present commonalty (Figure 3.2-5). For base asphalts used to prepare the PMAC sample, PG 64-22 and PEN 150, the presence of strong acids was not detected (Figure 3.2-6).

**Table 3.2-1 Concentration values for PMAC multiple dry PAV samples**

Hours dry PAV	Potentiometric titration meq/g	FTIR meq/g
0	1.28e-4	0
20	0.02694	0.01656
40	0.02754	0.01732
60	0.03956	0.01979
80	0.03992	0.02302
100	0.05581	0.02782

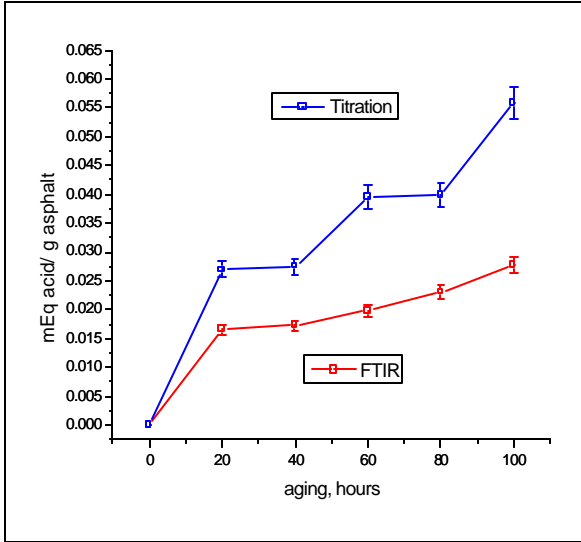


**Figure 3.2-1 Concentrations values from Potentiometric Titration and FTIR for PMAC samples**

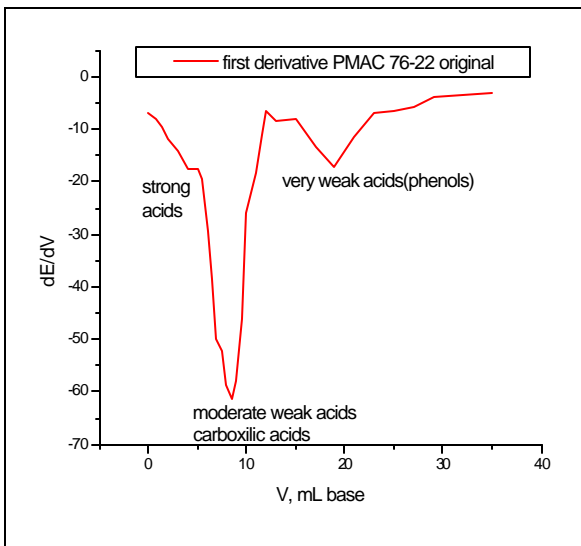


**Figure 3.2-2 First derivative of titration curve for PMAC original**

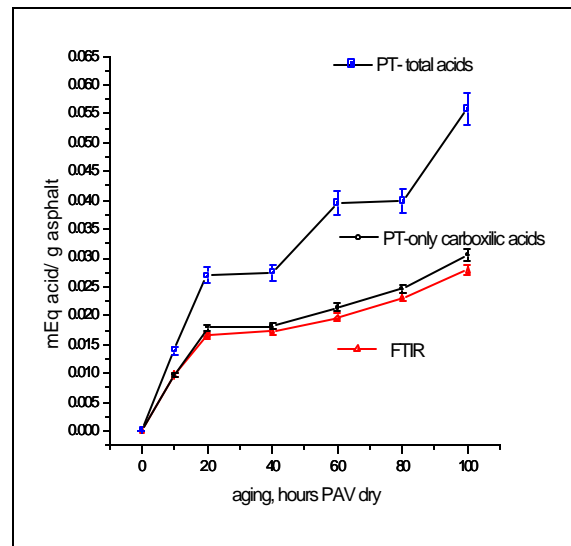


**Figure 3.2-3 Carboxylic acid concentration computed from titration data**

**Table 3.2-2 Carboxylic acids concentrations from FTIR and potentiometric titration experiments**

Hours PAV	Potentiometric titration (total meq/g)	FTIR meq/g	Potentiometric titration carboxylic acid
0	1.28e-4	0	0.8 e-4
20	0.02694	0.01656	0.0180
40	0.02754	0.01732	0.0182
60	0.03956	0.01979	0.0214
80	0.03992	0.02302	0.0247
100	0.05581	0.02782	0.0305

**Table 3.2-3 Acid concentration meq/g field samples from PT and FTIR**

Years in service	Potentiometric titration total meq/g	FTIR meq/g
3	0.013445	0.008460
5	0.025998	0.016567
7	0.039112	0.023020

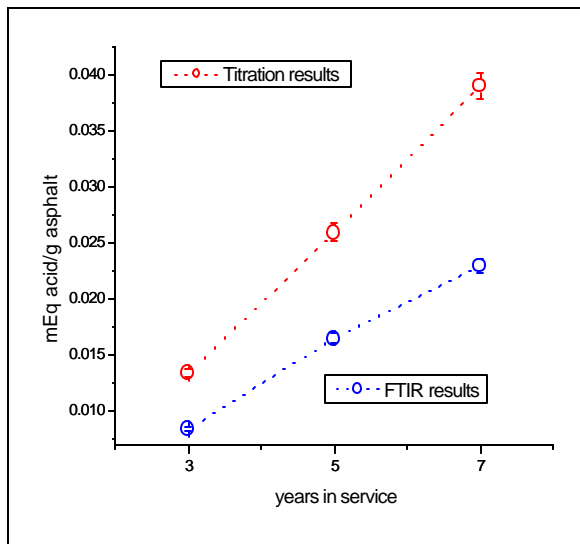


**Figure 3.2-4 Field samples- comparison potentiometric titration and FTIR**

**Table 3.2-4 Summaries of carboxylic acid concentrations, meq acid/g PMAC**

Hours	FTIR	FTIR	Titration	Years	FTIR	Titration
PAV	dry	wet	dry	Field		total
	mEq/g	mEq/g	mEq/g		mEq/g	mEq/g
0	0	0	0.00008			
10	0.0097	0.0098	0.0097	3	0.0084	0.0134
20	0.0165	0.0219	0.0180	5	0.0165	0.0259
30	0.0169					
40	0.0173	0.0316	0.0182			
60	0.0197	0.0341	0.0214			
80	0.0231	0.0388	0.0247	7	0.0231	0.0391
100	0.0278	0.0437	0.0305			

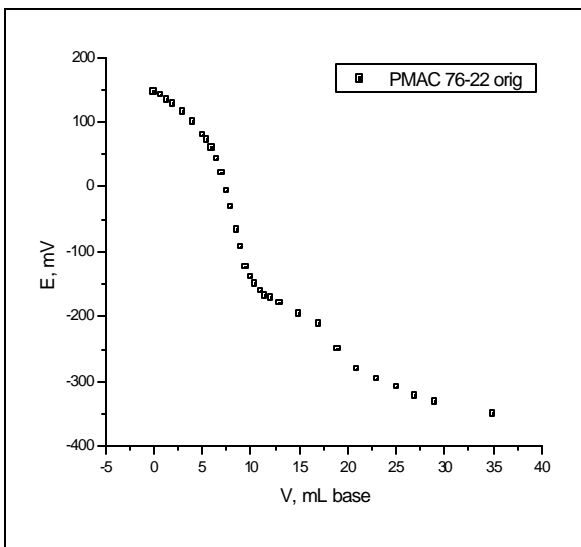


**Figure 3.2-5 Titration curve PMAC original**

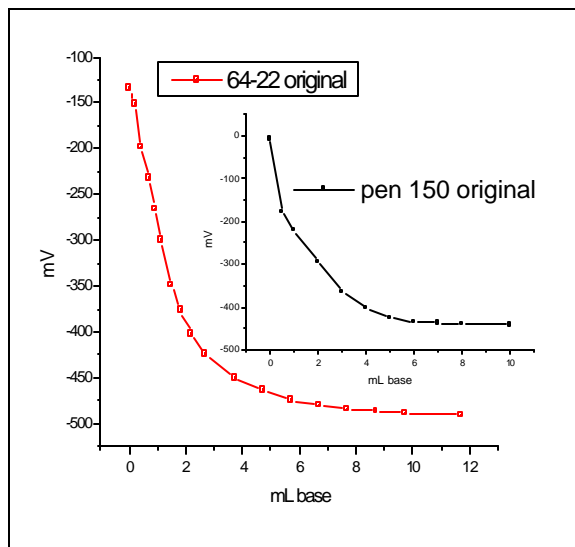


**Figure 3.2-6 Titration curve PG 64-22 and PEN 150 originals**

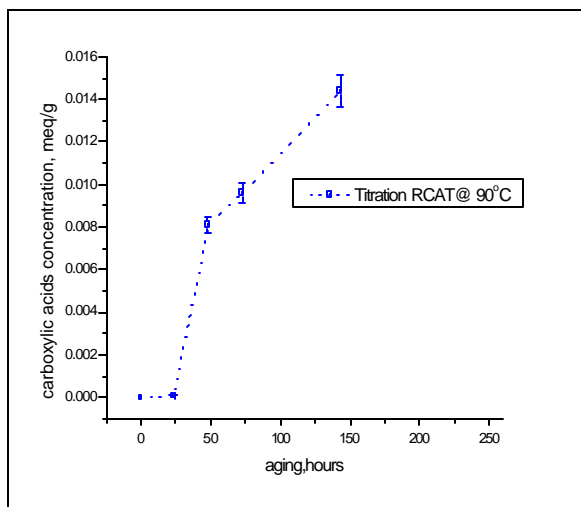


**Figure 3.2-7 Acids concentration PMAC after RCAT@90°C**

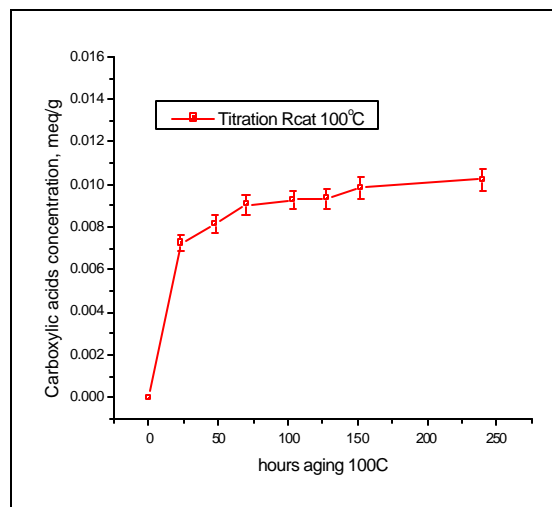


**Figure 3.2-8 Acids concentration PMAC after RCAT@100°C**

Sulfur is added during the polymer blending process to increase storage properties and polymer compatibility with asphalts. This process (vulcanization) creates disulfide bridges which, by oxidation in the presence of metal ions, can form sulfinic acids salts which initial can oxidize to sulfonic acids (very strong acids). The potentiometric titration experiment was run on RCAT samples as well for samples aged at 90°C, but also for the second sets of samples aged at 100°C (Figures 3.2-7 and 3.2-8). There were differences in carboxylic acid concentrations between samples aged at 90°C and 100°C for the first 48 hours (higher values for 100°C). PMAC showed an increased thermal oxidative susceptibility in this period of time. Between 48 and 73 hours, no noticeable differences were seen. After 73 hours, overheating compromised the first set of samples and it is not possible to make a comparison. The 3-year-old field aged asphalt exhibited a very close correlation to the 48-hour RCAT and it might be concluded that these materials just finished the accelerated stage of oxidation. To reach the level for 5-year-old asphalts it appears necessary to run more than 240 hour RCAT at 100°C (Table 3.2-5). This suggests that, in the field, carboxylic acid formation initially was influenced by the presence of aggregates (higher concentration of metal ions).

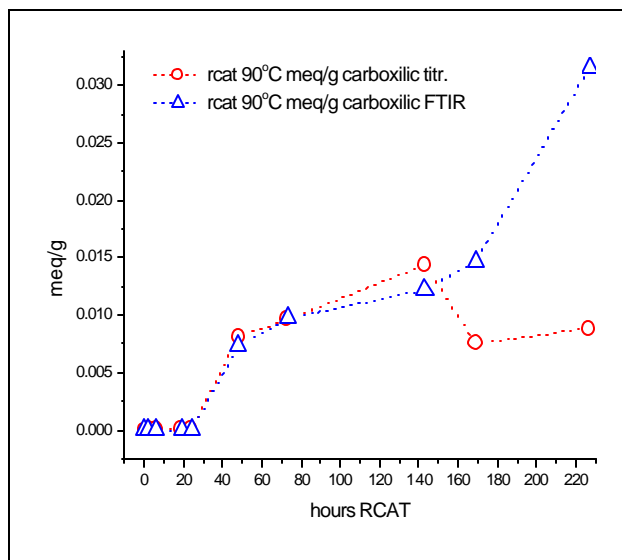


**Figure 3.2-9 Comparison of carboxylic acid concentrations both FTIR and PT measurements of RCAT-aged PMAC samples.**

**Table 3.2-5 Data collection for carboxylic acid concentrations**

Hours RCAT @100°C	Titration carboxylic acids conc., meq/g	Hours RCAT @90°C	Titration carboxylic acids conc., meq/g	hours dry PAV	Titration carboxylic acids conc., meq/g	Years Field	FTIR carboxylic acids conc., meq/g
0	0.00008	0	0.0000800	0	0.8 e-4		
23	0.00725	2	0.0000919	20	<b>0.0180</b>		
48	<b>0.00814</b>	6	0.0000875	40	0.0182	3	<b>0.0084</b>
70	<b>0.00906</b>	19	0.0000919	60	0.0214	5	0.0165
104	0.00927	24	0.0000900	60	0.0247		
128	0.00936	48	<b>0.0081100</b>	100	0.0305		
152	0.00982	73	<b>0.0096000</b>				
240	<b>0.01023</b>	143	<b>0.0143800</b>				
		169	0.0075000				
		227	0.0088700				

### 3.2.1 CONCLUSIONS

The potentiometric titration technique was used to measure the moderately strong and strong acids in unaged and oxidized asphalts. The method allowed for the quantification of the oxidation progress.

Comparison of the data with that obtained using FTIR yielded a satisfactory correlation. The technique was used to analyze RCAT samples to follow the initial oxidation kinetics. It was observed that carboxylic acid formation occurs primarily in the first 70 hours of aging under RCAT conditions.

Titration revealed the presence of strong acids which occurred due to oxidation of sulfur links. No strong acids were detected in neat or aged base asphalt cements, only in the PMAC sample. Sulfur is present in all types of asphalt, but being in such a low percentage, is not involved in oxidation.

During polymer modified asphalt production, sulfur is added to improve the physical better properties. But sulfur has a high capacity to take up oxygen. Sulfur bridges are first involved in the oxidation process with the formation of strong acids before other sulfur sites.

An increase in acidity, mostly strong acids, might lead to a higher degree of oxidative aging. If water is present, then the chances of early oxidation of the asphalt increase and the binder has more chances not to perform as was designed. In addition, strong acids have a strong possibility of reacting with basic aggregates, which may lead to a higher probability of adhesion failure.

On the other hand, oxidative aging creates more polar carboxylic groups that can improve asphalt-aggregates bonding.

Potentiometric titration is an easy and inexpensive method and can be readily adapted to automation, where automated titration systems can process larger volumes of samples with minimal analyst involvement.



### 3.3 GEL PERMEATION CHROMATOGRAPHY

During oxidative aging, polar and aromatic molecules interact through attractive forces to form molecular associations resulting in significant changes in the physical properties of asphalts. One consequence is that these associations have effective molecular weights and hydrodynamic volumes larger than the true molecular weights of their components. Therefore, a separation should be possible by techniques that separate mixtures into fractions of different molecular size. The most common technique is gel permeation chromatography (GPC) and there are many reports of earlier asphalt separation by this method.<sup>7</sup> Gel permeation chromatography is also a fast and reliable method to determine the polymer content in asphalt. Since polymer molecules typically weigh 10 times more than asphalt molecules, they can be easily identified using this method. Gel permeation chromatography is a form of size-exclusion chromatography. The smallest molecules pass through bead pores, resulting in a relatively long flow path while the largest molecules flow around beads, resulting in a relatively short flow path. The chromatogram shows detector response (DRI) versus time or elution volume ( $V_e$ ) with the largest molecules appearing first on the chromatogram. The organic solvent used should disturb the associations as little as possible and have a relatively low-boiling point. For our studies tetrahydrofuran (THF) was the choice. Using the calibration curve presented in chapter 2 the results from GPC were correlated with the macromolecular weights of the compounds. It was expected that, during oxidative aging, the polymer molecules from PMAC would be linked through stable chemical bonds, e.g., covalently bonded, crosslinked “aggregates” which are not soluble in THF. It is also possible that some highly aggregated asphaltenes are insoluble in THF.

Insoluble species and gels were precluded from entering the columns through filtration through a short guard column.<sup>18</sup>

The GPC studies presented in this chapter concern the water effect on laboratory oxidative aging of asphalt, the impact on the polymer only, on asphalt cements and on PMAC. The results from dry and wet PAV samples were compared with field-aged asphalts. As our interest was to have a closer look at what happens from the first moment of oxidative aging, RCAT samples were tested and compared with field results.

For a better view of changes taking place during oxidative aging of asphalts and analyzed by GPC, the regions of a GPC curve were defined in this work as: high molecular weight polymer species– HMW - region (polymer site) between elution volumes 16 to 20 mL correspondent to an proxy molecular weight range of 650 to 50 K; medium molecular weight polymer and asphalt cement species (asphaltenes size) –MMW- between 20 to 26 mL for 50 to 3 K molecular weight size compounds; and 26 to 31 mL elution volume for low molecular weight– LMW – asphalt components with a molecular weight of 3 to 0.4 K (Figure 3.3-1)

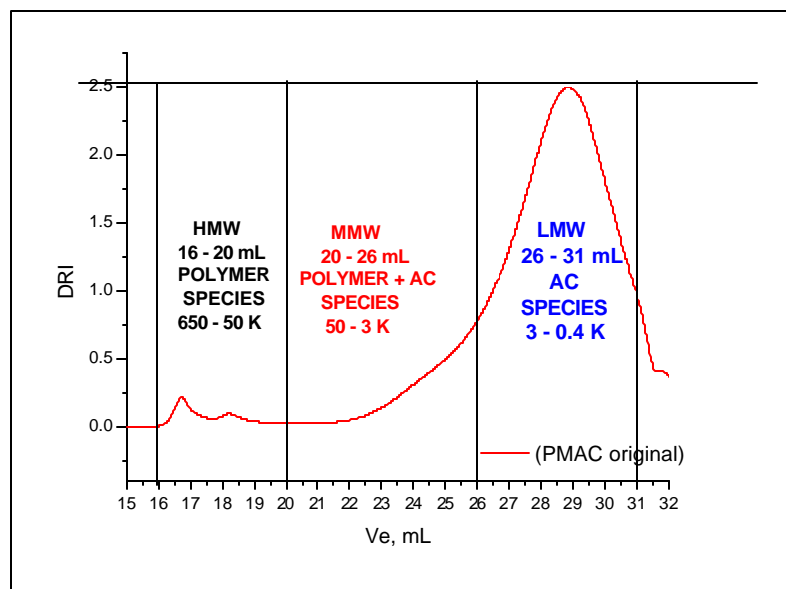


**Figure 3.3-1 Regions for a generally asphalt GPC curve, with correspondent in molecular weight values, based on calibration curve.**

For each of three regions a relative change of integrated area (increment and/or diminish) during oxidative aging was computed. The reference was the integrated area under the GPC curve for the original material. The integrate areas for the rest of aged samples were divided by the original value and presented graphically. An increment for the peaks in a certain region was observed when the values for relative changes were bigger than 1, respectively when there was less than 1 a decrease for the peaks observed. Areas under the GPC curve are an expression of compounds concentration. The dynamics of relative changes computation provide information about oxidative aging of asphalts. The first overview is for neat materials (Figure 3.3-2). Samples with only Calprene polymer dissolved in THF were analyzed to see the changes in the polymer during oxidation. The peak for HMW polymer (~ 650 K) was expected to have higher DRI magnitude than PMAC samples which contain only up to 3% polymer in asphalt.

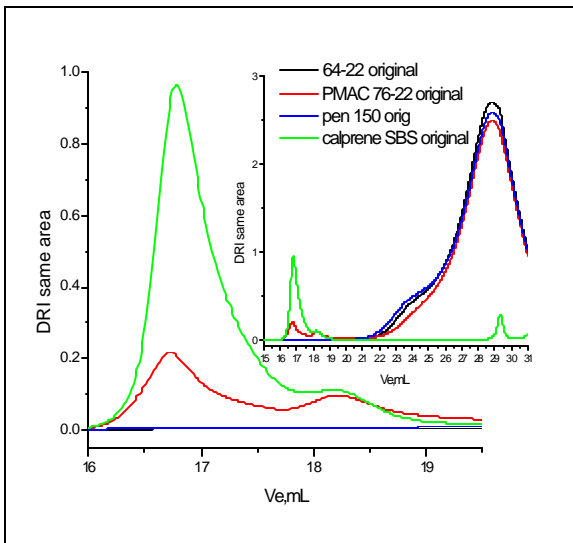


**Figure 3.3-2 GPC traces for the original materials.**

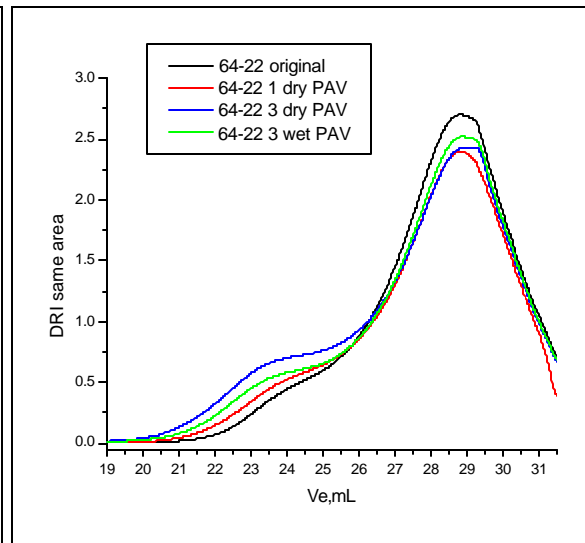


**Figure 3.3-3 GPC traces for 64-22, original and PAV aged in dry and wet conditions.**

Original base asphalts, PG 64-22 and PEN 150, which didn't have any polymer added, exhibited only slight differences in the MMW region (50 to 3K) during repeated PAV aging cycles (Figures 3.3-3 and 3.3-6). Looking for extreme changes in molecular weight distribution

the samples exposed for 3 cycles wet PAV were used for comparison. PG 64-22 exhibited an increase in asphaltenes area after multiple aging cycles (~ 65% more than original), but after aging in humid conditions the asphaltenes aggregation was less compared to dry PAV aged samples (~ 30 % more). The LMW peaks decreased with ~15% than original in dry PAV oxidative aging and only ~ 10% in humid conditions (Figure 3.3-4). This data shows us that it is diffusion inside of the arbitrary regions chosen.

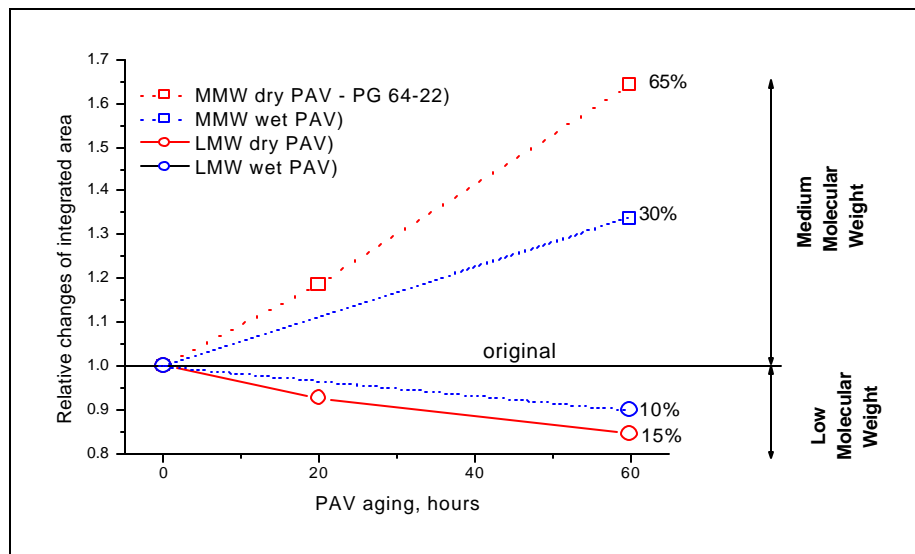


**Figure 3.3-4 Dynamics of relative changes of integrated area for 64-22 during dry and wet PAV operations**

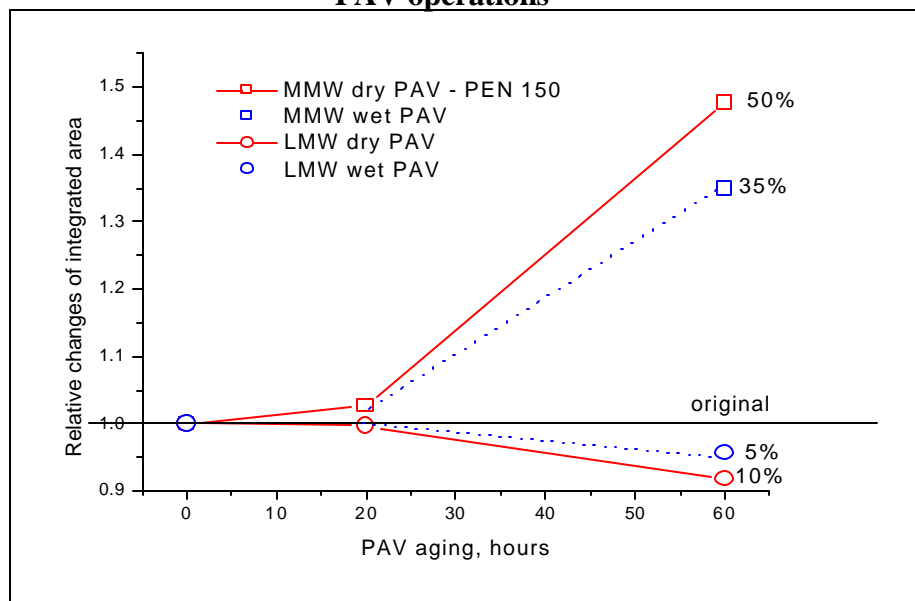


**Figure 3.3-5 Dynamics of relative changes of integrated area for PEN 150 during dry and wet PAV operations**

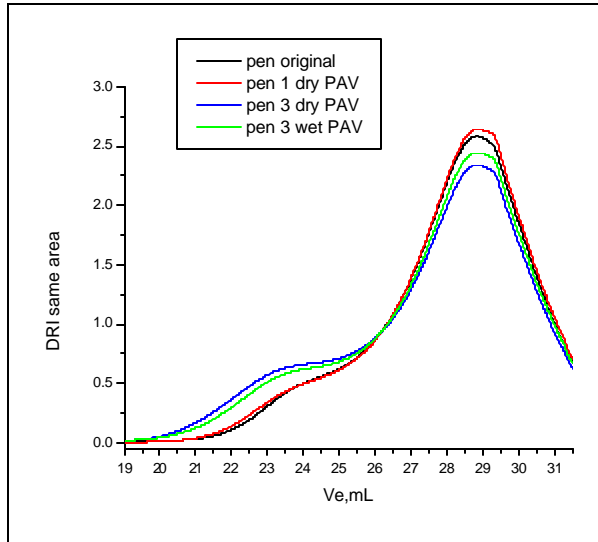


**Figure 3.3-6 GPC traces for PEN 150, original and PAV aged in dry and wet conditions.**

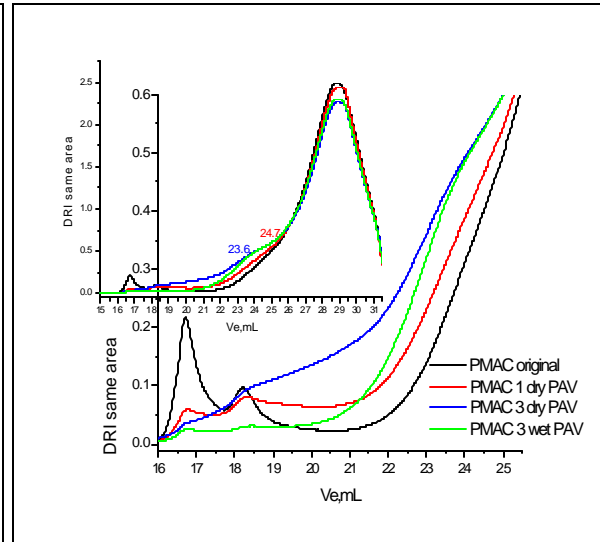


**Figure 3.3-7 GPC traces for PMAC, original and PAV aged in dry and wet conditions**

The increase in peaks for MMW came ~ 15% from LMW compounds aggregation and 40% from MMW asphaltenes association. Similarly for PEN 150 (Figure 3.3-5), wet PAV samples contained lower asphaltenes concentration (~35% more than original for wet conditions compared to ~45% in dry PAV cycles).

PMAC (Figure 3.2-7) aged in dry conditions exhibited an almost total degradation of high molecular weight polymer to the formation of low molecular weight polystyrene chains, which elute with the asphaltenes. The presence of water caused changes. The asphaltenes peak was lower and the polymer content appeared to be zero because of crosslinked molecules that are insoluble in THF.

After dry PAV oxidative aging, PMAC samples had an increment in MMW peaks of ~65% more than original samples, and around 10% is the contribution of LMW associations (Figure 3.3-8 and Table 3.3-1). The polymer contribution was approximately 5% to that increment as fragments from chain scission oxidative degradation were eluted in MMW region after 20 hours

dry PAV. The HMW region associated to the polymer site, after 20 hours PAV was ~20% lower in concentration than original and after 60 hours dry PAV was almost equal to the original.

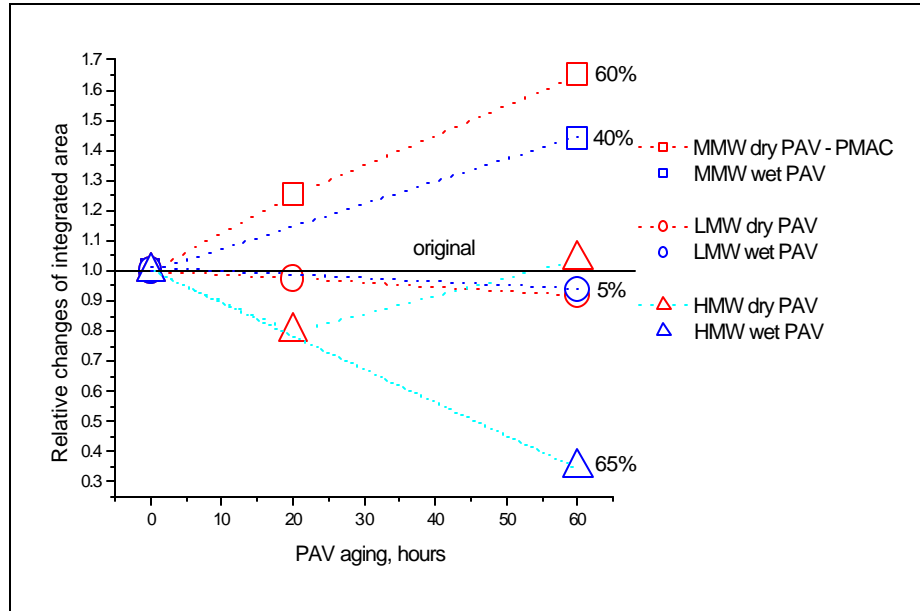


**Figure 3.3-8. Dynamics of relative changes of integrated area for PMAC during dry and wet PAV operations**

**Table 3.3-1 Integrated area values for asphalt binders after dry and wet PAV operations**

Asphalt	Integrated Area MMW 3 dry PAV	Area MMW 3 wet PAV	Area LMW 3 dry PAV	Area LMW 3 wet PAV	Area HMW 3 dry PAV	Area HMW 3 wet PAV
PG 64-22	2.9	2.3	8.3	8.9		
PEN 150	2.9	2.6	8.3	8.6		
PMAC	2.5	2.2	8.4	8.9	0.3	0.1

One reason is that extreme oxidation for 3 PAV cycles transformed the entire quantity of polymer in MMW species soluble in THF (around 30-20 K). As with the case of the wet PAV the MMW is decreasing, it can be concluded that in the presence of water polymer crosslinking effect was favorite with formation of a stable insoluble gel.

PMAC exhibited less oxidation effects in LMW region (3-0.4K) than PG 64-22 because of the presence of polymers. The dynamics under the MMW region was the same for PMAC and 64-22 (PMAC contains 85% 64-22 in composition). From compared GPC traces (Figures 3.3-9 and 3.3-10) for PMAC (asphalt blend with polymer) and PG 64-22 (asphalt without polymer) the region highly affected by oxidative aging was HMW polymer species for PMAC aged in humid conditions. There were no noticeable changes in concentrations of LMW species; a higher association of asphaltenes in MMW can be observed when the polymer additive was missing.

The polymer, by itself, was subjected to wet and dry PAV cycles using two different solvents: decaline (Figure 3.3-12) and DCM (Figure 3.3-13). During the high temperature TFOT process DCM was totally removed but this was not the case with decaline, which didn't evaporate, thus the polymer was in a decaline solution even after completion of PAV cycles. When decaline was used as solvent 1 cycle PAV aging in humid condition reduced the molecular weight for the polymer to ~70K and the second PAV cycles reduced Mw to ~ 20K. When DCM was used as solvent the molecular weight of the polymer was reduced after only one PAV cycle (dry or wet conditions) to ~20K. The water present in the PAV aging process increased carboxylic acid concentrations, so the polarity increased, and this might be connected with higher solvation for polymer decomposition products. It appears that water helped to slow down polymer chain scission. HMW soluble polymer chains with very low concentration can still be seen. (Figure 3.3-9 and 3.3-10). In the presence of decaline the humid aged PAV for 20 hours yielded compounds with four times more MMW species compared to the original solution (Figure 3.3-16). When the polymer was exposed for 20 hours in wet PAV conditions without solvent (after DCM evaporation, Figure 3.3-17) the chains length with MMW were 30 times more than the original. In all the samples analyzed by GPC, in humid PAV conditions, a higher autoxidation of polymer chains was observed.

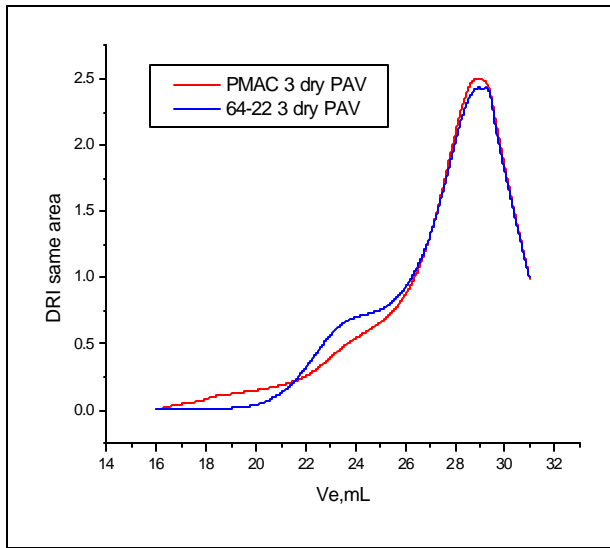


**Figure 3.3-9 Comparison PMAC vs. 64-22 after 3 cycles Dry PAV**

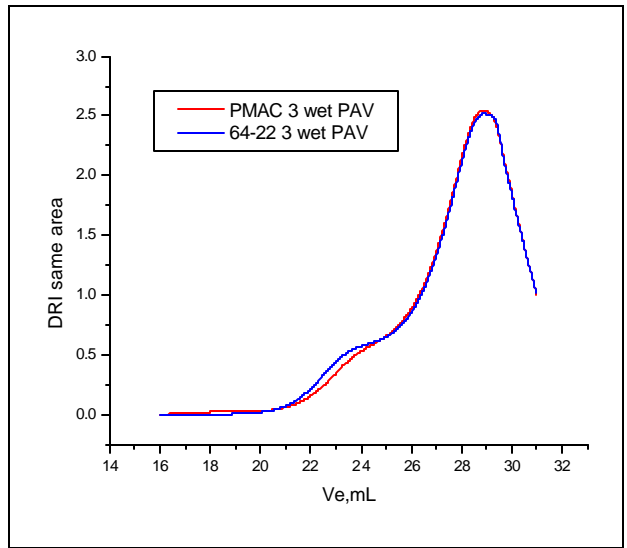


**Figure 3.3-10 Comparison PMAC vs. 64-22 after 3 cycles Wet PAV**

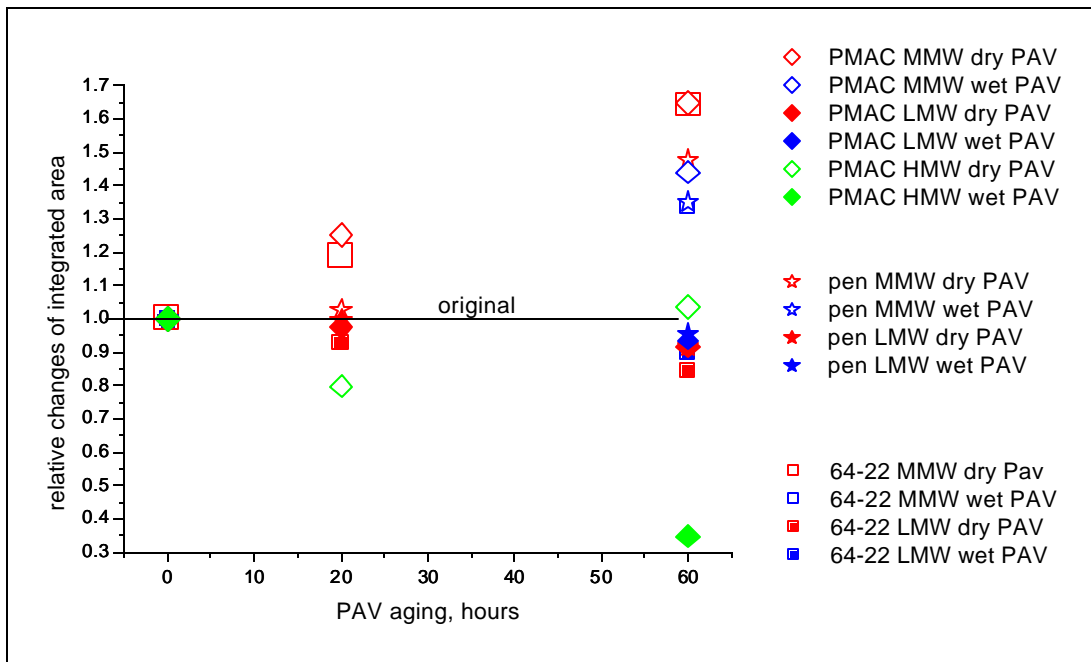


**Figure 3.3-11 Relative changes of integrated area for the asphalt binders analyzed by GPC**



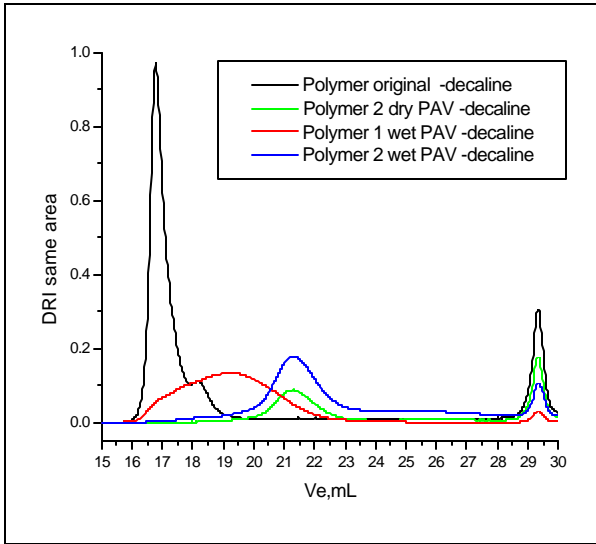


**Figure 3.3-12 GPC traces for the polymer/decaline aged in dry and wet PAV conditions**

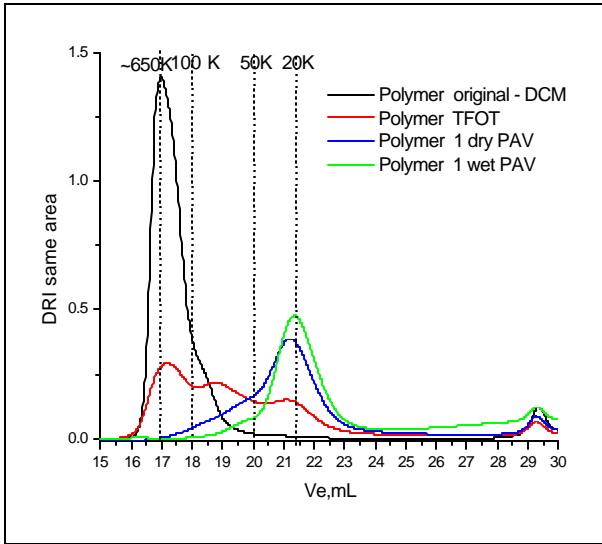


**Figure 3.3-13 GPC traces for the polymer/DCM aged in dry and wet PAV**

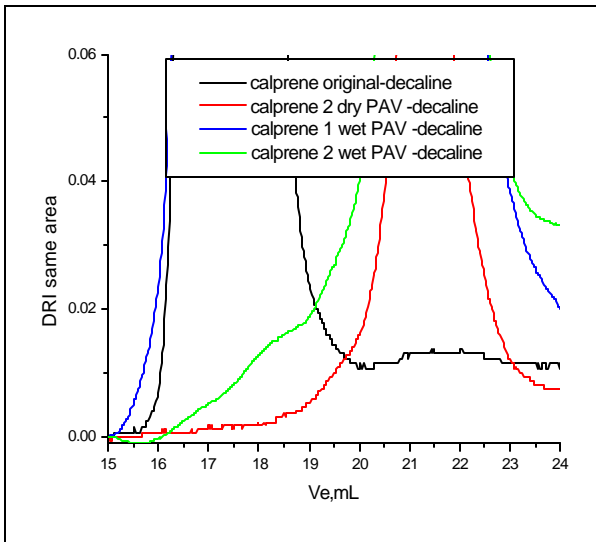


**Figure 3.3-14 GPC traces – details HMW polymer from Figure 3.3-12**

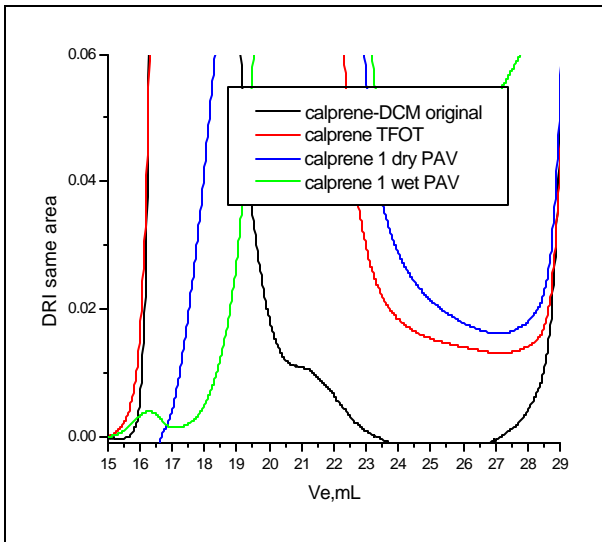


**Figure 3.3-15 GPC traces – details HMW polymer from Figure 3.3-13**

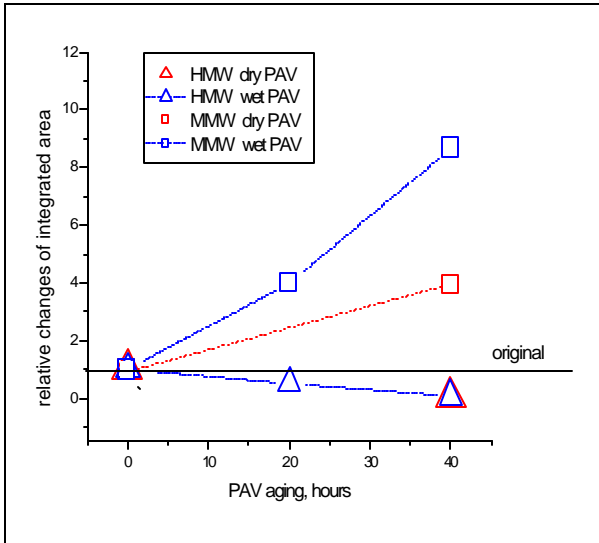


**Figure 3.3-16 Dynamics of relative changes of integrated area for polymer dissolved in decaline during dry and wet PAV operations**

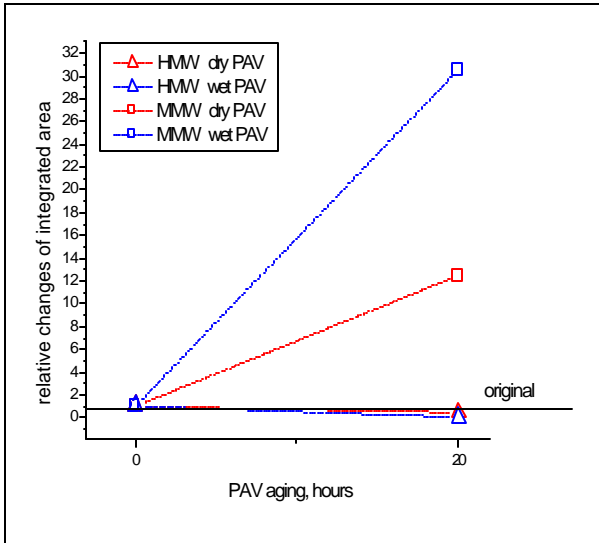


**Figure 3.3-17 Dynamics of relative changes of integrated area for polymer, after DCM volatilization, during dry and wet PAV operations**

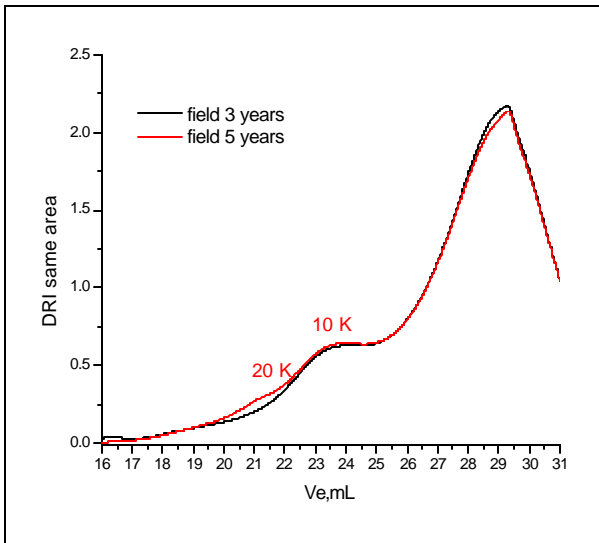


**Figure 3.3-18 GPC traces for asphalt binder extracted from field sample**

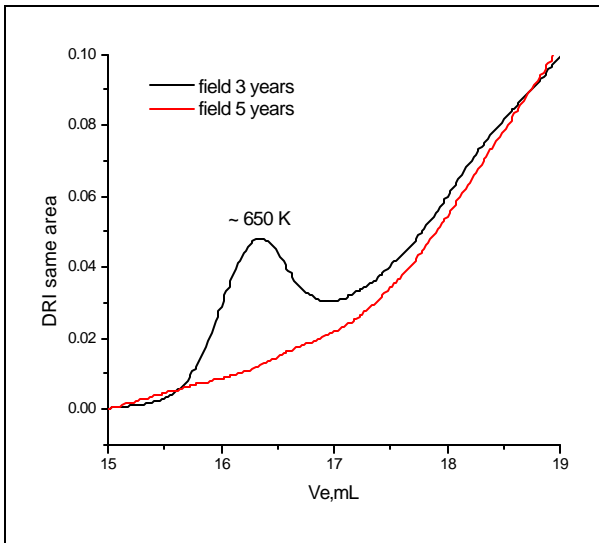


**Figure 3.3-19 GPC traces - details HMW from Figure 3.3-18**

**Table 3.3-2 Integrated area values for asphalt binders extracted from field samples**

Integrate area under GPC curves	HMW 650-50 K	MMW 50 – 3 K	LMW 3 – 0.4 K
3 years asphalt field aged	0.28	2.8	7.8
5 years asphalt field aged	0.26	2.9	7.6

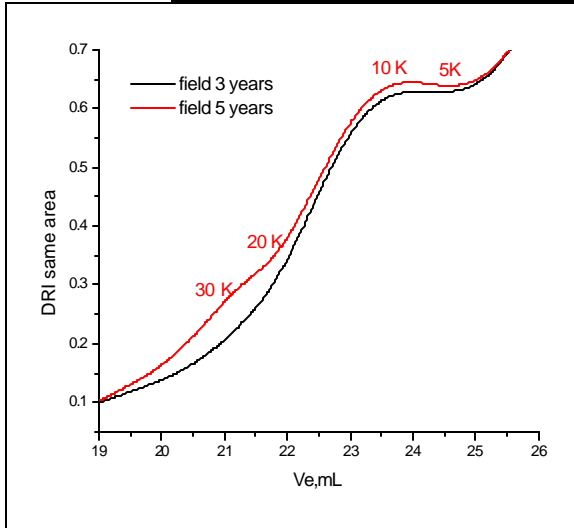


**Figure 3.3-20 GPC traces – details  
MMW from Figure 3.3-18**

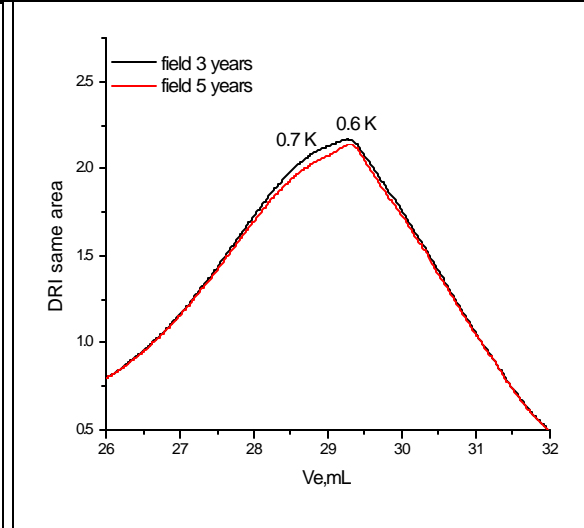


**Figure 3.3-21 GPC traces – details  
LMW from Figure 3.3-18**

GPC traces from Figures 3.3-18 to 3.3-19 show the oxidation progress in the field. It is easy to notice the polymer role in-field oxidation process (Figure 3.3-20). First the polymer cross-linked (3-year-old sample) with formation of soluble higher molecular weight species. After 3 years of service the polymer was still functional. The 5-year-old asphalt was in an advanced stage of polymer oxy-degradation (lower HMW polymer concentration than 3 dry PAV) and LMW polystyrene chains (30-20K) are “migrating” through asphaltene GPC site (Figure 3.3-21 and Table 3.3-2). There is not much of a difference between field samples. However, the asphaltene shoulder (MMW) of field samples is different from laboratory-aged asphalts. Inspecting all GPC curves, it was noticed that PG 64-22 and PEN 150 3 times PAV aged in dry conditions had the same magnitude for asphaltene as field samples but only PEN 150 3 times

aged in PAV wet condition had the same MMW “shape” as field samples (Figure 3.3-22). The “shape” shows the molecular distribution for species alone in the arbitrary slice chosen. The field samples, compared to laboratory samples, indicated a higher association of molecules with molecular weight of 5 K with a result of higher aggregation in the form of molecules with molecular weight of 10 K (Figure 3.3-23). A mixture between PG 64-22 and PEN 150 (Figure 3.3-24) was subjected to the same aging conditions. The shape for MMW (asphaltenes region) was similar to the field sample even though the polymer was missing. The samples were more similar in shape to the field samples when the asphalt mixture was aged in humid conditions.

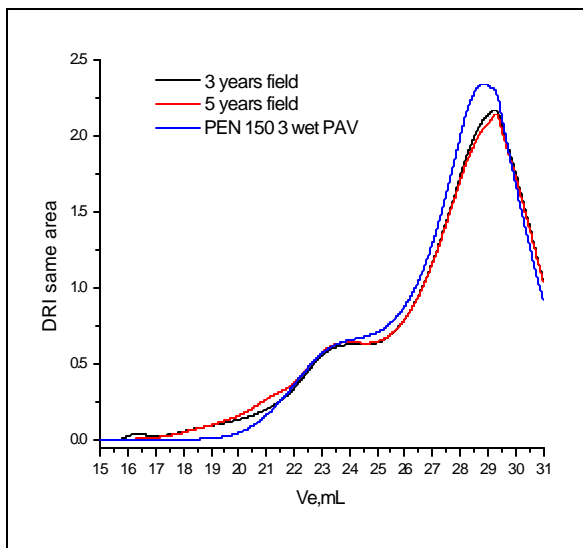


**Figure 3.3-22 GPC traces - comparison asphalt binder field aged to PEN 150 lab aged**

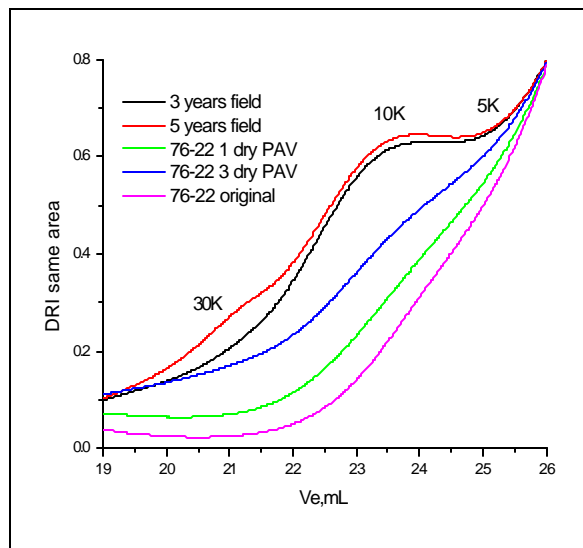


**Figure 3.3-23 GPC traces - comparison asphalt binder field aged to PMAC lab aged in dry PAV conditions**

The asphalt binder extracted for the 5-year-old field sample shown on GPC traces a peak for species with a molecular weight of ~30K (polystyrene chains) which was not observed in the traces for PMAC aged in the laboratory (Figures 3.3.23 and 3.3.25). A detailed view is presented in Figure 3.3.26 for the HMW polymer region in PMAC field aged and laboratory aged, and it appears that there is no match between samples.

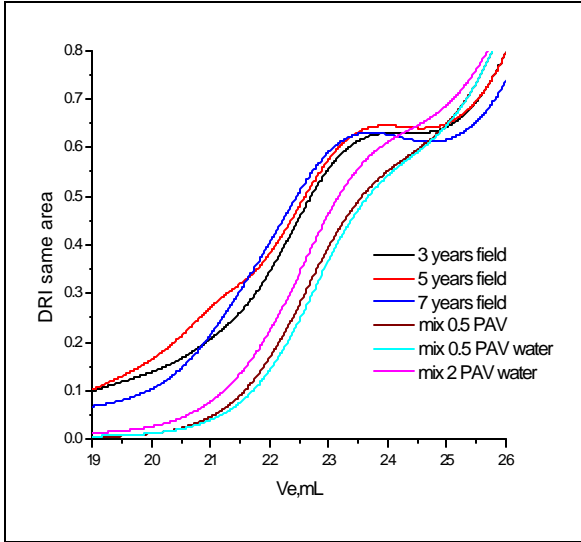


**Figure 3.3-24 GPC traces - comparison asphalt binder field aged to 64-22/PEN 150-mixture lab aged**

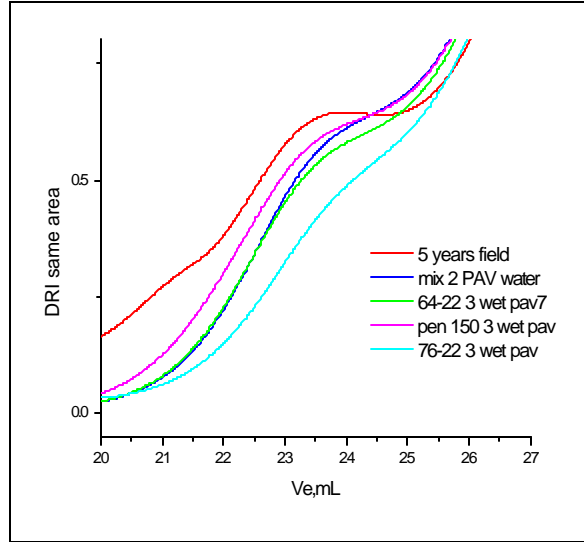


**Figure 3.3-25 GPC traces - comparison asphalt binder field aged to asphalts lab aged in wet PAV conditions**

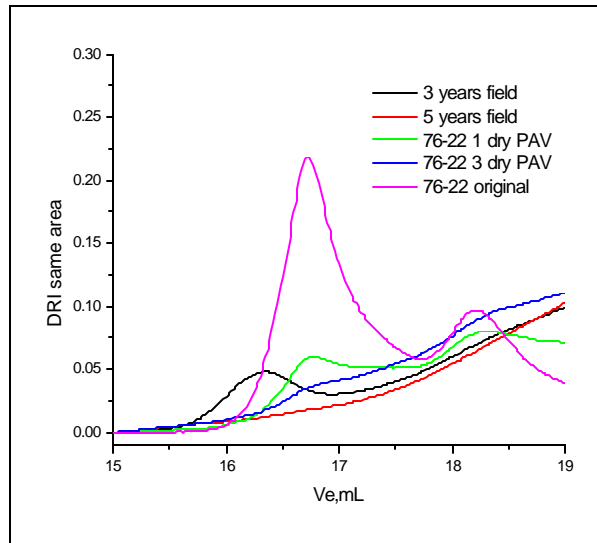


**Figure 3.3-26 GPC traces - comparison HMW polymer chains in asphalt binder field aged to HMW polymer chains in PMAC lab aged**

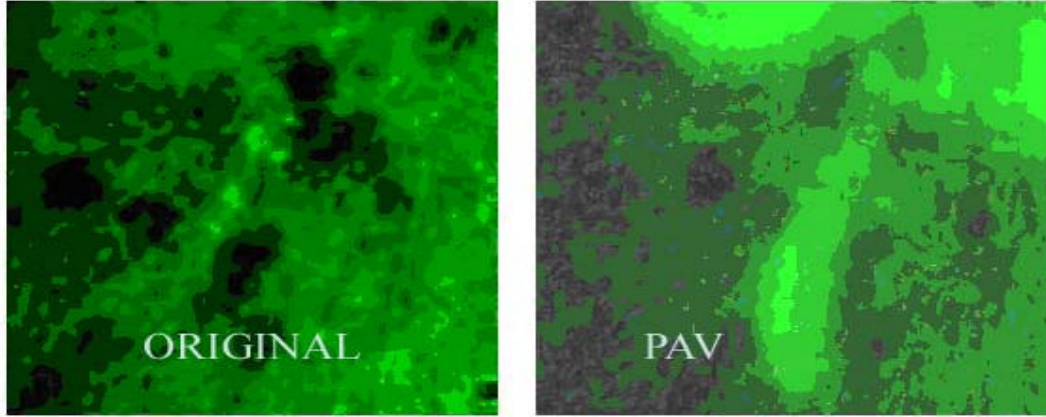


**Figure 3.3-27 Epifluorescence microscopy pictures**

Field aged asphalt binder showed the presence of polymer on GPC experiment, so an attempt to see the polymer phase was made. Epifluorescence microscopy was used to view the polymer asphalt blends (Figure 3.3-27). The asphalt is fluorescent and the polymer in the asphalt can be seen as dark globular like shapes. The polymer was clear and present and the phase separation between asphalt and polymer appears in the images, thus polymer remained in the binder cement even in the presence of aggregates.

Gel Permeation Chromatography RCAT 90°C. As a continuation of oxidation kinetic studies, the RCAT samples were analyzed by GPC.

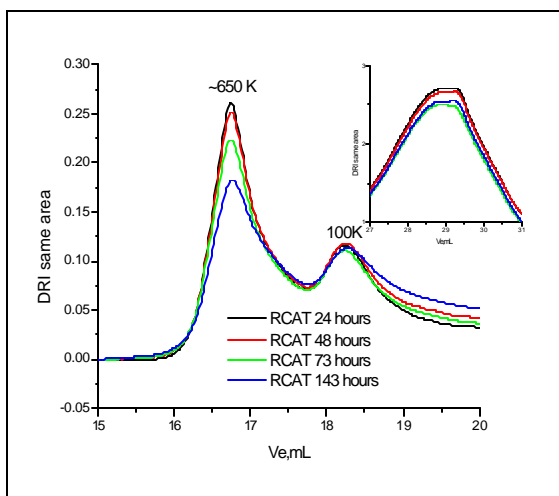


**Figure 3.3-28 GPC traces for PMAC RCAT aging conditions – changes in HMW polymer region**

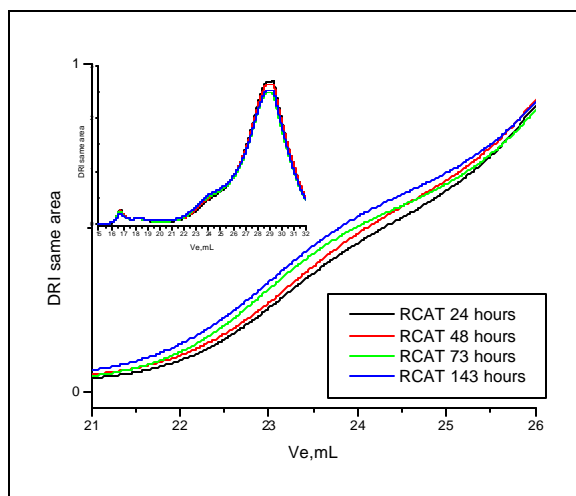


**Figure 3.3-29 GPC traces for PMAC RCAT aging conditions – changes in MMW polymer and AC region**

GPC traces for RCAT closely followed the polymer degradation, which increased with aging time (figure 3.3-28). The integrated area under the polymer peak (HMW) with a molecular weight around 650 K shows a decrease in concentration presented in Table 3.3-3 and Figure 3.3-30. It was observed that, after 70 hours, the oxidation process slowed down to a rate (integrated area under peak / hour aging) of four times slower than the beginning (table 3.3-3.). This result correlates with FTIR and PT results that showed the same accelerated carboxylic acids formation into 70 hours aging by RCAT. Compared with the original PMAC the polymer exhibited higher concentration for samples aged up to 48 hours and equal concentration for 73 hours (Figure 3.3-31 and 3.3-32). The polymer was more soluble than original PMAC, possibly because of the oxidation of disulfide crosslinks. It can be observed that the decrease of the HMW peak for the polymer (~650 K) is correlated to an increase in MMW region (30 -5 K) and no significant changes in the LMW (1-0.4K) site. This can sustain the conclusion that polymer oxidizes first and lower molecular weight polymer fragments elute in MMW range bringing an increase in the concentration of the species in that region (30 – 5K). The samples didn't yet reach the 3-year-old asphalt level of aging. Overall the GPC traces for RCAT samples are very useful to study early stages of aging for the PMAC.

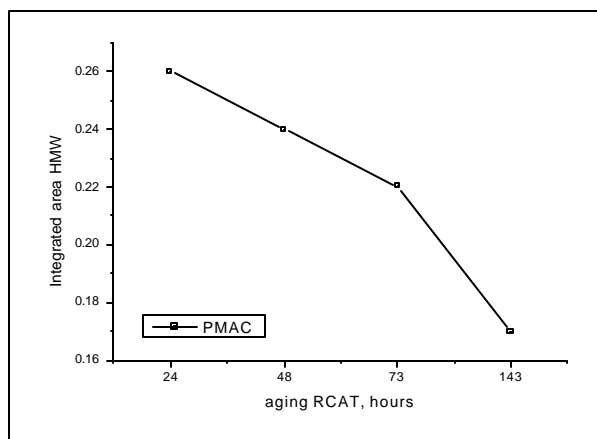


**Figure 3.3-30 Polymer content changes in PMAC subjected to RCAT aging conditions**

**Table 3.3-3 Integrated area of PMAC-RCAT aged for HMW polymer chains**

Aging exposure, hours 90°C	Integrated Area for ~ 650 K
24	0.26
48	0.24
73	0.22
143	0.17

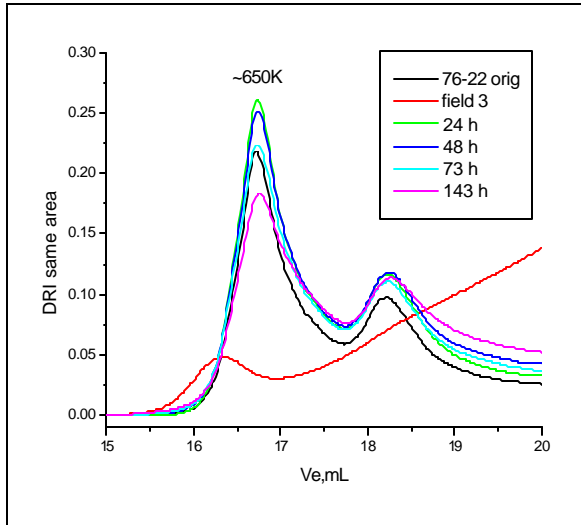


**Figure 3.3-31 GPC traces- comparisons PMAC original, PMAC aged under RCAT condition and PMAC aged 3 years in field – HMW region**

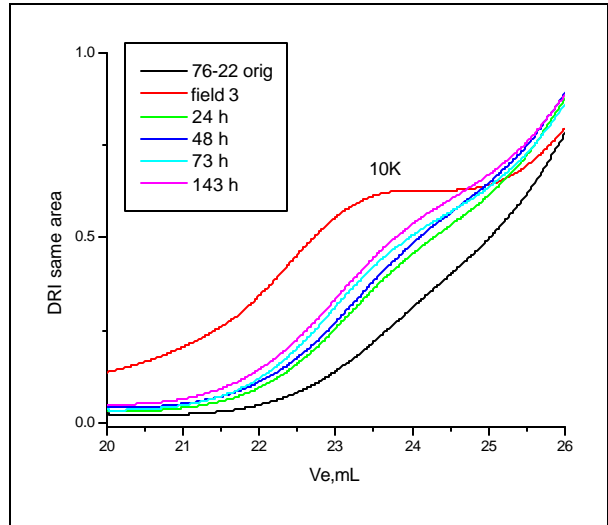


**Figure 3.3-32 GPC traces- comparisons PMAC original, PMAC aged under RCAT condition and PMAC aged 3 years in field – MMW region**

### 3.3.1 CONCLUSIONS

The changes in molecular weight distribution of the asphalt component were estimated using gel permeation chromatography (GPC). Laboratory aged samples were compared with field aged asphalt and the impact of water on the oxidative degradation was observed.

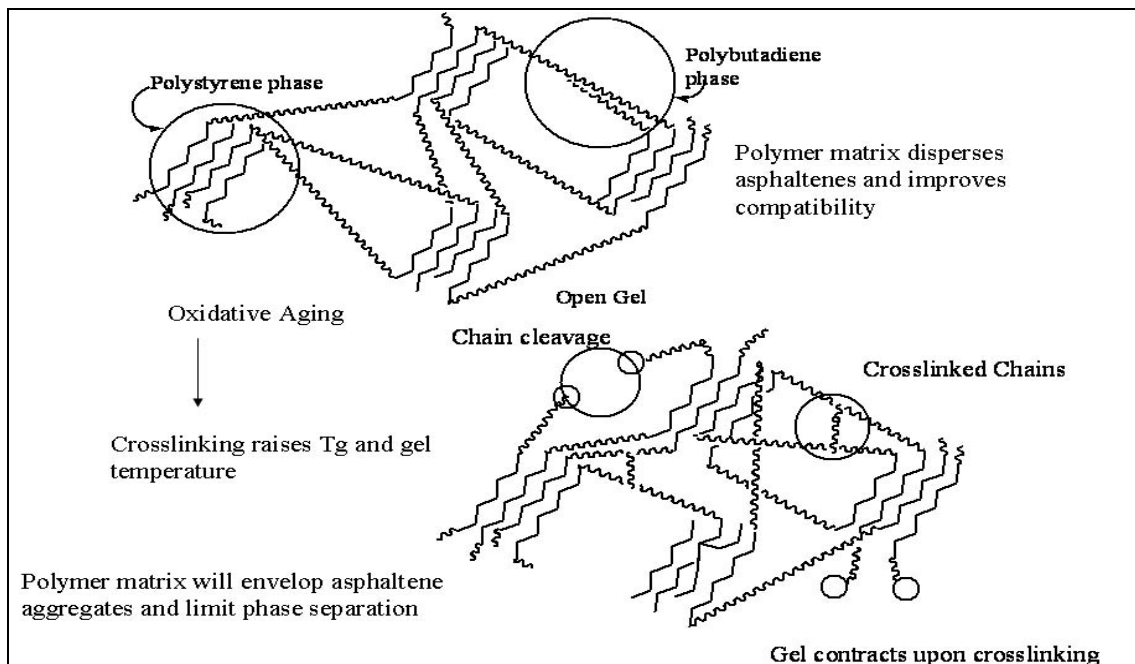


**Figure 3.3.1-1 Schematic oxidative aging representation of polymer additive <sup>36</sup>**



Generally, the aging in the presence of water had the following effects: less asphaltene association in the MMW region, less association for LMW asphalt species, and lower polymer concentration in the HMW region. In the wet aging processes for PMAC samples, there was no evidence of an increase in concentration for species with molecular weight 30-20 K as was observed for polymer samples. The water may terminate the chain propagation of free radical autoxidation of the polymer additive by crosslinking. Highly crosslinked insoluble polymer gels are not shown in GPC traces, but their influence is shown by more dispersed asphaltenes (Figure 3.3.1-1).

After dry PAV oxidative aging, PMAC samples had an increment in MMW peaks of ~65% more than the original samples showing less insoluble polymer species and higher asphaltene association compared to PMAC samples aged in the presence of water (Figure 3.3.1-2).

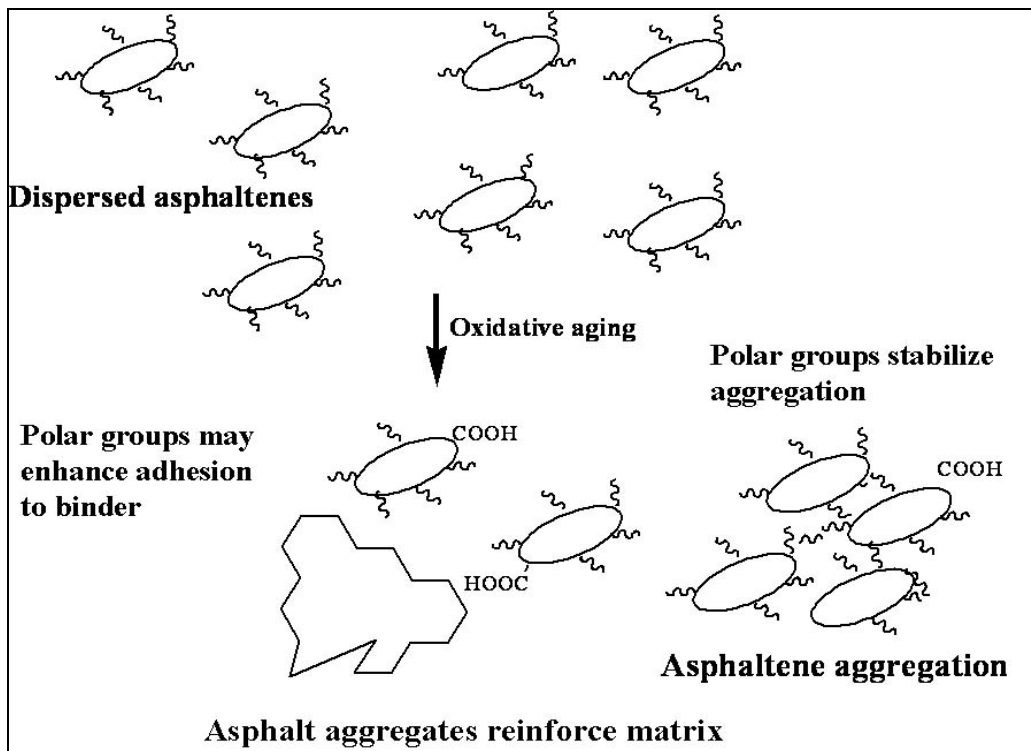


Figure 3.3.1-2 Schematic representation of asphaltenes association during oxidative aging <sup>3</sup>

The FTIR and potentiometric titration studies showed that, during aging, more polar carboxylic acid groups were produced. Increasing the polarity of the asphalt-aged blend had an effect in a higher stabilization of the asphaltenes in aggregation forms. GPC traces indicated that when polymer additive was present in asphalt blends this association was a diminution during aging, thus we know from FTIR measurements that the carboxylic acids concentration will increase with aging. The increase in carboxylic acid concentration may have come mainly from polymer additive oxidative aging and less from asphalt species.

Oxidative aging in humid PAV conditions yielded higher carboxylic acid concentration than the dry operations (FTIR and PT results). GPC traces revealed that for extended PMAC oxidation in humid PAV conditions; asphaltenes association was lower compared to the dry aging oxidation process.

GPC compared data between field and laboratory aged polymer modified asphalt binder showed that after 3 years in field aging conditions the asphalt blend presented a peak in the HMW polymer region (~700K), peak higher than original PMAC. These polymer species created in field aging were not observed in our laboratory-aged samples. The 5-year-old field aged asphalt GPC traces indicated a higher degradation of HMW polymer species. Both field-aged asphalt blend samples exhibited a higher association of species with a molecular weight of ~ 10K (asphaltene conglomerations), mainly produced from interaction between species with molecular weight of ~5K. This effect was not observed in laboratory-aged samples.

There is a need to better simulate the oxidation aging following more closely the possible field influences. One important influence might come from metal ions present in aggregates. The next step in this work is to simulate oxidative aging of asphalt samples in the presence of metal ions and hydroperoxides.

## CHAPTER 4

### INDUCED DECOMPOSITION OF ASPHALT COMPONENTS

There are differences between laboratory and field aged asphalt samples as shown in the previous chapters. The oxidation mechanism that takes place during chemical aging could be a free-radical reaction mainly to the SBS polymer chains. Free-radical oxidation by molecular oxygen is often referred to as autoxidation. The general mechanism is outlined in Figure 4-1. Thermal energy, mechanical stress, metal catalysts, and the addition of initiators can form radicals that initiate autoxidation in polymers. Radicals rapidly abstract hydrogen, but most radicals are highly reactive toward oxygen. In the presence of oxygen, radicals will form a peroxy radical reactive toward a hydrogen donor yielding a hydroperoxide. Various catalysts, notably the transition metals and derivatives of these, induce the decomposition of hydroperoxides.

The degradation mechanism of SBS polymer has been suggested to be at 1,4 and 1,2 groups by oxygen to peroxides that leads to the formation of carbonyl or carboxylic groups.<sup>11</sup> The degradation of the PB block proceeded mainly by  $\alpha$  and  $\beta$  chain scissions whose fragments may consequently stabilize by cyclization reaction. From analysis of these spectra the conclusion was that the 1,4 PB groups were more easily degraded than the 1,2 PB units.<sup>12</sup>

The autoxidation process is controlled by the chemical composition of asphalt blends; the presence of transitional metal ions; and the oxygen uptake. In the field the conditions for a free-radical oxidative aging are present.

To simulate a long term in-the-field autoxidation process of asphalt binder, laboratory samples were mixed with cobalt naphthenate as a source of metal ions and cumene

hydroperoxide as radical source (redox pairs) and the changes in molecular weight distributions were analyzed using GPC. The autoxidation was accelerated by various redox system concentrations. The ratio asphalt: cobalt: hydroperoxide used were 1:0.2:20 (redox1), 1:1:20 (redox2), 1:3:20 (redox3), 1:1:100 (redox4) and 1:1:4 (redox5). Samples of polymer, asphalt cement and polymer asphalt cement, with and without redox systems, were aged under TFOT conditions, followed by dry or wet PAV aging. Changes of integrated area and relative integrated area, for arbitrary regions defined as high molecular weight polymer species (HMW), medium molecular weight polymer and asphalt species (MMW) and low molecular weight asphalt species (LMW), were compared. Laboratory simulations were balanced with the asphalt binders extracted from field samples 3 and 5 years old.

The induced decomposition of cumene hydroperoxide, catalyzed by cobalt ions via a redox mechanism, used to accelerate the laboratory simulation of autoxidation process is presented in Figure 4-2.

Having FTIR results as a guideline for the oxidation level, a mixture of 1.65 grams of cobalt naphthenate (6% cobalt), 5 milliliters of cumene hydroperoxide and 50 grams of asphalt was chosen to start with. This first redox system was named redox2 in Chapter 2 and the ratio expression for 1 gram of asphalt used in this work is 1:1:20. The aggregates and asphalts carry different concentrations of metal ions. In an effort to more closely simulate the on-the-road oxidation process; various concentration ratios of redox pairs were used. The redox1 system had five times less cobalt salts with the same amount of hydroperoxide used for redox2, named 1:0.2:20. Redox3 had five times more hydroperoxide than redox2, expressed by ratio 1:1:100. When cobalt salts were added at a ratio of three times more than redox2 the ratio was presented as 1:3:20 for the redox4 system. As in the field, it could be possible that a lower concentration of hydroperoxides in the redox5 system was prepared by adding five times less cumene

hydroperoxide with a ratio expressed 1:1:4. Just for identifying the peaks for hydroperoxide excess samples with asphalt and only peroxide was prepared, the case of 1:0:20 ratios. The oxidation process was analyzed using the GPC procedure, and the results were compared to field samples.

The general mechanism of free-radical chain oxidation (autoxidation) follows the initiation, propagation and termination steps. If relatively electron rich substrates are available for hydrogen abstraction (i.e. benzylic, allylic and tertiary positions) reaction propagation will be granted. A proposed reaction sequence, which might apply in oxidative aging of asphalt blends, is presented by the reaction scheme in Figure 4.3. Once the autoxidation is initiated by molecular oxygen ( $O_2$ ), it can propagate by the abstraction of allylic PB hydrogen as illustrated in scheme 4.3.A. Reaction of the allylic radical produced with oxygen yields peroxy radicals is shown in reaction 4.3.B. Peroxy radicals will abstract hydrogen to produce hydroperoxide and a new carbon radical (from polymer or from asphalt components) as in reaction scheme 4-3.B.

In the presence of a transitional metal M (cobalt in this case) the reductant donates an electron to the oxidant (metal ion) with formation of an oxy-radical (reaction scheme 4-3.C).

The propagation sequence can go in different ways:

- Oxygen radical abstracts hydrogen. This reaction will yield an alcohol (with further oxidation to a ketone) and a new active radical;
- Oxygen radical will stabilize by disproportion (chain scission). The yields will be an aldehyde and a new carbon radical.

The new radical formed in step C will react either with oxygen and form peroxy radical or will form new bridges - crosslink reaction. The peroxy radical also can continue a chain propagation step yielding a hydroperoxide. The hydroperoxide will be reduced to an oxygen

radical by the metal ions (reaction scheme D). The new oxygen radical might abstract hydrogen, with formation of an allylic alcohol followed by a rearrangement and ending with a ketone. It also might follow the oxidation steps and yield aldehydes, followed by oxidation to a carboxylic acid. Oxy-radical formed in step D may stabilize to an aldehyde (step E) with generation of a new carbon radical.

Polystyrene chains under oxidative aging condition will form a benzylic radical. Following the similar step for free-radical oxidative mechanism in the presence of metal ions presented above, it might form an oxy-radical, which by disproportionation and oxidation would form benzoic acid (step F). Another chain termination possibility is when two radicals meet to form crosslinked or cyclic compounds (reaction scheme G). Chain scission will lower the molecular weight of the block copolymer and lead to a loss of mechanical properties. The polar compounds formed might enhance adhesion of asphalt to aggregates, but in the same time will induce asphaltene aggregation.

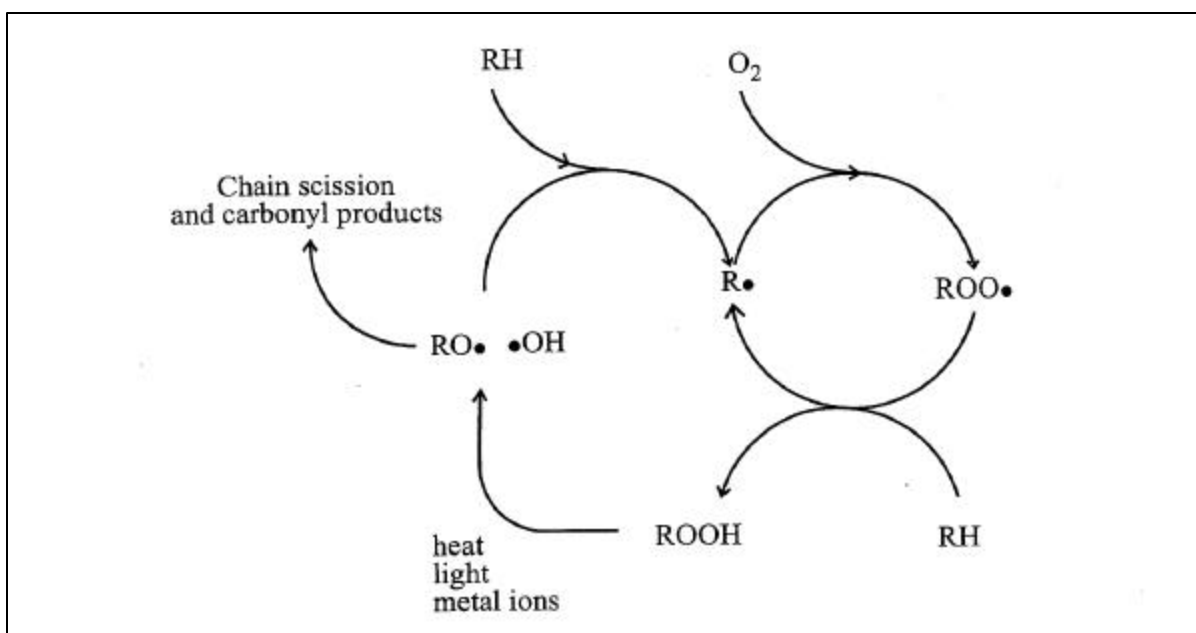


**Figure 4-1 General representation of a free-radical oxidation of an organic molecule catalyzed by metal ions<sup>3</sup>**

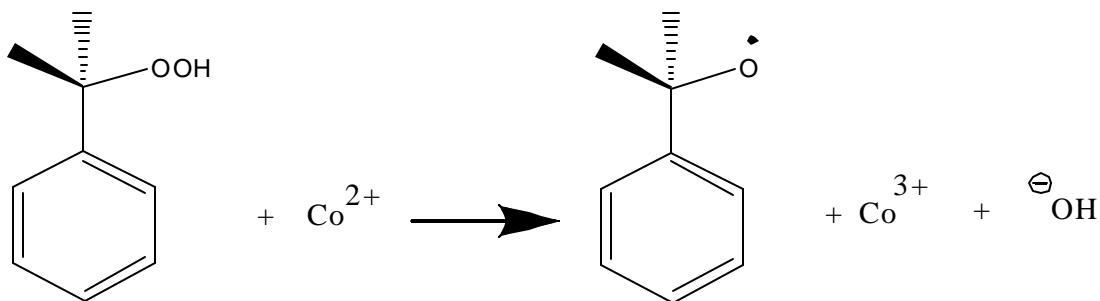
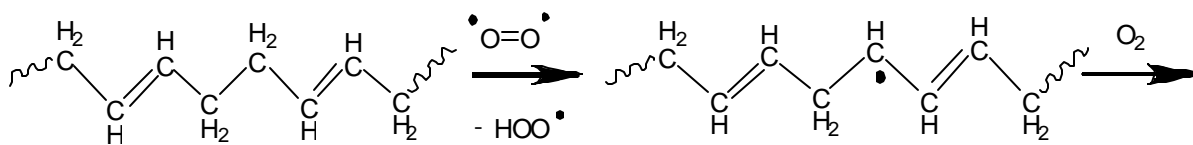
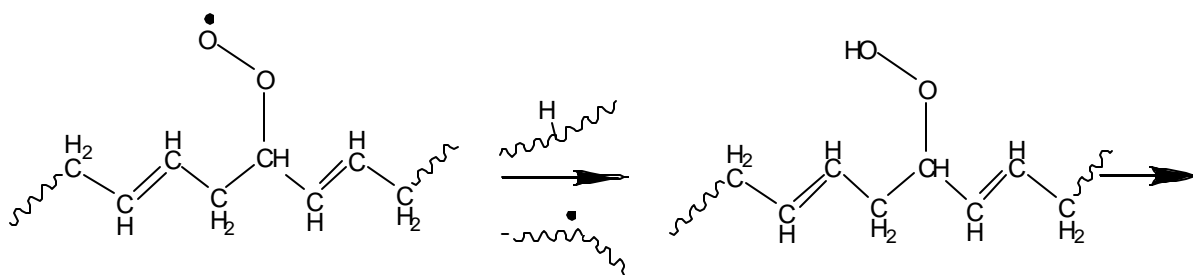


**Figure 4-2 Cumene hydroperoxide decomposition in the presence of cobalt ion**



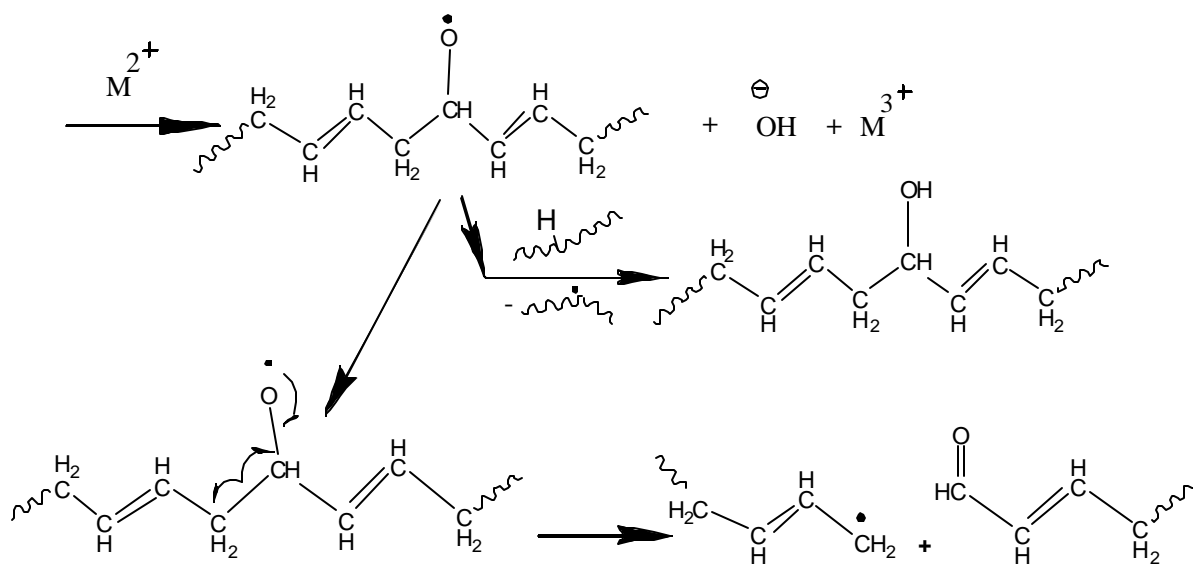
**A**



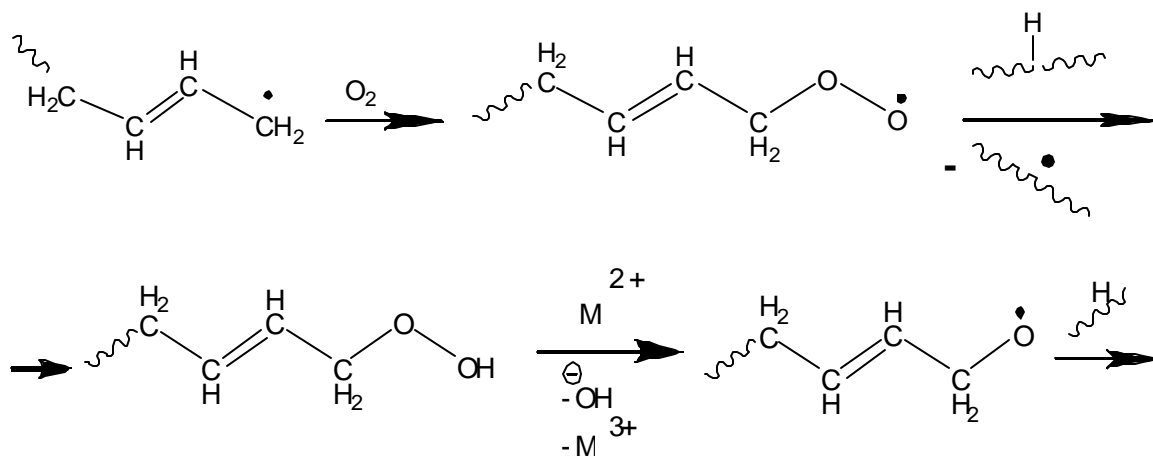
**B**

**Figure 4-3 Reaction scheme (A, B, C, D, E, F and G)**

**Figure (Continued)**



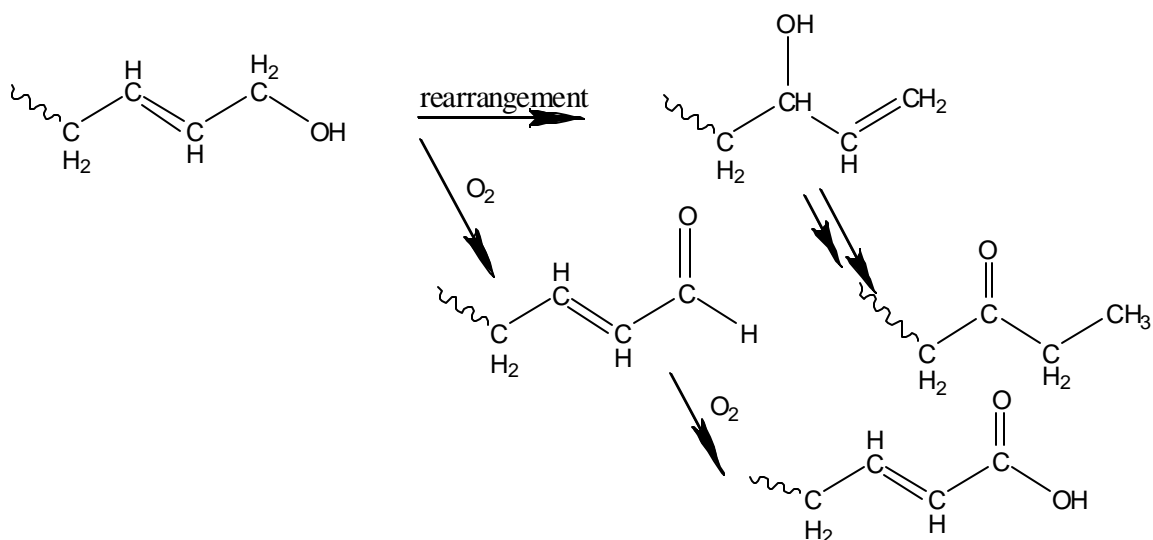
C



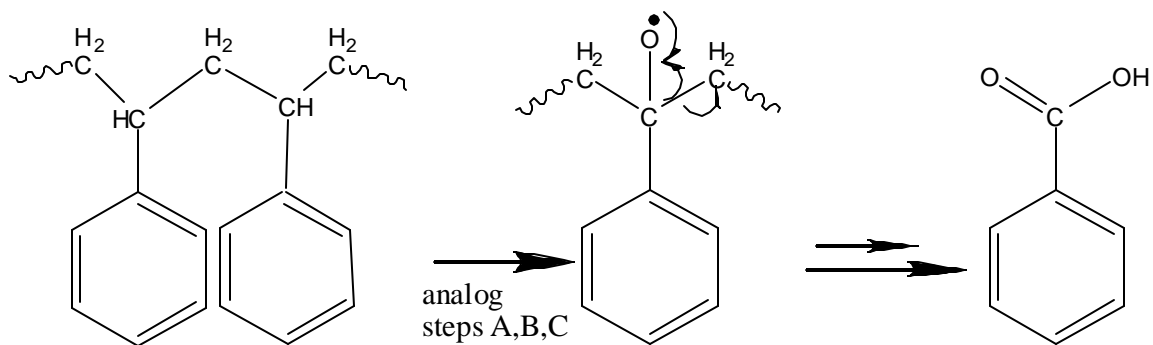
D

Figure (Continued)

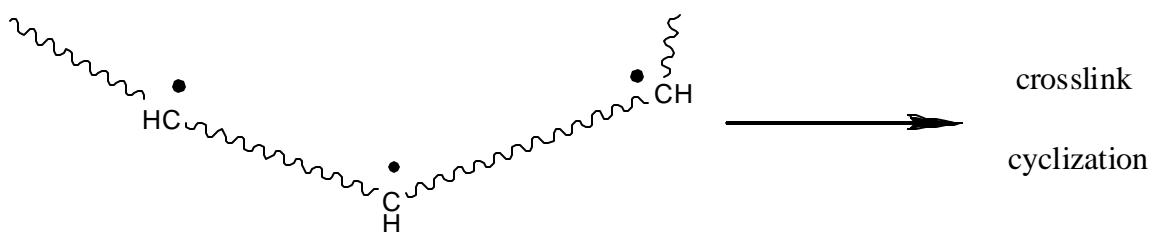




**E**



**F**



**G**

To verify if the model proposed is the case of in-field oxidative aging, the free-radical oxidation reaction was simulated in laboratory. Both wet and dry PAV aging processes were

employed on mixtures of redox systems with asphalt cement, polymer modified asphalt and polymer samples. The changes in composition of asphalt and polymer mixtures were compared with the observations of the field samples.

Impact of oxidative agents on polymer was analyzed using GPC. The GPC trace on the original polymer exhibited a molecular weight distribution with peaks around ~650 K for high molecular weight polymer chains, around 0.9K for very low molecular weight species (could be an inhibitor), and around 0.3K for the THF solvent (Figure 4-4). The autoxidation was initiated at room temperature by mixing polymer, cobalt naphthenates with cumene hydroperoxide. The polymer oxidation occurred quickly and changes in molecular weight were observed by formation of a new peaks ~700K (crosslinked chains) and ~ 50-20 K (chains scission). As regards the extent of degradation, there were no noticeable differences for diverse cobalt concentrations. However, when the hydroperoxide concentration was increased (1:1:100) the oxidation process slowed down. The dilution effect of five times more hydroperoxide could be one reason for the slowdown. The excess of hydroperoxide was seen around a molecular weight value of 0.2K (33 mL).

After TFOT (Figure 4-5) GPC traces for the polymer exposed with redox2 (1:1:20) exhibited a higher concentration for HMW species (~700K) compared to polymer-redox 1 mixture (1:0.2:20). The cobalt salts concentration (five times higher in redox 2) made this difference. The TFOT temperature increased the reaction rate and more medium molecular weight polystyrene chains were formed (~20K) if redox pairs were present, compared to polymer samples without redox system.

As was expected, during the TFOT process, the decomposition of the polymer without redox system was slower than systems with redox compounds. The polymer and redox 3 mixture (1:1:100) could not pass through the TFOT test yet. Every day, for 2 weeks, the sample was

heated for 30 minutes starting with 90°C achieving 145°C in the last day, and every time the heat was stopped because of the fumes, hydroperoxide smell and danger of explosion.

After dry PAV (Figure 4-6) GPC traces for polymer and redox2 indicated that the hydroperoxide it was almost consumed and also the 2 K species were gone. The polymer mixed with redox 2 (1:1:20) still showed a small percentage of soluble HMW (~700K) polymer besides MMW species (~20K). The proportions chosen for redox2 were more stoichiometric, and were expected to give a more realistic effect. The GPC curve for a mixture of polymer and redox1 (less cobalt than redox2), exhibited a higher concentration for species with molecular weight distribution around 20K, without any peaks for HMW polymer species. As can be seen, after dry PAV oxidative aging, the difference in concentration in metal ions induced different final products (Figure 4-7 and 4-8).

With less cobalt present (less catalyst for free radical reaction propagation), more insoluble HMW polymer species were revealed by GPC traces.

The GPC traces for polymer mixed with redox2 showed less short polystyrene chains and more soluble HMW compared to polymer-redox1 mixture. An explanation may be that cobalt contains 6% naphthenates in mineral oils. With more oil present, there was more surface area (dilution) with the effect of decreasing oxidation speed.

Using the same regions (Figure 4-9) defined in Chapter 3 for a GPC molecular weight distribution (HMW, MMW and LMW); the relative changes of integrated area for various species, with respect to integrated area for the original polymer (before and after dry PAV) are computed and presented in Figure 4-10 and 4-11.

The GPC trace for the dry-aged PAV polymer, without redox systems, showed a decrease in HMW of around 55% while MMW increased with 15% than the original polymer.

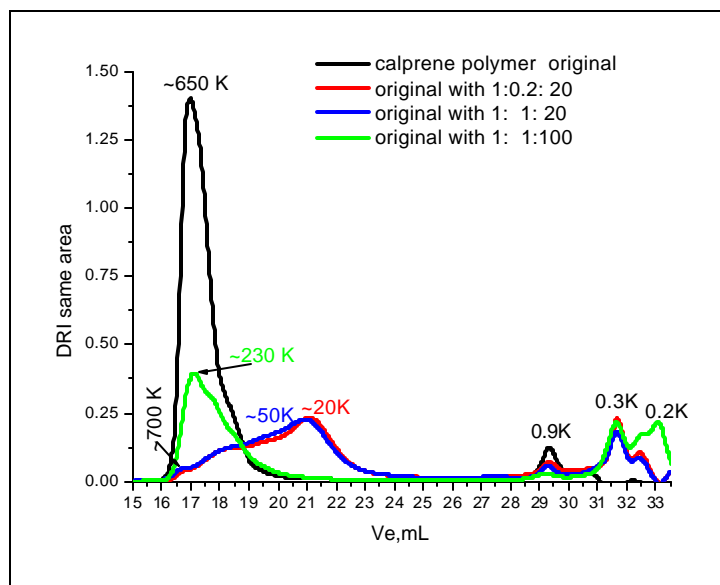


**Figure 4-4 GPC traces for the polymer, polymer-redox1 mixture 1:0.2:20, polymer-redox2 mixture 1:1:20, polymer-redox3 mixture 1:1:100, at room temperature**

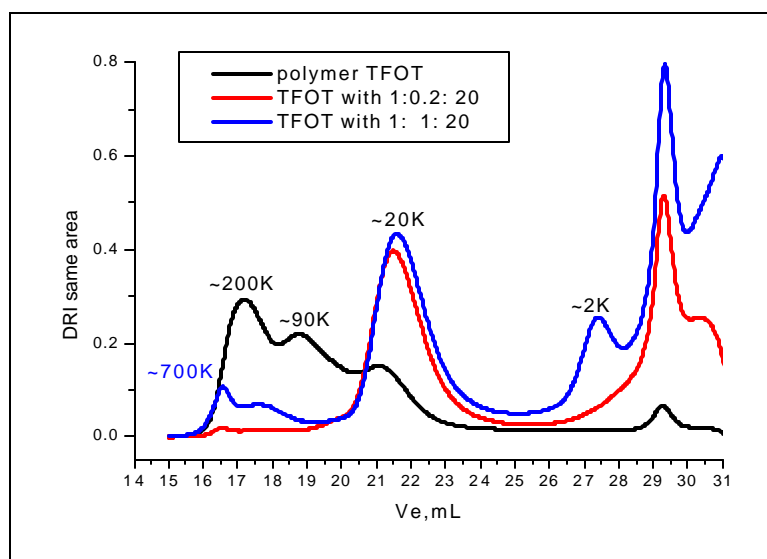


**Figure 4-5 GPC traces for the polymer, polymer-redox1 mixture 1:0.2:20, polymer-redox2 mixture 1:1:20, after TFOT**

At room temperature both redox1 and redox2 pairs accelerated polymer autoxidation, the concentration of HMW species decreased with 80% and MMW increased with 25% than the original polymer. The difference of around 55% not shown in GPC traces was insoluble crosslinked polymer species.

After dry PAV aging, the product of redox pairs produces a further diminution of HMW of around 15-20% loaded to total reduction of original HMW. For the polymer-redox1 mixture the MMW increased after aging only 20% compared to PAV-aged polymer (45% compared to original polymer) while polymer aged in the presence of redox2 did not bring significant increases in this regions compare to PAV-aged-polymer.

We have seen how the polymer degraded in the presence of redox systems. The next step is to analyze the impact on asphalt cement (AC) PG 64-22 by itself (Figure 4-12).

The peak at 0.9 K was higher for the asphalt cement mixed only with hydroperoxide. The presence of cobalt had an effect of decreasing this peak as it consumed the hydroperoxide. The more cobalt there was in the system (Figure 4-13) the higher the asphaltenes peak (9.8K) became. However, various concentrations of redox compounds induced only a slight difference (Figure 4-14), but the main conclusion is that oxidation can occur to asphaltic materials when in contact with a redox system. All the samples exhibited almost the same percentage increment in the asphaltenes region. Small differences can be seen around 0.9K (Figure 4-15) and around 0.2K for excess of hydroperoxide. TFOT (Figure 4-16 and 4-17) aging caused a slight increase in the oxidation differences between samples but the changes were not significant.

After PAV aging, the curves displayed a more normal (expected) trace (Figure 4-18 and 4-19). After TFOT and dry PAV, the samples of asphalt-redox system showed some increase in the asphaltenes content (MMW region) while the sample mixed only with HP had the same trace as asphalt alone, which indicates that HP did not have any major influence on the asphalt. This

sustained the conclusion that what we see in figure 4-19, from the sample with the higher concentration in HP (redox 5 1:1:100), was only a solvation effect caused by HP excess and not asphalt degradation.

From GPC traces magnitude the conclusion is that there were no significant changes in molecular weight distribution of asphalt species due to accelerated oxidation induced by redox systems. To have detailed information about the changes brought by adding redox pairs to the original AC, the medium molecular weight species regions was divided in two new zones MMW 1 (50-7K) and MMW 2 (7-3K) as presented in Figure 4-20 and 4-21. The changes of the extended oxidation were noticeable more in the region MMW 2 (lower molecular weight) than in MMW 1.

The overall changes in MMW region of asphalt cement are presented in Figure 4-22. At room temperature the redox systems induced acceleration in asphaltenes association up to 37% more than original asphalt integrated area for MMW species. After the dry PAV operation, the integrated area for the same region computed using GPC traces was higher with 50% than asphalt aged without redox systems. Analyzing the LMW region it was observed that around 10% of these species diffused in MMW region before aging, regardless of the PAV exposure (Figure 4-23). For both regions MMW and LMW the mixture with redox5 (1:1:4) indicated the highest acceleration in oxidation effects.

A blend of asphalt and 3% polymer was prepared in the laboratory. The polymer concentration in asphalt was verified by GPC data (Figure 4-24). The peak at 0.9K from the original polymer could be seen overlapping on the asphalt peak for the blend trace. After blending, the polymer in asphalt appeared at a slightly different peak at 16.6 mL, compared with 16.9 mL (~650K) of the original. The polymer elution was influenced by the high concentration of asphalt compounds in the solution.

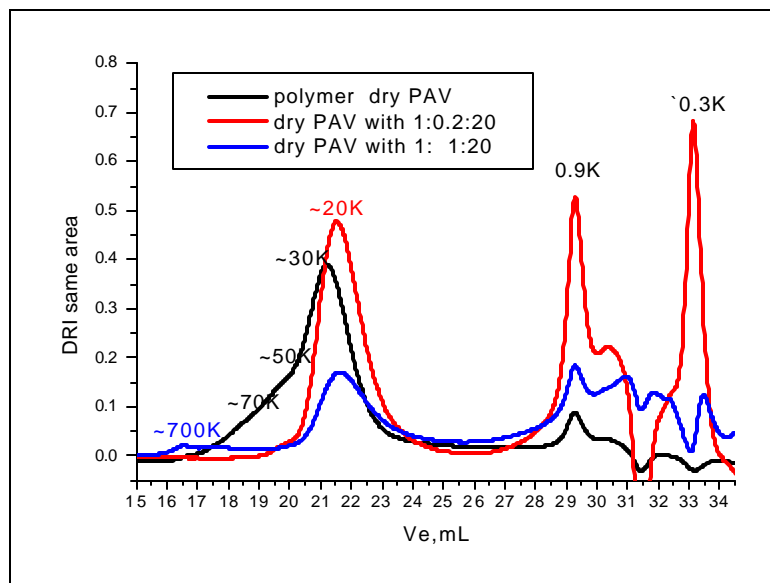


**Figure 4-6 GPC traces for the polymer, polymer-redox1 mixture 1:0.2:20, polymer-redox2 mixture 1:1:20, after dry PAV aging**

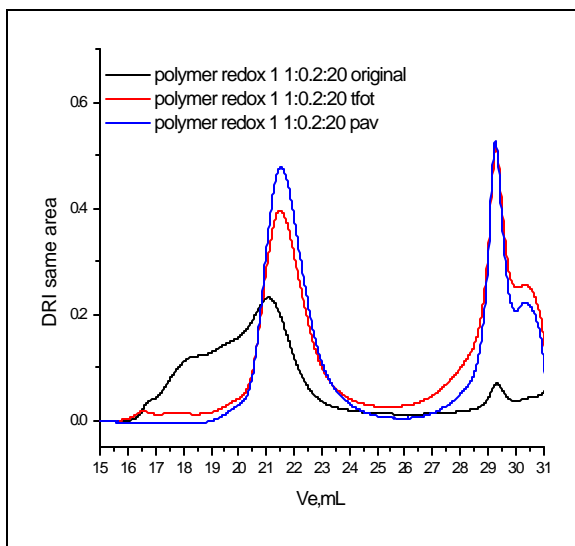


**Figure 4-7 Changes in molecular weight distribution from GPC traces for polymer and redox1 (1:0.2:20) mixture (original, TFOT, dry PAV)**

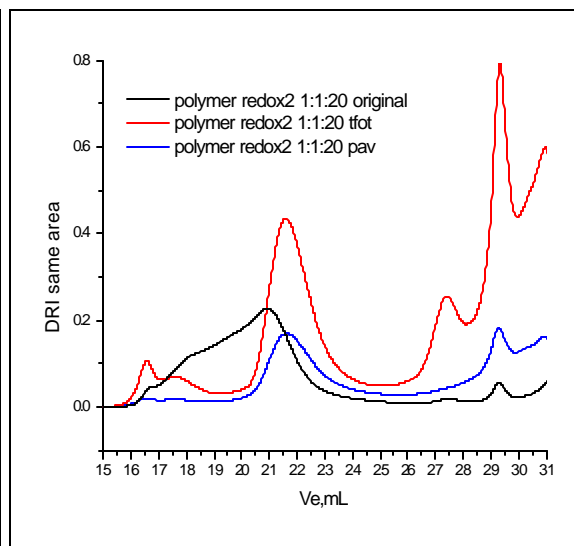


**Figure 4-8 Changes in molecular weight distribution from GPC traces for polymer and redox2 (1:1:20) mixture (original, TFOT, dry PAV)**

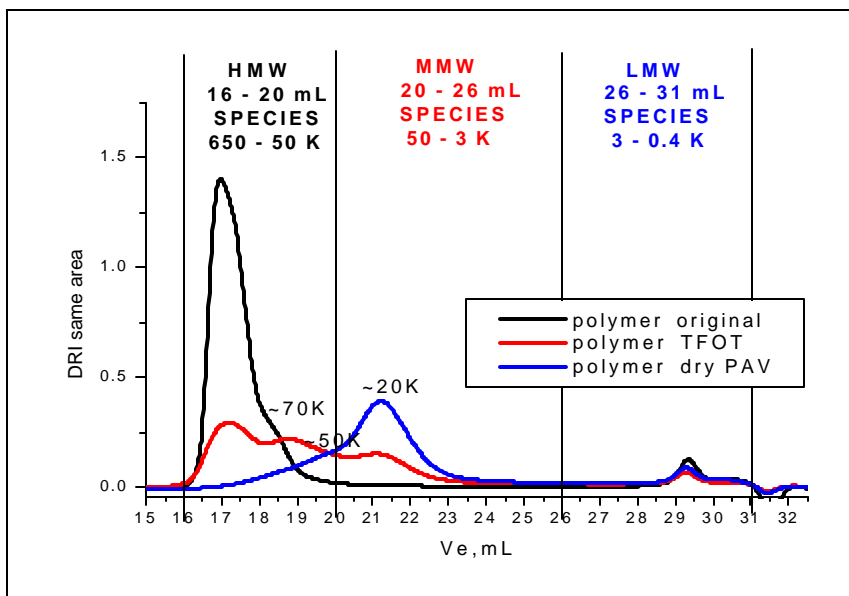


Figure 4-9 GPC traces for polymer after oxidative aging without redox systems

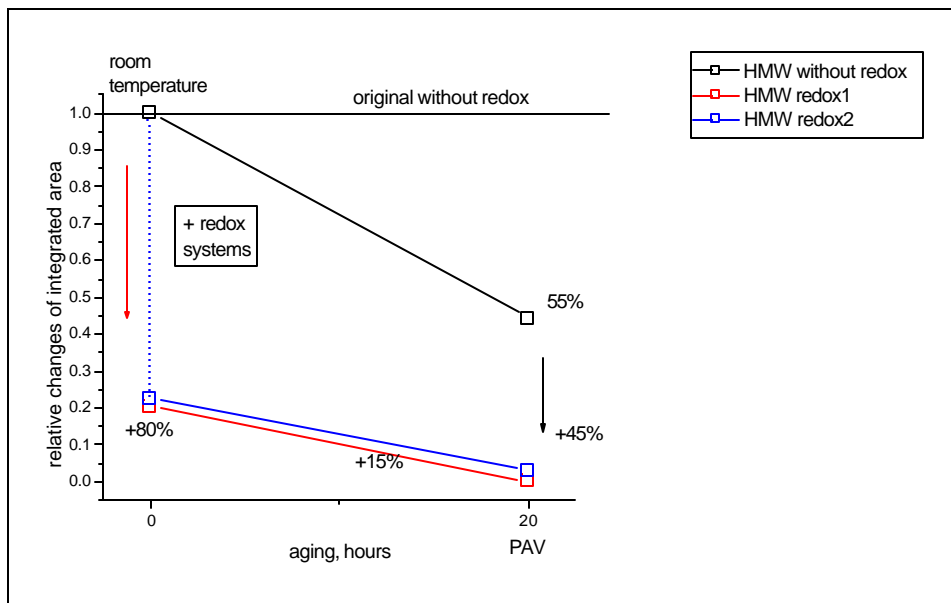
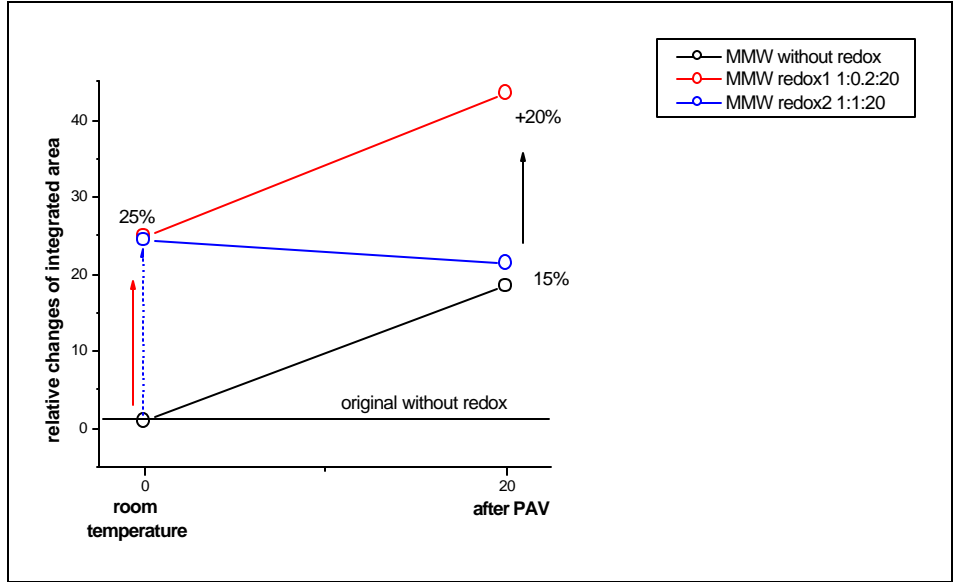
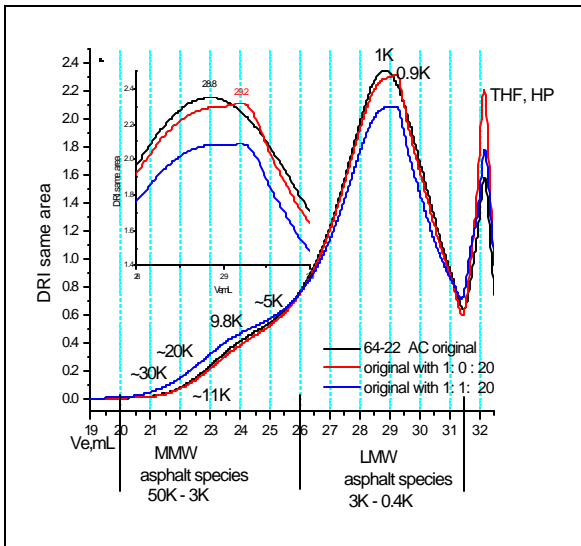


Figure 4-10 Relative changes of integrated area in HMW region, before and after dry PAV process, for polymer, polymer and redox1, polymer and redox2 samples





**Figure 4-11** Relative changes of integrated area in MMW region, before and after dry PAV process, for polymer, polymer and redox1, polymer and redox2 samples



**Figure 4-12** GPC traces for the AC 64-22 original, AC with HP (1:0:20), AC-redox 2 mixture 1:1:20, at room temperature

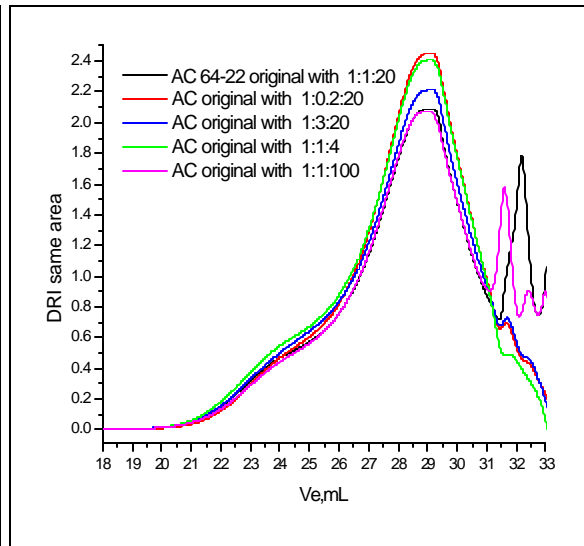


**Figure 4-13** GPC traces for the AC 64-22 mixtures with redox1 (1:0.2:20), redox2 (1:1:20), redox3 (1:1:100), redox4 (1:3:20), redox5 (1:1:4) and at room temperature

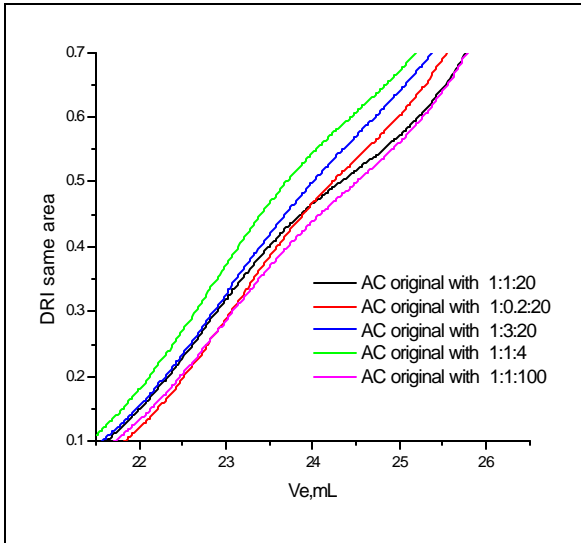


**Figure 4-14 GPC traces for the AC 64-22 mixtures with redox1 (1:0.2:20), redox2 (1:1:20), redox3 (1:1:100), redox4 (1:3:20), redox5 (1:1:4) and at room temperature-details**

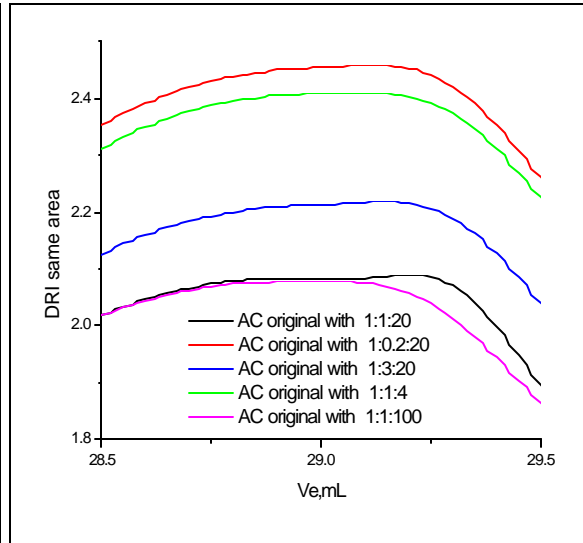


**Figure 4-15 GPC traces for the AC 64-22 mixtures with redox1 (1:0.2:20), redox2 (1:1:20), redox3 (1:1:100), redox4 (1:3:20), redox5 (1:1:4) and at room temperature-details**

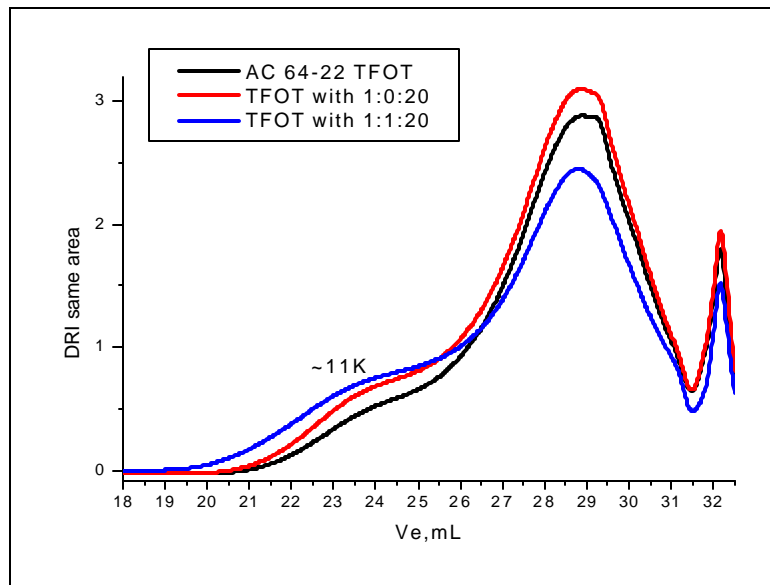


**Figure 4-16 GPC traces for the AC 64-22, AC 64-22 mixtures with HP (1:0:20), redox2 (1:1:20), after TFOT**

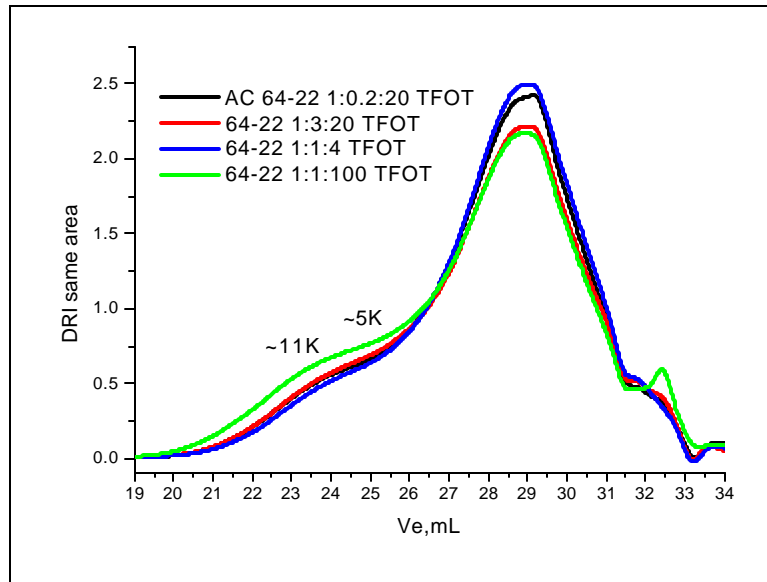


**Figure 4-17 GPC traces for the AC 64-22 mixtures with redox1 (1:0.2:20), redox3 (1:1:100), redox4 (1:3:20), redox5 (1:1:4) after TFOT**

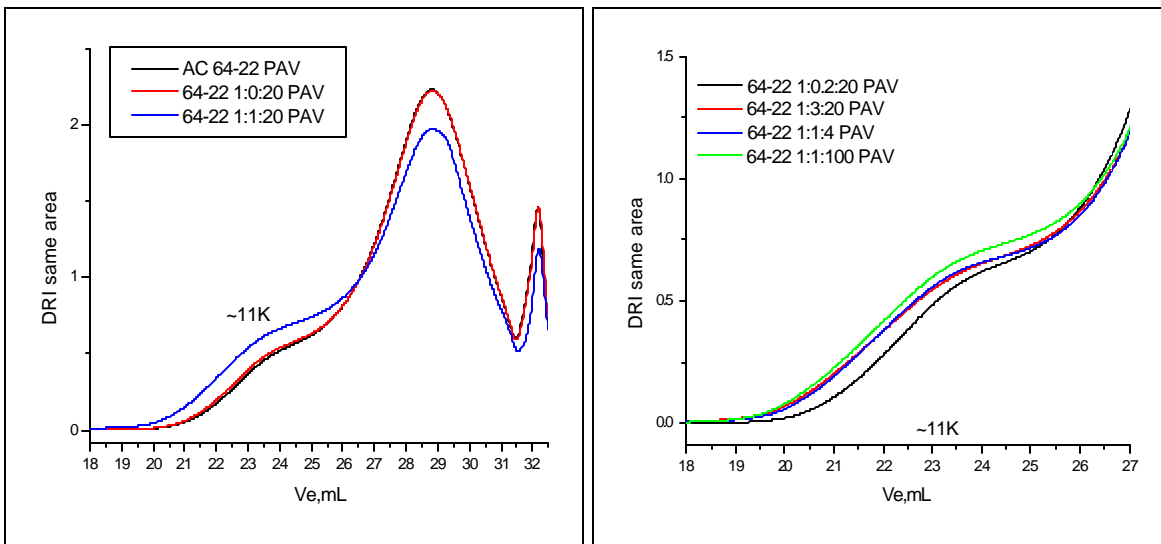


**Figure 4-18 GPC traces for the AC 64-22, AC 64-22 mixtures with HP (1:0:20), redox2 (1:1:20), after dry PAV aging**

**Figure 4-19 GPC traces for the AC 64-22 mixtures with redox1 (1:0.2:20), redox3 (1:1:100), redox4 (1:3:20), redox5 (1:1:4) after PAV**

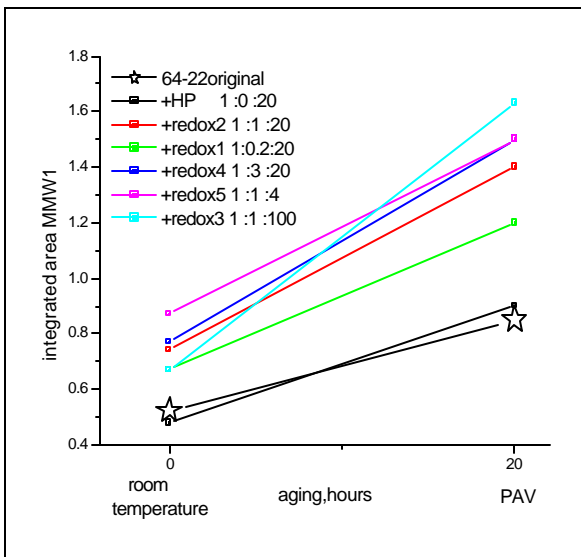


**Figure 4-20** Changes in integrated area from GPC curves for the molecular weight region 50-7K for AC 64-22 original, AC and HP, AC mixtures with redox1, redox2, redox3, redox4, and redox5, at room temperature and after dry PAV

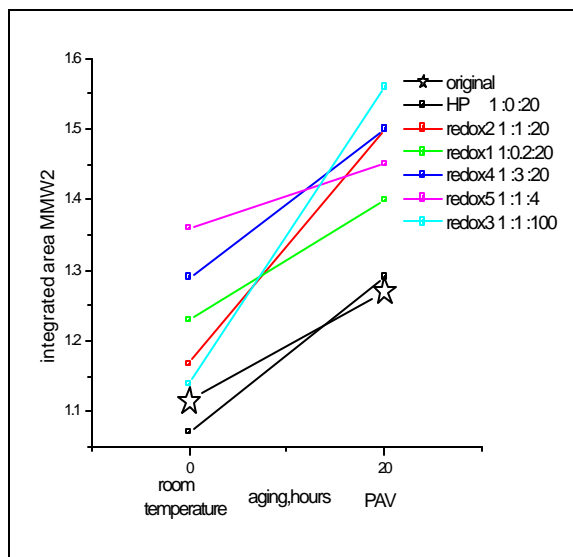


**Figure 4-21** Changes in integrated area from GPC curves for the molecular weight region 7-3K for AC 64-22 original, AC and HP, AC mixtures with redox1, redox2, redox3, redox4, and redox5, at room temperature and after dry PAV

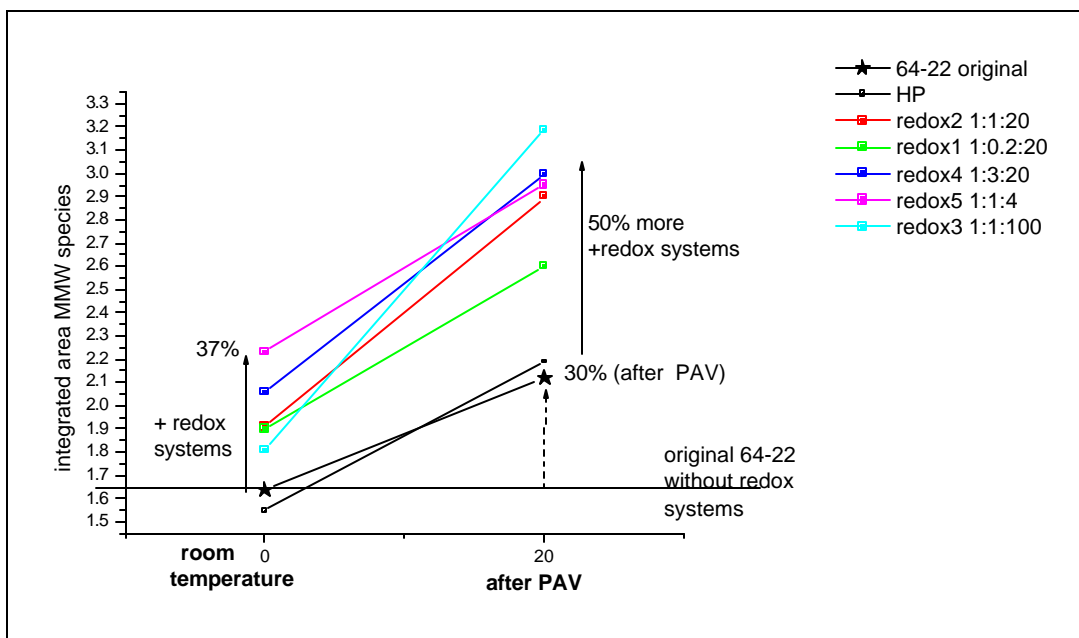


**Figure 4-22** Changes in integrated area from GPC curves for the molecular weight region 50-3K for AC 64-22 original, AC and HP, AC mixtures with redox1, redox2, redox3, redox4, and redox5, at room temperature and after dry PAV

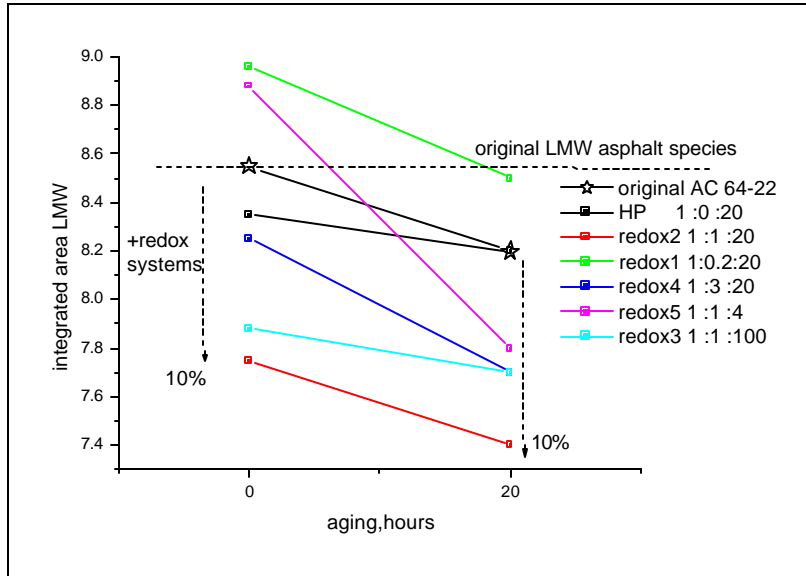


**Figure 4-23** Changes in integrated area from GPC curves for the molecular weight region 3-0.4K for AC 64-22 original, AC and HP, AC mixtures with redox1, redox2, redox3, redox4, and redox5, at room temperature and after dry PAV

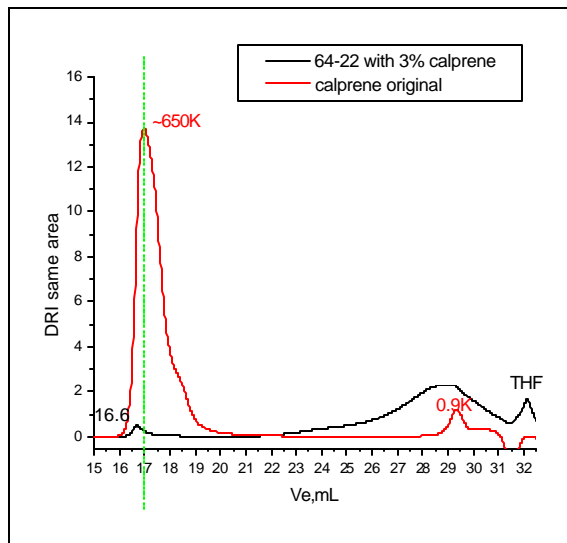


**Figure 4-24** Area correlation for blend prepared

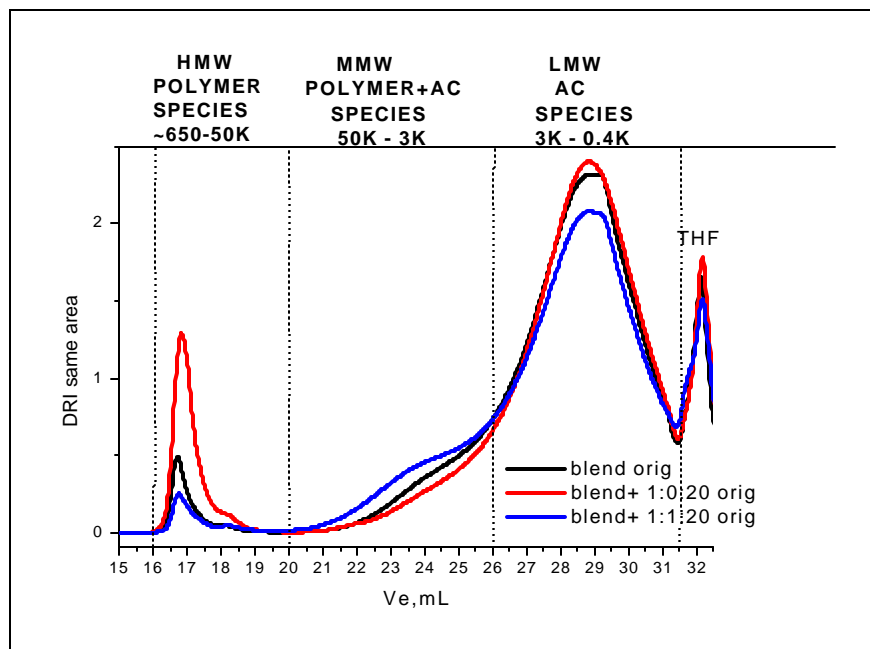


**Figure 4-25 GPC traces of the original blend, blend and HP, blend and redox2 (1:1:20), at room temperature**

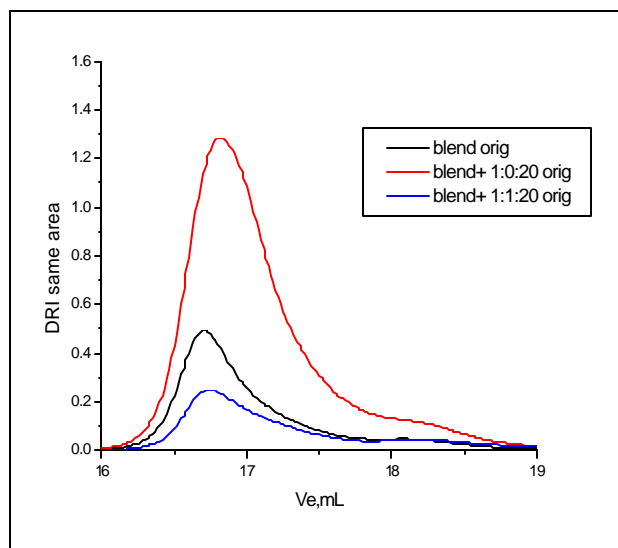


**Figure 4-26 GPC traces-details from Figure 4-25**

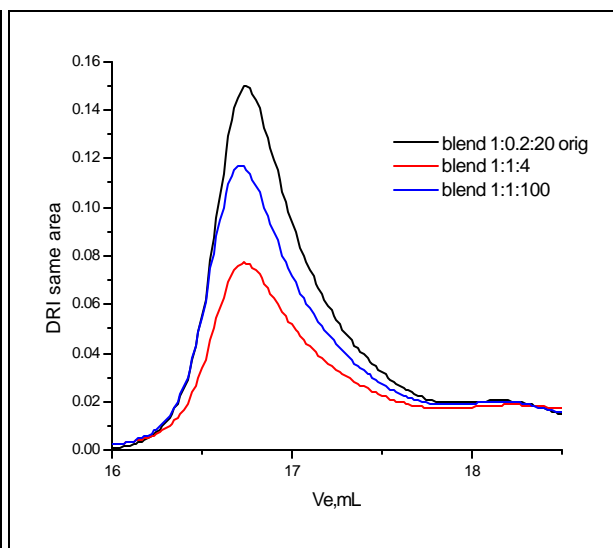


**Figure 4-27 GPC traces for HMW region original blend with redox1 (1:0.2:20), redox3 (1:1:100), redox5 (1:1:4), room temperature**

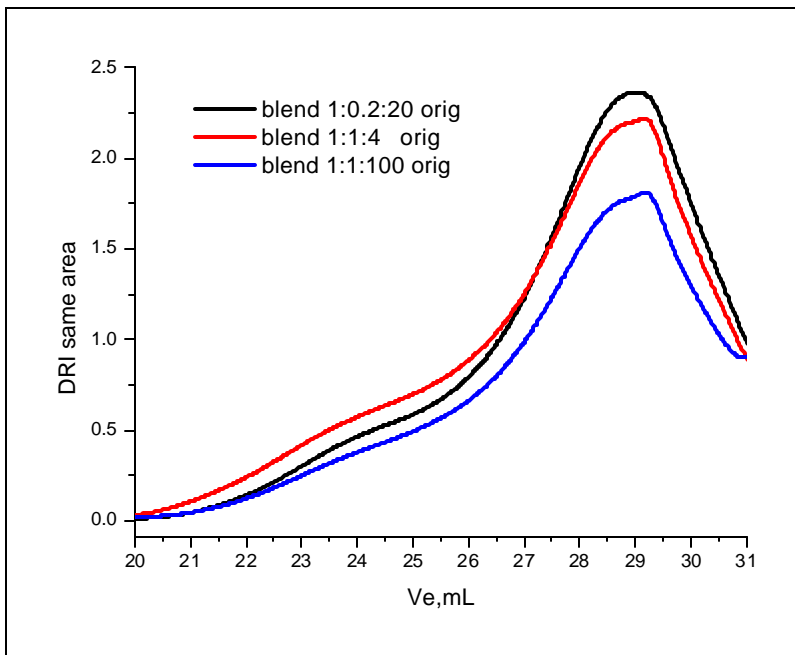


**Figure 4-28 GPC traces for MMW and LMW region of original blend with redox1 (1:0.2:20), redox3 (1:1:100), redox5 (1:1:4).**

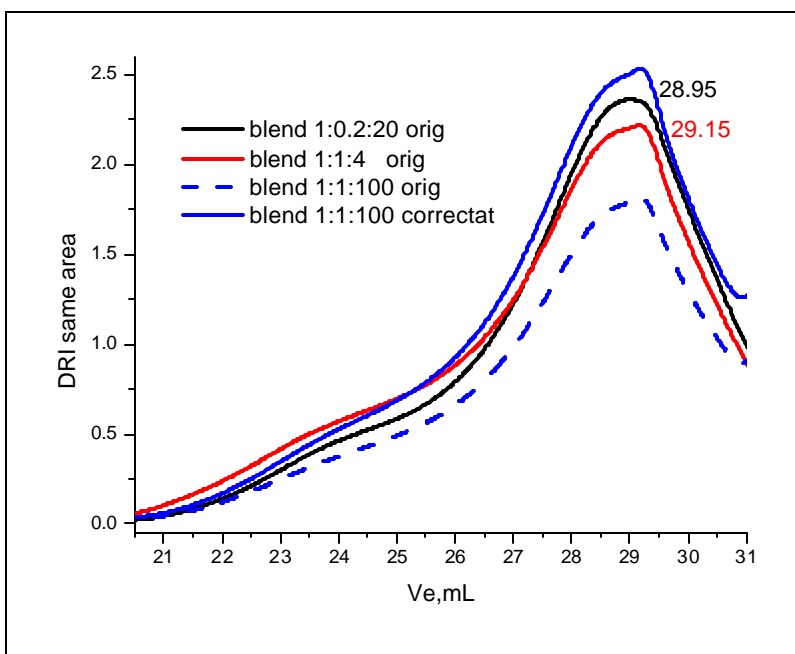


**Figure 4-29 GPC traces for MMW and LMW region of original blend with redox3 (1:1:100) corrected**

When cobalt was present the polymer peak decrease was accompanied by elution of shorter species in the MMW region (Figure 4-25 and details in Figure 4-26). Higher concentration of metal ions of cobalt did lower the concentration of HMW species (Figure 4-27).

Less cobalt caused less damage on polymer and asphalt sites (Figure 4-28). The sample with more cobalt and less HP sample showed more damage on the polymer site and some on asphalt. There was an error for the blend sample with HP (1:0:20); the polymer DRI signal was higher than the sample with original blend (Figures 4-25 and 4-26)

Keeping in mind the solvation effect of HP in excess, the area for GPC curve with a high content of HP (redox3) was integrated from 50K to 0.3K and the HP peak was excluded. The graph from Figure 4-28 was re-plotted in Figure 4-29. This image shows that HP, when used in excess, had only a dilution effect. In the discussion below fewer references will be made to the samples with high concentration of hydroperoxide as it is suspected that there was only a dilution effect revealed by GPC traces.

The graphic comparison presented in Figure 4-30 shows polymer oxidative degradation in the presence of redox2 system without changes in molecular weight distribution of asphalt components in the region 30K through 0.3K.

It might be concluded that when polymer was present as an additive in asphalt blends, the induced oxidation would occur first at the polymer chain. Intermediate stages of molecular weight distributions of oxidative aging in GPC traces of TFOT samples are seen (Figures 4-31 to 4-34). After TFOT aging the molecular weights of the species around 11K showed an increment in concentration for the blend aged in the presence of redox2 system (1:1:20). This increment was accompanied by a lower concentration for species that elute in LMW and also by a lower concentration of HMW polymeric species.



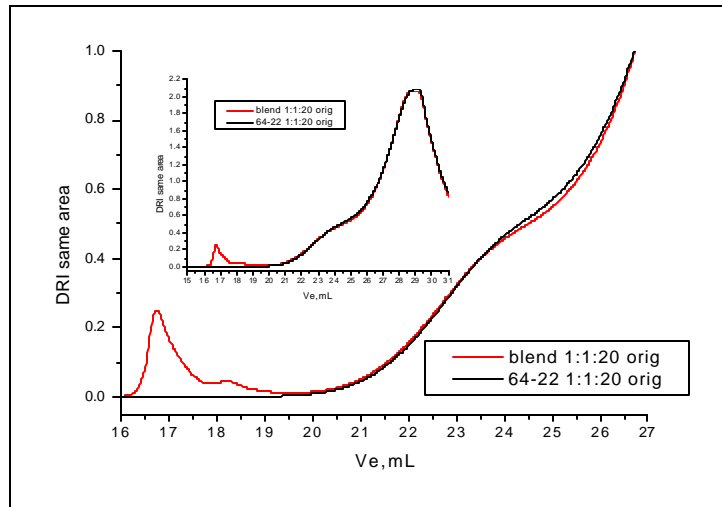


**Figure 4-30 Comparison of GPC traces for blend and redox2 and for AC 64-22 and redox2, at room temperature**

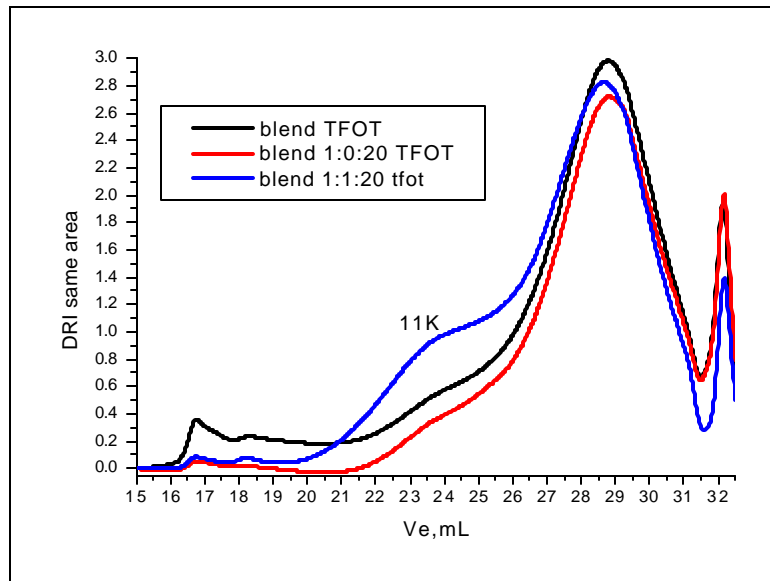


**Figure 4-31 GPC traces for original blend with redox1 (1:0.2:20), redox2 (1:1:20), redox5 (1:1:4), after TFOT**

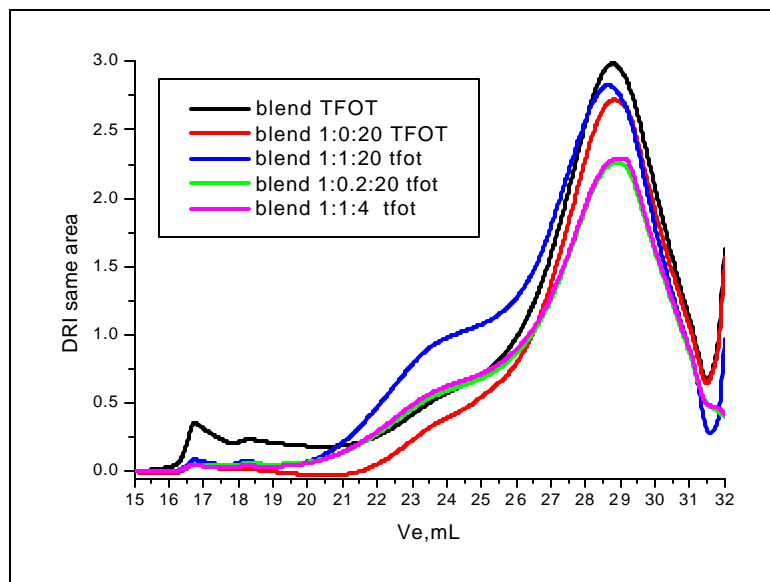


**Figure 4-32 GPC traces for blend, blend with HP, with redox1 (1:0.2:20), redox2 (1:1:20), redox5 (1:1:4), after TFOT**

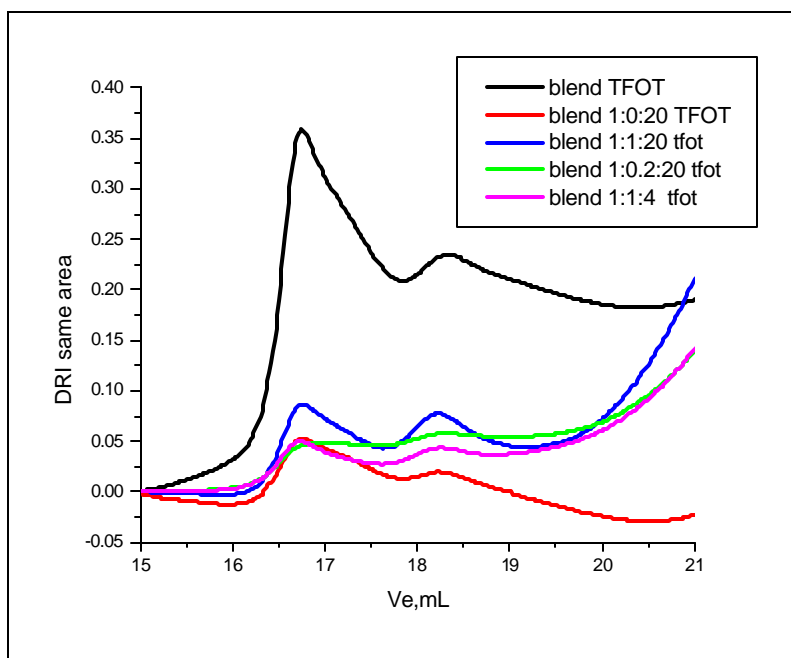


**Figure 4-33 GPC traces - HMW detail from Figure 4-32**

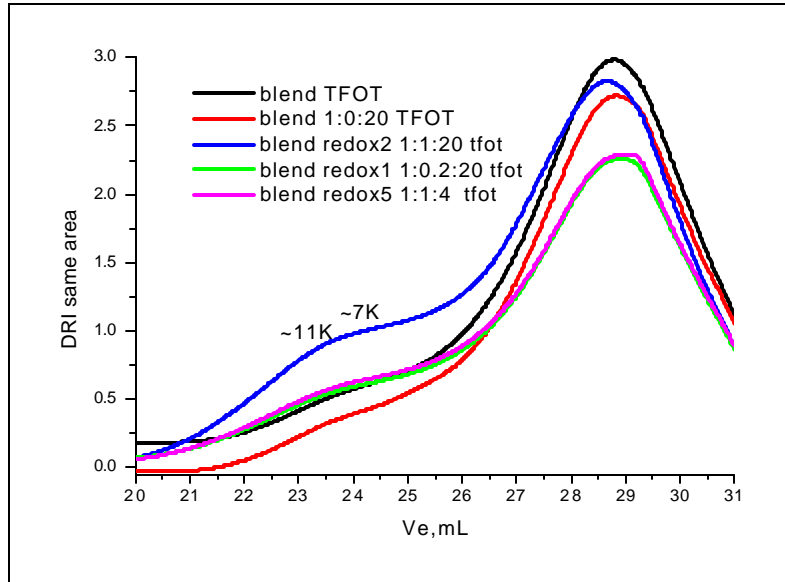


Figure 4-34 GPC traces – details MMW and LMW from Figure 4-32

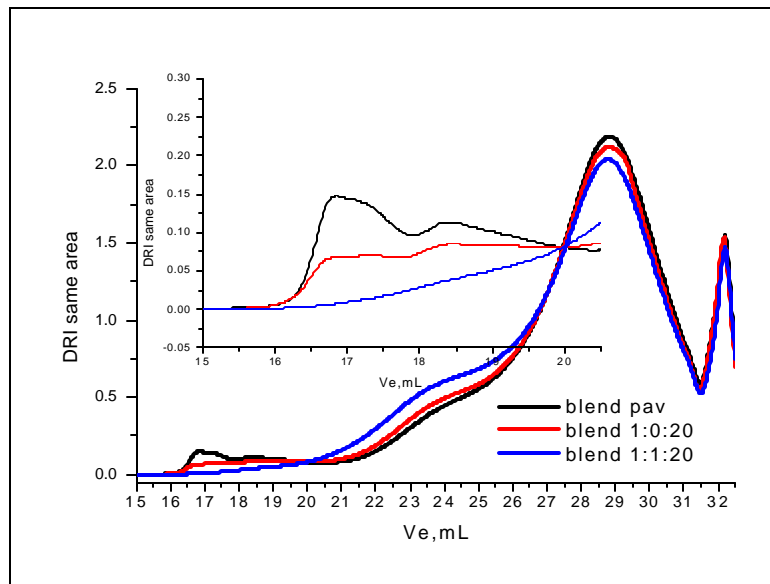


Figure 4-35 GPC traces for blend, blend with HP, blend with redox2 (1:1:20), after PAV

From the composition of the mixtures formed with redox pair the effects of a redox2 treatment could easily be seen. After the TFOT process the concentration of species which eluted around 11K (asphaltenes) was maximized in the presence of asphalt: cobalt: HP ratio of 1:1:20 (redox2).

The HMW species (polymer), after TFOT aging operation, contained a higher concentration for samples treated redox2 than with redox1 or redox5.

It can be concluded that HMW polymer chains subjected to aging in the presence of a low concentration of free-radicals and/or low concentration of metal ions catalyst formed an insoluble crosslinked network (case of sample redox1 and redox5). This statement is correlated with the observations of MMW for these samples, where a noticeable increase in that region is not revealed by GPC measurements. When the ratio, blend: cobalt: HP was 1:1:20, the oxidative aging of HMW polymeric chains is propagating through formation of short chains which diffuse in MMW region. After dry PAV aging (Figures 4-35 to 4-38) the trend observed after short term TFOT aging is changed. The samples of blend mixed with redox1 and redox5 (lower concentration of cobalt 1:0.2:20 and lower concentration of HP 1:1:4) show a continue propagation of free-radical reaction. Some of the crosslinked insoluble polymer is cleaved after a dry PAV process in smaller molecular weight species, which elute in the range 50K to 20K. The effect is shown by GPC traces; the concentration in MMW region for these samples is increasing. Very low concentrations of high molecular polymer chains are still present. This was not observed when the polymer was oxidized by itself. As the polymer was present at only a 3 % in asphalt, some protection from the asphalt site is expected. A higher concentration of MMW species was coming from degradation of HMW polymer chains than from LMW associations. After dry PAV the samples do not exhibit significant changes in LMW region. An extra peak is observed for GPC curves for redox1 and redox4 pairs eluting around 29.12 mL that

it can be an excess of redox components as there was not a stoichiometric proportion to consume them. The changes in molecular weight distribution occurred in induced oxidation of the blend prepared in laboratory (asphalt cement 64-22 and 3% polymer additive) might be better understood using the comparative values of integrated area for a specific range of molecular weights (Figure 4-39 and 4-40).

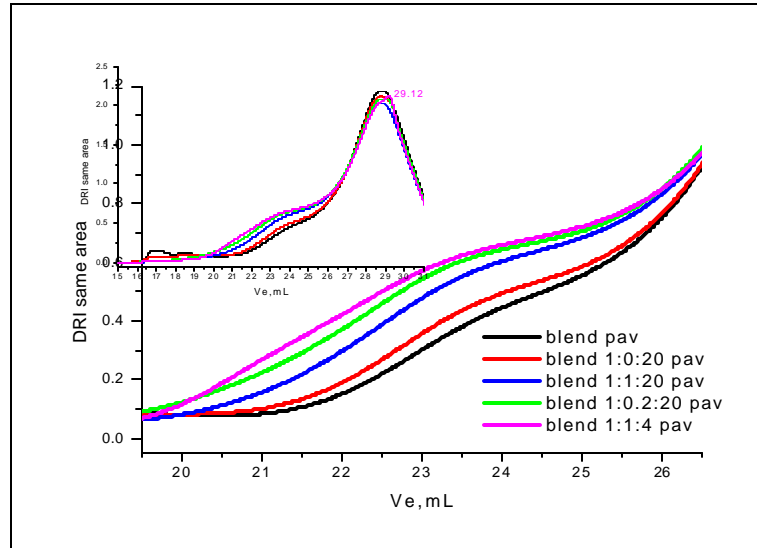


**Figure 4-36 GPC traces – MMW details - for blend, blend with HP, with redox1 (1:0.2:20), redox2 (1:1:20), redox5 (1:1:4), after PAV**

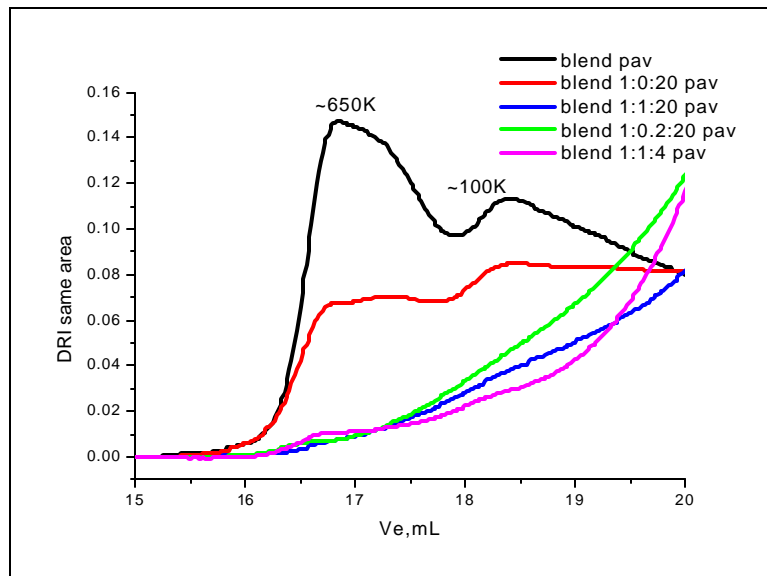


**Figure 4-37 GPC traces - HMW details- for blend, blend with HP, with redox1 (1:0.2:20), redox2 (1:1:20), redox5 (1:1:4), after PAV**

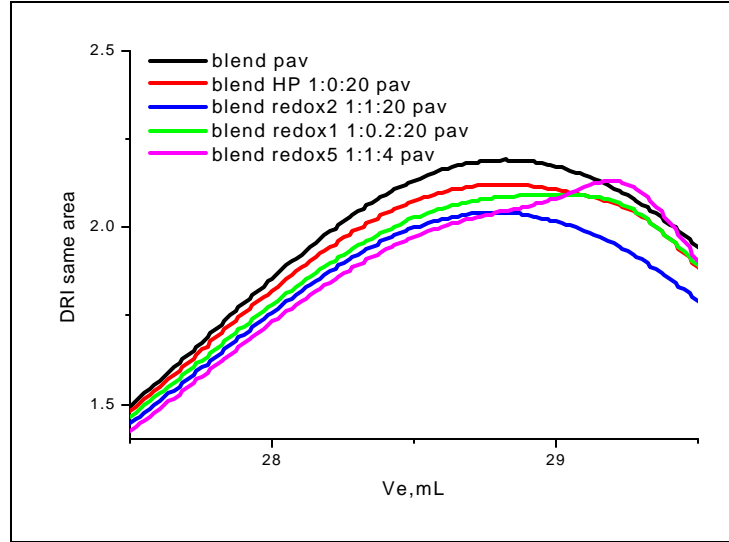


Figure 4-38 GPC traces – LMW details- for blend, blend with HP, with redox1 (1:0.2:20), redox2 (1:1:20), redox5 (1:1:4), after PAV

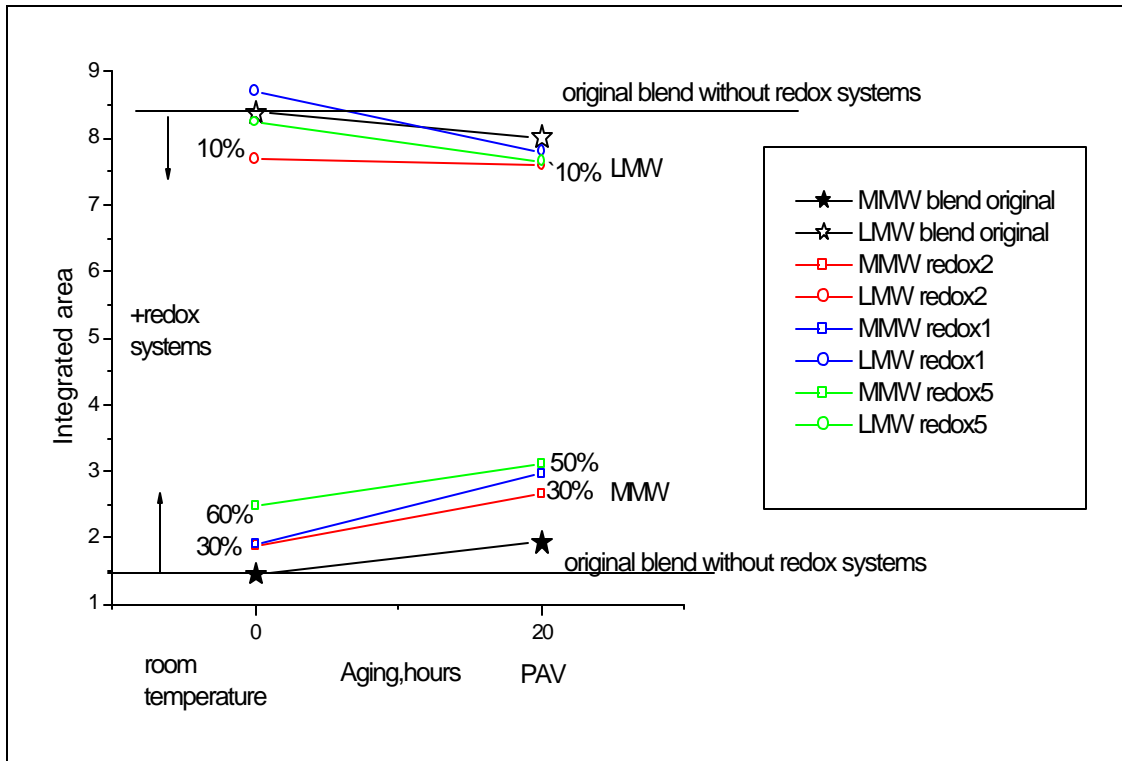
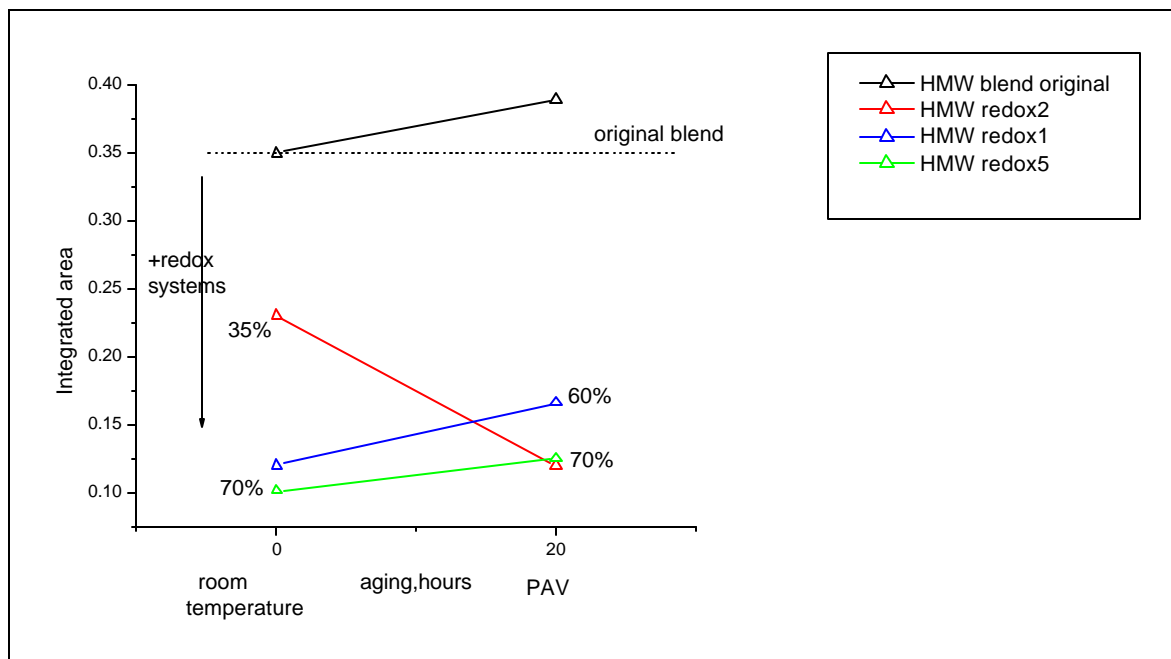


Figure 4-39 Changes of integrated area in MMW and LMW region, before and after dry PAV process, for blend, blend and redox1, redox2, redox5



**Figure 4-40 Changes of integrated area in HMW region, before and after dry PAV process, for blend, blend and redox1, redox2, redox5**

At room temperature the polymer autoxidation was initiated and the integrated area for changes after blend was mixed with redox systems show that redox2 (1:1:20) induced 35% lower concentration of HMW species while redox1 (1:0.2:20) and redox5 (1:1:4) were inducing a decrease in HMW concentration of 70%.

Different for the redox1 and redox5 was a lower concentration in cobalt ions-catalyst donor and hydroperoxide- radical donor systems. These two systems, both redox1 and redox5, induced a slow propagation of free-radical reaction in polymer chains giving enough time to the active radicals to close an insoluble crosslinked network. After PAV aging redox2 and redox5 exhibited the same percentage of polymer degradation (around 70% more than blend PAV aged).

Analyzing the integrated area for MMW and LMW it can be observed that redox5 systems accelerated the increment in the 50-3K ranges by 60% (redox5) with a decrease in 3-0.4K ranges by 10%. This 10% was diffusing from the LMW to the MMW region. The rest of 50%

increment in MMW appears to come from HMW, which allows us to estimate that around 20% polymer crosslinked at room temperature. After PAV in LMW there were no new changes brought by redox systems. The PAV process gave enough time for redox5 to extract 10% more from crosslinked network, transforming the species in soluble molecules. In the MMW region, at room temperature, there was 60% higher the concentration than in the original material. The concentration was only 50% higher after PAV than aged blend. The loss was 10%. It may be possible that there was a diffusion back-and-forth of the molecules passing the arbitrary borders we drew for computation purposes. It also may be a high association of asphaltenes with an effect in formation of insoluble species.

A similar set of blend samples were PAV aged in a humid condition in order to understand water influence during oxidative aging (Figures 4-41 to 4-44).

Samples containing asphalt, polymer and hydroperoxides showed slightly higher degradation of HMW species in wet rather than dry PAV conditions (Figure 4-42). In MMW and LMW there were no differences between samples of blend mixed in a ratio of 1:1:20 with cobalt and hydroperoxide after wet and dry aging.

For the samples of asphalt without polymer the water present in the aging vessel increased asphaltenes aggregation is observed (Figure 4-45). These associations were enhanced by the presence of cobalt and hydroperoxide. The highest asphaltenes association took place when a redox system and water were present (Figures 4-45 and 4-46). One reason for this may be a solvation effect caused by the water, which increased the surface contact area.

The GPC studies presented in chapter 3.3 showed that, in the presence of water, the asphalt aging was slowed down. It was shown also that polymer protected the asphalt during oxidative aging. The wet or dry aged PMAC samples consistently had a lower asphaltenes shoulder than aged asphalt cements.



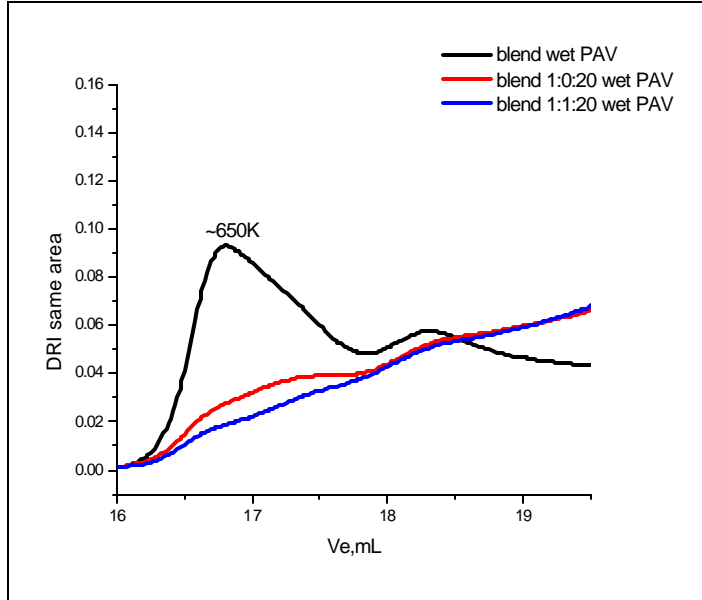


Figure 4-41 GPC traces –HMW details for blend, blend with HP, and blend with redox2, after wet PAV aging.

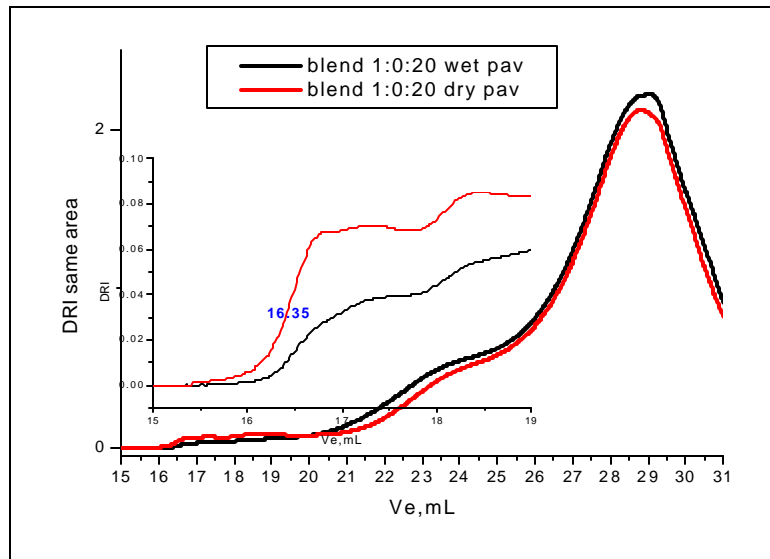


Figure 4-42 GPC traces for blend with HP, after dry and wet PAV aging.

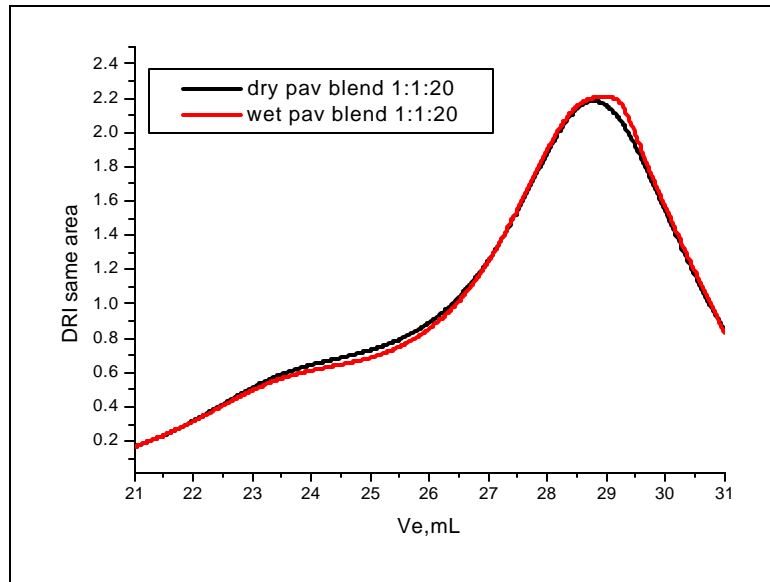


Figure 4-43 GPC traces –MMW and LMW details for blend, with redox2, after dry and wet PAV aging.

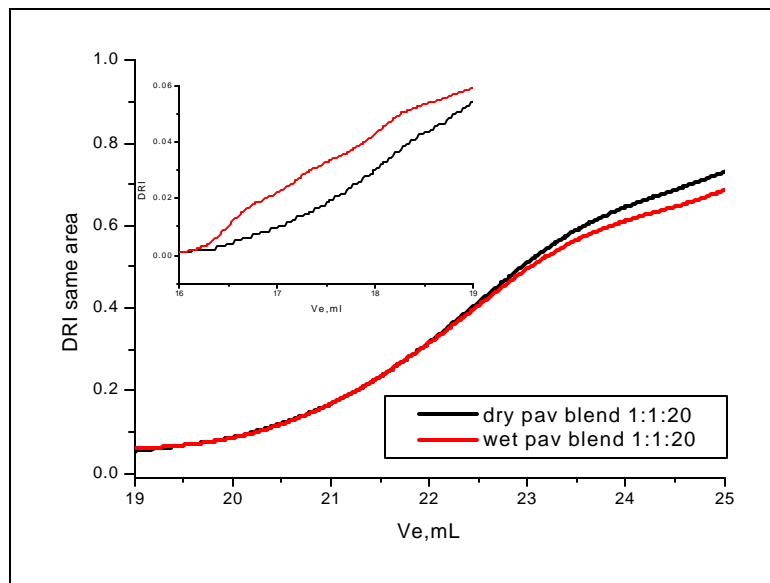
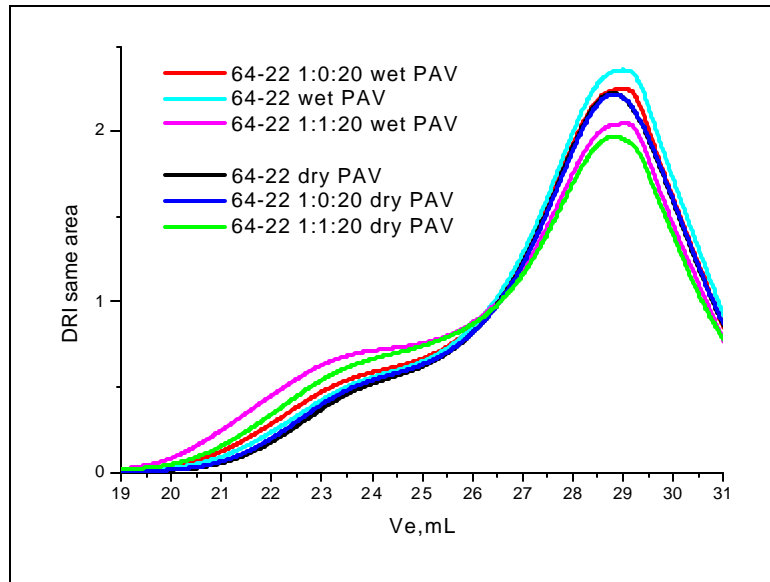
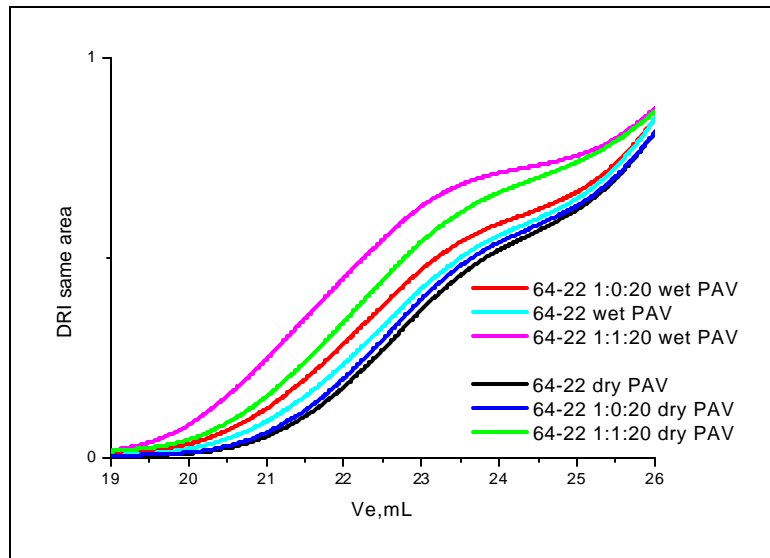


Figure 4-44 GPC traces –MMW details for blend with redox2, after dry and wet PAV aging.



**Figure 4-45 Comparison GPC traces for dry and wet PAV aged asphalt cement with and without redox system**



**Figure 4-46 GPC traces – MMW details - for dry and wet PAV aged asphalt cement with and without redox system**

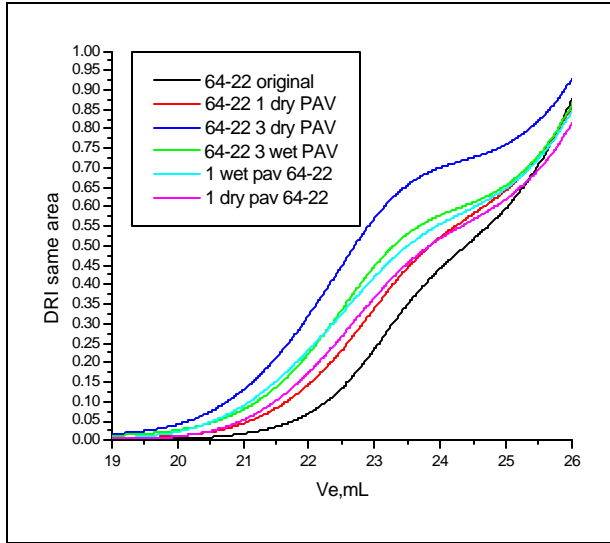


**Figure 4-47 GPC traces – MMW details - for dry and wet PAV aged asphalt cement without redox system**

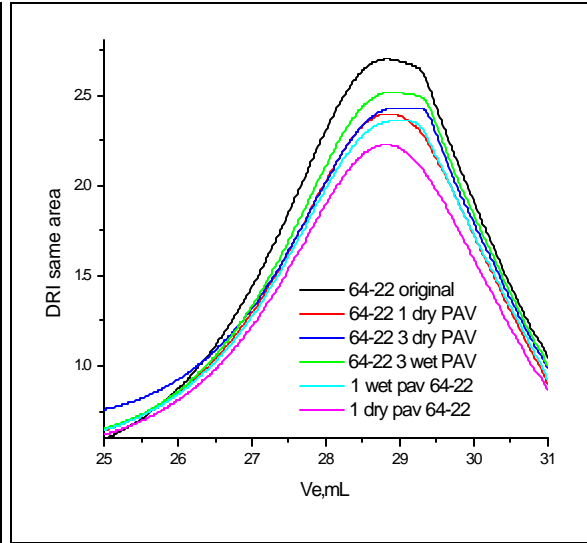


**Figure 4-48 GPC traces – LMW details - for dry and wet PAV aged asphalt cement without redox system**

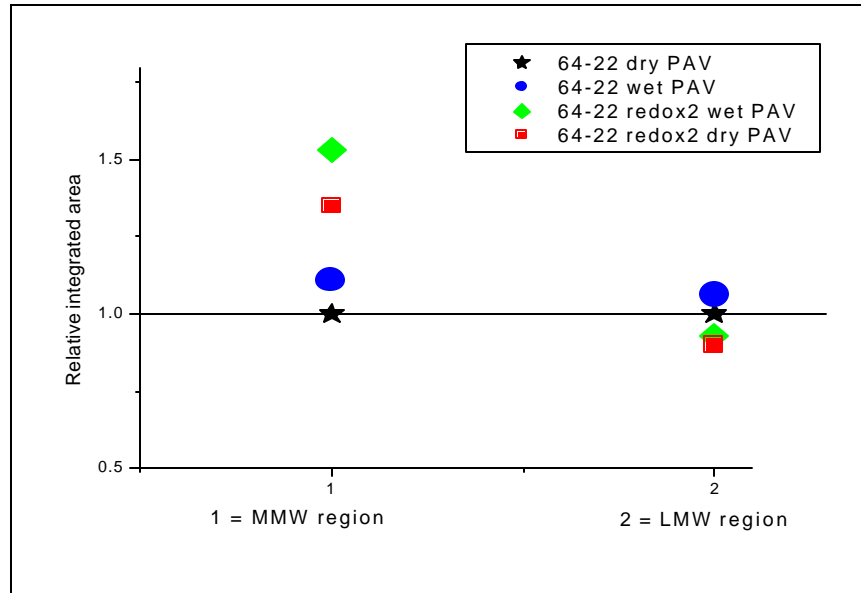


**Figure 4-49 Changes in integrate area from GPC curves for the molecular weight regions MMW (50-3K) and LMW (3-0.4K) for AC 64-22 dry and wet PAV aged, AC mixture with redox2 (1:1:20) dry and wet PAV aged**

In all the samples run in Chapter 3.3 the water had a beneficial influence against oxidation. But the samples analyzed in Chapter 3.3 were treated 3 times under dry or wet PAV conditions. These new sets of samples showed that, before 60 hours of aging, water promoted oxidation (Figures 4-47 to 4-48). As can be seen in Figure 4-47, two samples were tested for 1 dry PAV. There was a difference of one year between the GPC measurements for these samples. This is a proof that data from Chapter 3.3 can be compared to the new samples from Chapter 4 because there were insignificant differences between 1 dry PAV samples. Unexpectedly, 1 and 3 times wet PAV were almost the same age. The 1 wet PAV was a little more aged than 1 dry PAV while 3 wet PAV was less aged than 3 dry PAV. We might say that in the long term water will protect asphalt against oxidative aging. The changes in integrated area for medium and low molecular weight asphalt components showed the same conclusions can be made after reading the GPC curves. The highest concentration in degraded species, translated in asphaltene aggregation, was observed for AC 64-22 with redox2 aged in wet conditions (Figure 4-49). The diffusion of asphaltene with a molecular weight close to 3K by association into molecules with molecular weights closer to 11K was the reason for concentration increment observed in MMW region. This observation is based also on the fact that in LMW region the changes were not comparable to the addition in content of the MMW species. Figure 4-50 shows that, once the redox system was added, 1 dry PAV with cobalt and hydroperoxide complex equaled 3 dry PAV without redox complex. The highest asphaltene aggregation took place after only 1 PAV in the presence of redox system and water. It may be concluded that asphalt is susceptible to a complex metal ions/hydroperoxide/water. Figure 4-51 brings together GPC curves for blend (asphalt with 3% polymer) and AC 64-22 exposed to wet PAV mixed or not with redox pairs (redox2). The conclusion from that figure sustained by the changes of integrated area presented in Figures 4-52 and 4-53 is that the presence of polymer protected the asphalt cement in all the cases.

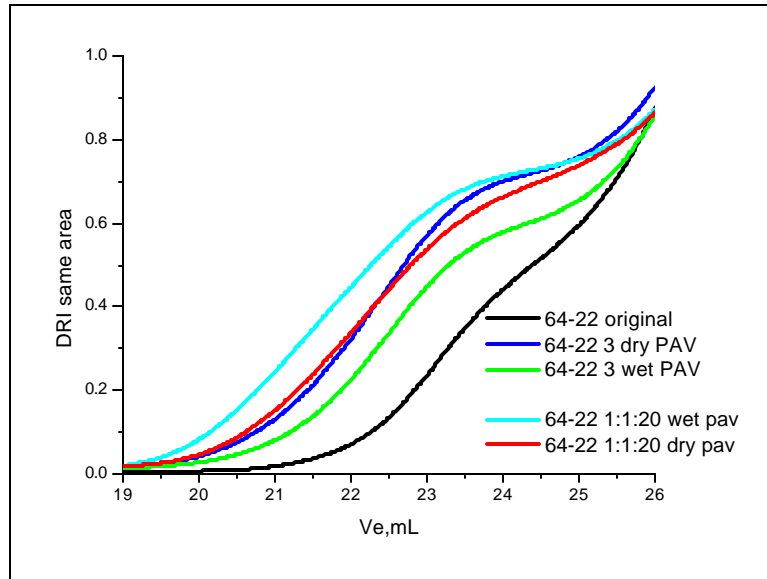


**Figure 4-50 GPC traces – MMW details - for original AC, for 3 dry and wet PAV aged asphalt cement, and for AC mixed with redox2 dry and wet aged**

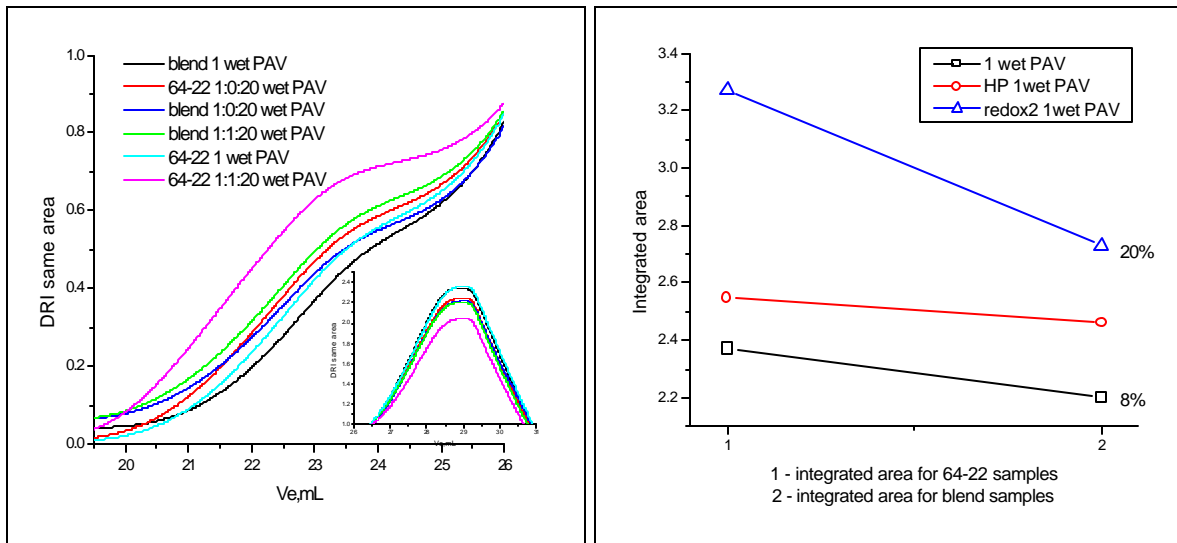


**Figure 4-51 GPC traces – MMW details – comparison for wet aged samples contain AC, AC and HP, AC and redox2, blend, blend and HP, blend and redox2**

**Figure 4-52 GPC results – integrated area for region MMW of the samples from Figure 4-51**

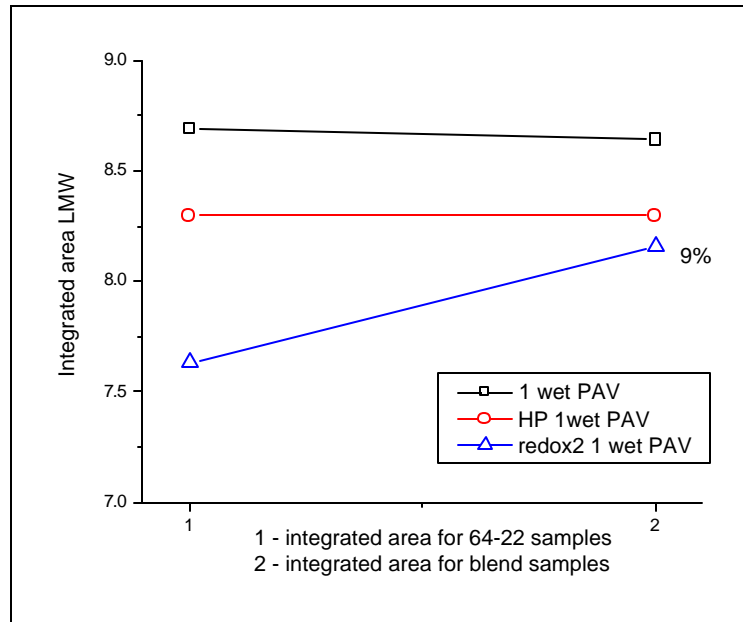


**Figure 4-53 GPC results – integrated area for region LMW of the samples from Figure 4-51**

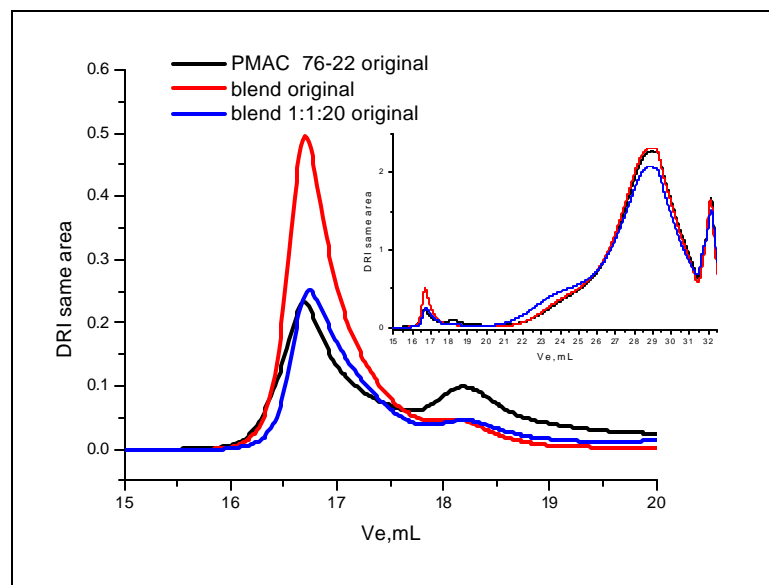


**Figure 4-54 Polymer molecular weight distribution in various blends**

The polymer was primarily subject to oxidative aging and was sacrificed in protection of the asphalt. When polymer was present, as an additive in asphalt, there was a 9% lower content in species in MMW. Oxidative induced aging for blend yielded a lower accumulation in MMW with 20% than samples of asphalt cement without polymer. At the same time LMW species did not indicate a noticeable diffusion into the MMW region.

Figure 4-54 brings together GPC curves for PMAC, blend and blend exposed to induce oxidation by the presence of redox pairs (redox2). The difference between PMAC 76-22 and laboratory blend 64-22 with 3% Calprene polymer was that 76-22 contained at least 15% PEN 150. Also, we know that 76-22 original had around 6.9% of species insoluble in THF.

The GPC (Figure 4-51) shows that the polymer in original 76-22 was already in the degradation process. When polymer was mixed with asphalt, for a better compatibility and storage, sulfur was added, so a crosslinked insoluble polymer was formed. The presence of sulfur has further implications.

Potentiometric titration showed that PMAC samples had strong acids besides carboxylic acids; acids, which can be generated from sulfur, compound oxidations. The presence of sulfur will accelerate the polymer oxidation process. It was expected that the polymer concentration would be lower than with our blend (but not that low).

The next results attempt to compare the laboratory blend to the PMAC already prepared by the supplier 76-22. As the asphaltenes area show the same values for PMAC and the blend, it can be concluded that the polymer from PMAC suffered only crosslinkage not chain scission. Once the redox system was added to the blend, induced oxidation was started at room temperature with scission of polymeric chains (Figure 4-55).

The closest curve to the field sample for MMW asphaltenes and short polymer chains was the dry aged blend (asphalt + polymer) with redox ratio 1:1:4 (Figure 4-56), but the HMW



polymer degradation showed by GPC traces for these samples was not a match with field samples (Figure 4-57).

Another close example is the mixture blend with 1:0.2:20 after 1 dry PAV (Figure 4-58) but, again, there were differences for polymer degradation in the HMW region (Figure 4-59). The PMAC in the field had enough time for slow diffusion process of species with molecular weight of ~3K to form aggregates with higher molecular weights; we might not find the perfect match for it.

The GPC trace for HMW polymer species in the blend with asphalt subjected to TFOT in the presence of redox2 system 1:1:20 came closer to the field samples, but with a different magnitude. The integrated areas for “the best matches” with asphalt samples extracted from the field are presented in Table 4-1. This means that the stoichiometric ratio used might work to model aging if a lower concentration of redox agent per gram of asphalt was added. It is reasonable to conclude that a ratio 1:0.2:4 will give closer results to the field. It is also reasonable to consider controlling free-radical oxidation in laboratory simulation to a slower rate by adding very small concentrations of hydroperoxide and cobalt at longer difference in time.

**Table 4-1 Comparison of integrated area for field aged asphalt samples and laboratory blend with redox1 and redox5 dry PAV aged**

	Integrated Area HMW	Integrated Area MMW	Integrated Area LMW
3 years field aged	0.27	2.82	7.80
5 years field aged	0.25	2.98	7.68
Blend +redox5 1 dry PAV	0.12	3.12	7.65
Blend +redox1 1 dry PAV	0.16	2.90	7.80

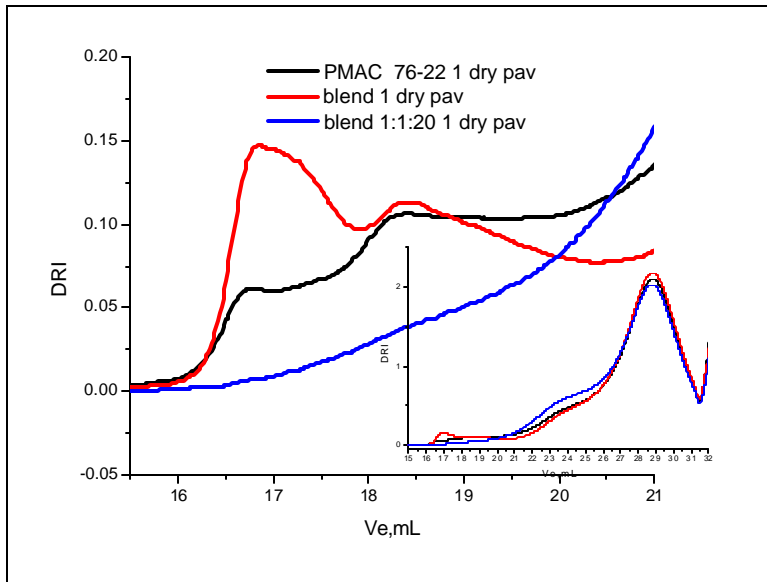


**Figure 4-55 PAV aging effect on polymer in different blends**

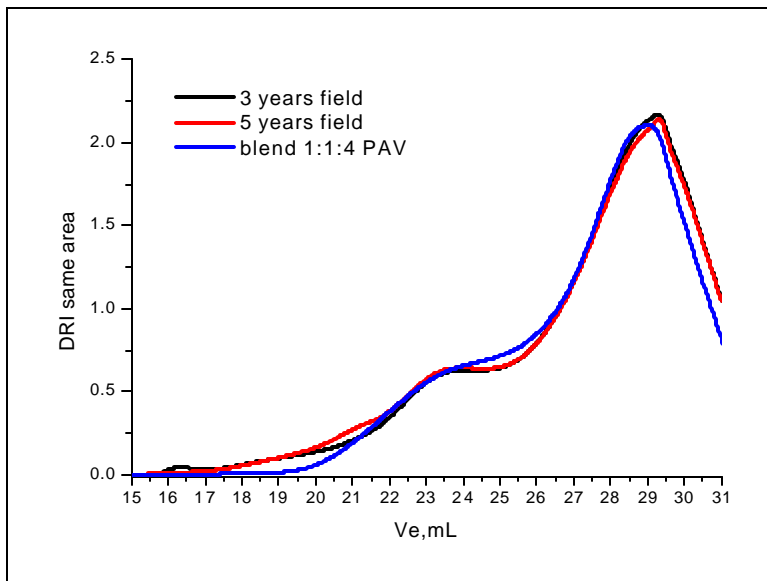


**Figure 4-56 GPC traces for 3 and 5 years old-field aged asphalt compared to trace for blend with redox5 dry PAV aged**

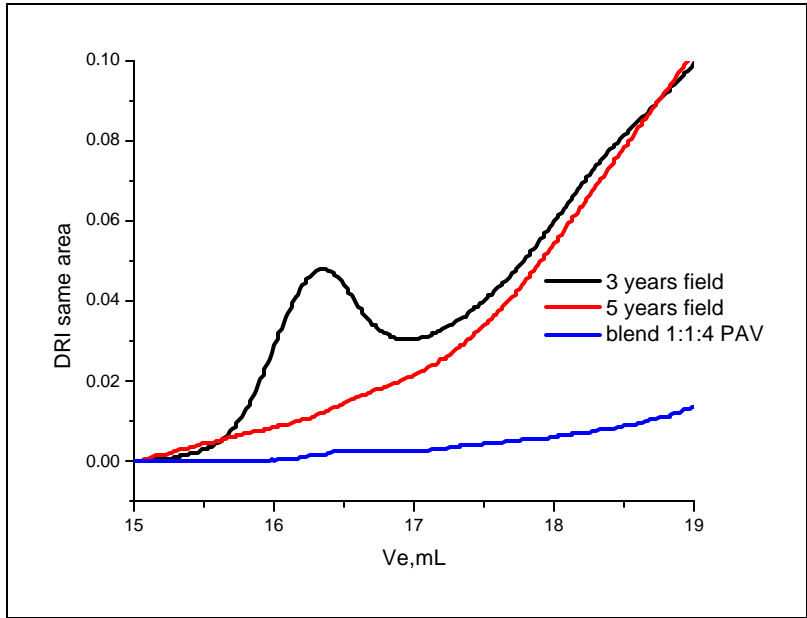


**Figure 4-57 GPC traces for 3 and 5 years old field aged asphalt compared to trace for blend with redox5 dry PAV aged –details HMW region**

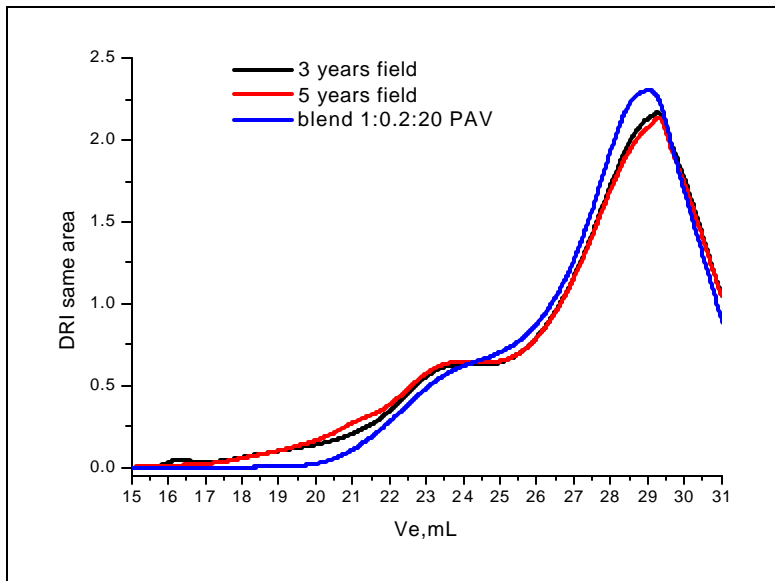


**Figure 4-58 GPC traces for 3 and 5 years old-field aged asphalt compared to trace for blend with redox1 dry PAV aged**

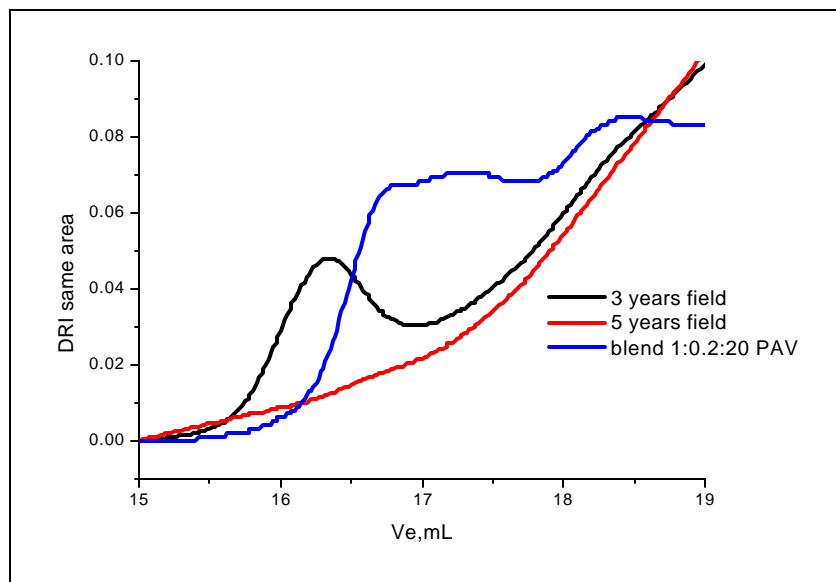


**Figure 4-59 GPC traces for 3 and 5 years old-field aged asphalt compared to trace for blend with redox1 dry PAV aged- details HMW region**

#### 4.1 CONCLUSIONS

The expected results from oxidation reaction were to have a decrease in HMW polymer species with a segment diffusing to MMW and another segment to become insoluble. This was the case for the samples with polymer. PAV aging yielded 55% degradation of HMW, but only 15% of the fragments were found in MMW region, leading to the conclusion that 40% of the polymer components became insoluble crosslinked species. At room temperature the induced oxidation accelerated HMW loss, leading to a decline in concentration of 80% compared to the original polymer concentration. The reduction in HMW was accompanied by the diffusion of a 25% of the fragments to MMW and the formation of 55% insoluble species. The chain propagation of induced oxidation continued with scission of network bridges during PAV. Redox1 (less cobalt) promoted the cleavage of 45% of the insoluble species (80%) created by the initial mixing of polymer with redox1; 35% of the fragments created were seen in HMW range and 10% diffused to MMW region. Redox2 (1:1:20) provoked solvation of 75% of species which

initially crosslinked at room temperature and brought them in HMW range. After these computations it looks that after redox1 and PAV there are 10% more insoluble species than were after polymer PAV aged and after redox2 and PAV the value for insoluble polymer is the same with PAV-aged polymer.

The expected molecular distributions for asphalt cement species after being subjected to oxidative aging was a rise in concentration of MMW species due asphaltene associations along with a lower concentration in LMW region. The dry PAV operation on AC 64-22 produced a 30% increase in MMW asphaltene associations; to this increment 4% was molecule diffused from LMW region, and 26% was a rearrangement of MMW species, molecules with around 3K molar mass to associated molecules with ~11K molar mass.

At room temperature redox systems brought an increase in asphaltenes association at up to 37%, 10% came from LMW and 27% within the region diffusion. After dry PAV redox systems do not continue the degradation of LMW species but intra-region diffusion in MMW continue with another 23% LMW are not susceptible to redox more than 10%. The higher damage is brought by redox5 (1:1:4)

The blend prepared in laboratory (AC 64-22 with 3% polymer) showed after dry PAV operation a 10% increment in HMW, 30% increment in MMW and 5% decrease in LMW. At room temperature the addition of redox systems accelerated polymer oxidation. GPC curves for Redox5 and redox1 showed 60-70% less concentration in HMW species while for redox2 shown 35%.

Redox2 (1:1:20) at room temperature determined a growth in MMW concentration of 30% and lower LMW content of 10%. So, 10% from LMW diffused to MMW and 20% of HMW diffused to MMW. This yielded 15% insoluble species.

Redox1 (1:0.2:20) induced an increase of concentration in LMW range of 5%, which could be derived from MMW region. This increase might also be connected with the excess of hydroperoxide. As MMW showed a 30% increment, a 35% from decomposition of HMW was transferred to MMW, leaving uncounted a 25% insoluble species. The lowest uncounted insoluble percent, 10%, was computed for Redox5 (1:1:4) which did not produce any changes in LMW range, and a 60% increment to MMW was observed from chain scission of 70% polymer.

At room temperature dilution by asphalt protected the polymer against redox (lower extend of degradation was observed in HMW for the blend mixtures). Polymer protected the asphalt against the redox system, as the MMW concentration is lower relative to asphalt alone exposed with redox systems. In the case of redox5 the 60% increment in MMW is due to a massive chain scission reaction since the GPC trace for this sample showed this diffusion from HMW to MMW. It was observed that LMW could not associate more than a total 10% (5% more when redox system were present than PAV aged blend). An increase in MMW of 20-30% more for the blend-redox systems mixtures compared to aged PAV blend was observed. Without polymer additive, the MMW for asphalt cement alone with redox pairs went up to 50% more

After dry and wet PAV operations the GPC traces for AC and AC mixed with redox2 were analyzed. Examination of GPC curves led to a conclusion that 1 wet PAV might have been very close to 1 dry PAV. Relative integrated area computations showed that there are 10% more MMW species for sample aged in humid conditions with respect of dry-aged asphalt. Higher concentration in MMW (20% more) was observed for asphalt mixed with redox2 aged in wet conditions compared to asphalt-redox2 aged in dry conditions.

The polymer served as a sacrificial antioxidant and protected the asphalt components from oxidation. (Figure 4-51 to 4-53). When polymer is present, as additive in asphalt, there is a lower content in species in MMW of 9%. Oxidative induced aging for blend yielded a lower

accumulation in MMW with 20% than samples of asphalt cement without polymer. At the same time LMW species do not show a noticeable diffusion to the MMW region.

Comparison of the integrated areas for asphalt binders aged 3 and 5 years on the road, showed that a blend (asphalt and polymer) with redox system 5 (1:1:4) and redox system 1 (1:0.2:20) closely matched field aging. It is reasonable to conclude that a ratio 1:0.2:4 will give closer results to the field. It is also reasonable to consider controlling free-radical oxidation in laboratory simulation to a slower rate by adding very small concentrations of hydroperoxide and cobalt at longer difference in time could be a better model.

From the induced oxidation test it can be concluded that polymer protects the asphalt. It is necessary to have a stoichiometric ratio between metal ions and hydroperoxides to induce higher polymer degradation. If water is present, the oxidation reaction effects increased in the presence of redox system. However the water will keep the oxidation aging to a constant level (simulated in laboratory by 3 times PAV wet cycles).

## CHAPTER 5

### RHEOLOGY ANALYSIS

For practical purposes it is important to correlate chemical changes due to oxidative hardening with changes occurring in physical properties. Upon aging, in-service asphalt cement becomes stiffer, suggesting systematic microstructural changes as steric hardening is observed with rheological measurements.<sup>37</sup> Rheology is the study of deformation and flow of matter. Deformation and flow of the asphalt binder in HMA is important in determining HMA pavement performance. HMA pavements that deform and flow too much may be susceptible to rutting and bleeding while those that are too stiff may be susceptible to fatigue or thermal cracking. HMA pavement deformation is closely related to asphalt binder rheology.

To characterize the viscous and elastic behavior of the asphalt binder a AR 2000 TA Rheometer instrument set up in Dynamic Shear mode was used to measure complex shear modulus  $G^*$  (total resistance of a material to deforming when repeatedly sheared) and phase angle  $\delta$  (relative amounts of recoverable and non-recoverable deformation). By measuring  $G^*$  and  $\delta$ , the DSR software is able to determine the total complex shear modulus as well as its elastic ( $G'$ ) and viscous ( $G''$ ) components.<sup>38</sup>

An elastic material (Figure 5-1a) experiences recoverable deformation when subjected to a constant (or creep) load and will immediately return to its initial shape when the creep load is removed ( $\delta=0^\circ$ ,  $G'=G^*$ ). The deformation of the viscous material (Figure 5-1c), however, will remain after the load is removed; hence, a viscous material experiences non-recoverable deformation ( $\delta=90^\circ$ ,  $G''=G^*$ ). A visco-elastic response is presented in Figure 5-1b; after the load is removed the material will partially recover, accumulating a permanent deformation. Asphalt



binders are viscous at high temperature and elastic at a low temperature below service temperature. At temperatures where most pavements carry traffic, asphalt acts as a visco-elastic material.

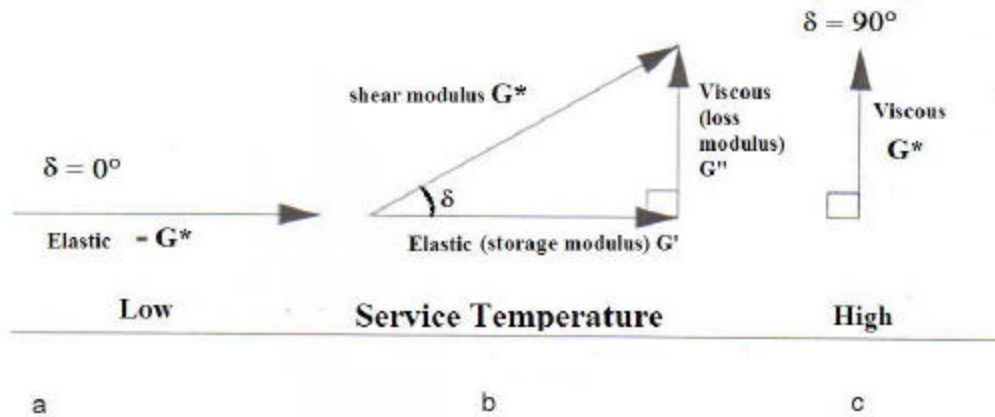


Figure 5-1 Principle of visco-elasticity <sup>29</sup>

## 5.1 CRITICAL TEMPERATURE

By adding polymers, such as cross-linkable SBS, the gel character of asphalt cements is enhanced. The three dimensional network resists deformation and recovers the initial shape at temperatures at which the storage modulus ( $G'$ ) is superior to the modulus describing the viscous character of the asphalt, i.e., the loss modulus ( $G''$ ). The effectiveness of the network diminishes rapidly above the cross-over temperature at which these two moduli become equal ( $G' = G''$  at  $\delta = 45^\circ$  for which  $\tan\delta = 1$ ).<sup>39</sup> This cross-over temperature (to be called critical temperature,  $T_c$ , in the following) was proposed to discern the changes in rheological characteristics of polymer modified asphalts brought about by aging. The cross-over temperature depends, however, on the frequency at which the test is conducted: the higher the frequency, the higher the temperature. Therefore for each temperature a relaxation time can be determined, corresponding to the frequency at which the moduli are the same: the higher the temperature, the shorter the time. An

example is shown in Figure 5.1-1 that describes the variation of  $\delta$  of the 30 hours PAV dry-aged PMAC sample. In this example  $\tan\delta=1$  for  $T_c=42.8^\circ\text{C}$ .<sup>3</sup>

The results are presented in Figure 5.1-2 and table 5.1-1. Extremely high critical temperatures have been recorded after 60 hours dry PAV aging. Surprisingly, wet-aging produced much softer materials, with a  $T_c$  of samples wet-aged for 50 hours equivalent to that of dry-PAV samples aged for only 30 hours.

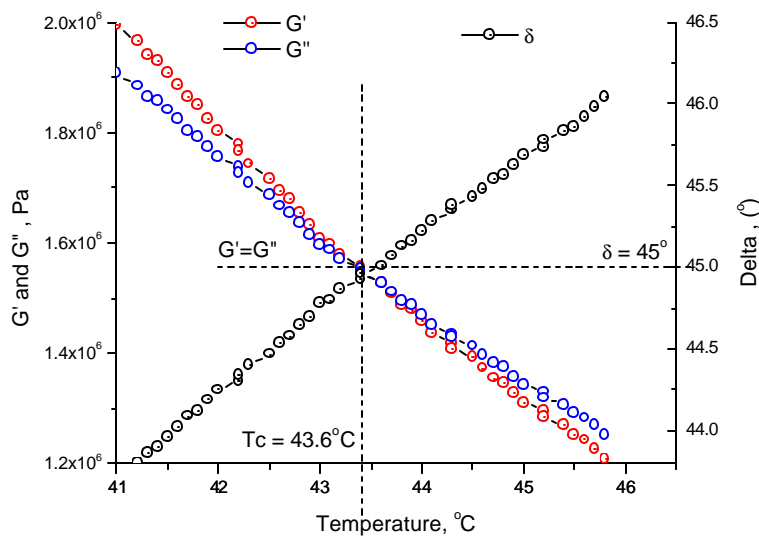


**Figure 5.1.1 Plot of  $G'$  and  $G''$  vs. frequency applied to the determination of the cross-over temperature of the AC 64-22 aged without water for 30 hrs (1.5 PAV)<sup>3</sup>**

Critical temperatures of PMAC laboratory aged samples were compared with that of asphalt samples extracted from field aged pavements.

Perusing data listed in this table we might conclude that the maximum critical temperature exhibited by the sample aged for 7 years is somewhere between the PMAC sample aged for 20 hours in the presence of water (one dry PAV cycle) and without water, while shorter periods of aging on the road (3-5 years) produced samples with a cross-over temperature somewhat closer

to that of PMAC samples aged for 10-20 hours. These data are almost in the same direction with the conclusion from previous measurements (FTIR and GPC).

**Table 5.1-1 Critical Temperatures data collection**

Hours PAV	T <sub>c</sub> , °C Dry PAV	T <sub>c</sub> , °C Wet PAV	field years	T <sub>c</sub> , °C
0	9.5			
10	23.7	20.3	3	21
20	30.8	22.1	5	27.3
30	42.8	35.5	7	29.4
40	55	41		
50	58.9	43.2		
60	71	63.2		
80	89.4			
100	104.1			

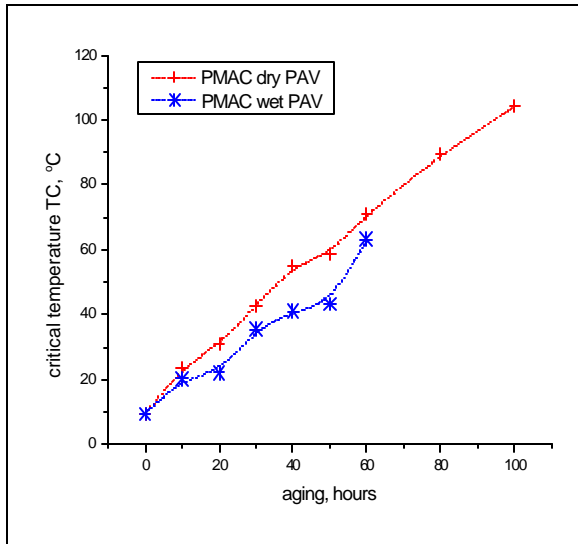


**Figure 5.1-2 Variation of critical temperature of multiple PAV dry-aged and wet-aged PMAC samples**

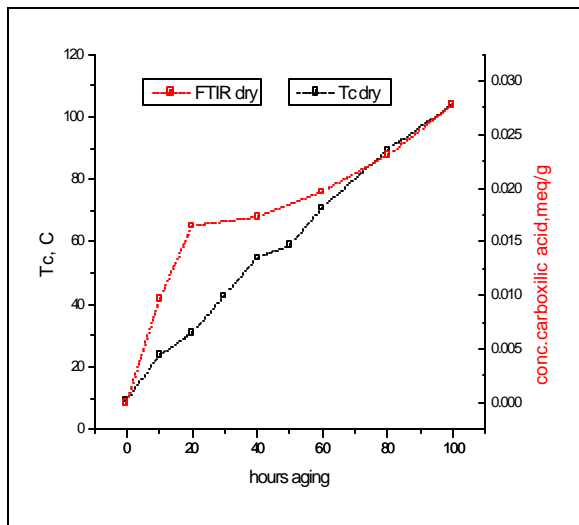


**Figure 5.1-3 The correlation between carboxylic acid concentrations determined from FTIR data and T<sub>c</sub> of samples aged in dry PAV conditions**

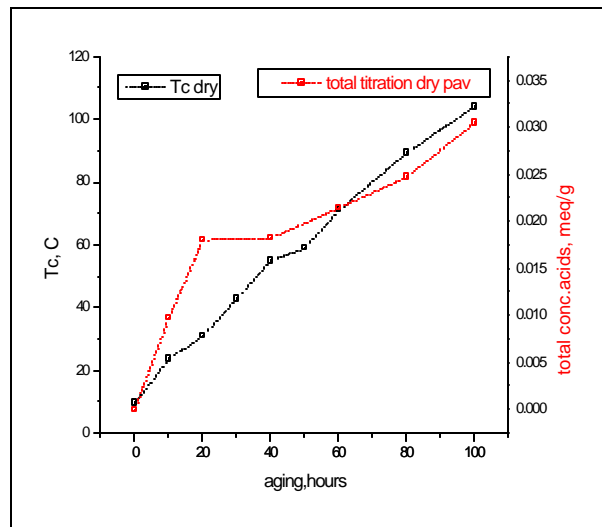


**Figure 5.1-4 The correlation between carboxylic acid concentrations determined from PT data and T<sub>c</sub> of samples aged in dry PAV conditions**

A short overview about how chemical changes by oxidation influence physical changes for PMAC aged in laboratory are presented in Figures 5.1-3 and 5.1-4. Formation of acid groups during oxidative aging analyzed with potentiometric titration and FTIR methods does not follow critical temperature changes. This means that chemical changes analyzed address primarily the polymer and less to the asphalt species. However, the critical temperature values, as a measure of physical changes, are determined by changes in the asphalt composition. Figure 5.1-5 shows a parallelism between rheological determinations of critical temperature for PMAC and the changes of integrated area from GPC traces for medium molecular weight distribution (MMW ~50-3K). The changes of integrated area for HMW polymer species do not follow the changes in critical temperature. The percentage of insoluble polymer values for aged polymer in PMAC is still under study in our laboratory. When SBS is used as an asphalt additive, the oxidative aging changes the polymeric matrix towards an open gel structure still capable of stabilizing asphaltene/maltene emulsion. As has been mentioned in previous chapters, the oxidation process is controlled at a given temperature by the reactivity of the binder and the rate of diffusion of oxygen into the binder. As the viscosity of asphalt increases, the coefficient of diffusion of oxygen decreases. The coefficient of diffusion was found to also be dependent on the concentration of chemically bound oxygen, viz., as the later increases the coefficient decreases.<sup>40</sup> The concentration of chemically bound oxygen was found to be higher in asphalt samples aged in the presence of water both in this work and in other investigations.<sup>17</sup> Therefore, water might moderate the aging process towards a more open gel structure that translates to a “softer” material with a corresponding lower  $T_c$ .<sup>3</sup> From previous chapters an idea about a comparison between those two aging methods has been formed. It is the aim of rheology to provide a clearer picture of this comparison, as shown in Figure 5.1-6. It appears that the RCAT oxidative aging

needed an induction period of several hours. Therefore equivalence was observed between 24 hours airflow RCAT-aged samples and 10 hours dry PAV. After that, both the PAV- and RCAT-aging processes developed divergently with an almost linear progress (Figure 5.1-7). This linear progress was not observed from the FTIR RCAT-PAV data correlation (Figure 5.1-8). The much higher reaction rate determined by PAV conditions (100°C and 300 psi vs. 90°C and 6-7 psi RCAT parameters) resulted in an equivalence of 2 PAV operations (40 hours) with >200 hours RCAT (as compared to 4 PAV vs. ~200 hours RCAT for FTIR equivalence). These findings do not compare well with data on RCAT aging in air at 90°C of different asphalt binders, both plain and polymer-modified which indicated that simulation of long term aging – as obtained in 1 PAV operation – required some 140 hours of continuous operation.<sup>41</sup> Moreover, comparison of  $T_c$  of laboratory- and field-aged samples (Table 5.1-2) shows that less than 19 RCAT aging hours were necessary to achieve the same  $T_c$  as that of the field PMAC sample extracted from cores collected from MS Hwy 155 after 3 years of service (as compared to more than 48 RCAT hours to achieve an FTIR acidic group equivalence, Table 3.1-4). The equivalence for the sample extracted from cores after 5 years of service was achieved after 48 RCAT hours (as compared to 193 RCAT hours for FTIR equivalence). The equivalent RCAT time was <70 hours (~ >200 hrs FTIR equivalence, Table 3.1-4).<sup>24</sup>

**Table 5.1-2 Critical temperatures  $T_c$  ( $\tan \delta = 1$ ,  $G' = G''$ ) of aged PMAC samples determined at a frequency of 10 rad/s**

PAV Aged, Hrs	T (°C) @ $\tan \delta=1$	RCAT Aged, Hrs	T (°C) @ $\tan \delta=1$	Field Aged, Hrs	T (°C) @ $\tan \delta=1$
0	9.5	6	18.6		
10	23.7	19	22.7	3	21.0
20	30.8	24	23.2		
30	42.8	48	27.4	5	27.3
40	55.0	73	31.6		
60	71.0	143	42.4		
80	89.4	169	45.6		
100	104.1	227	56.4		

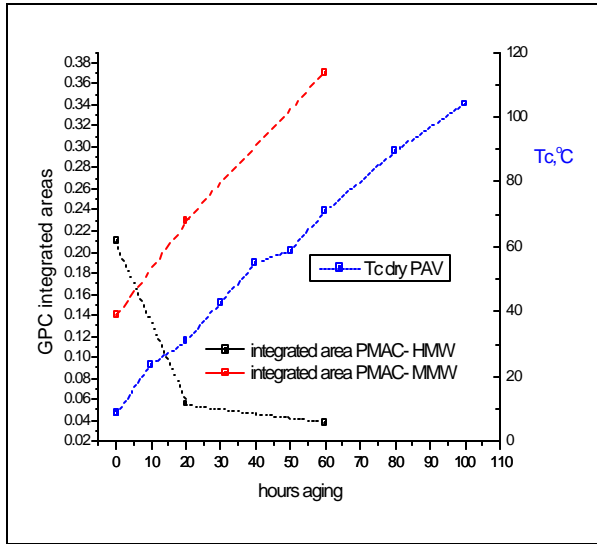


**Figure 5.1-5** The correlation between integrated area from GPC traces and Rheology results for PMAC samples - dry PAV

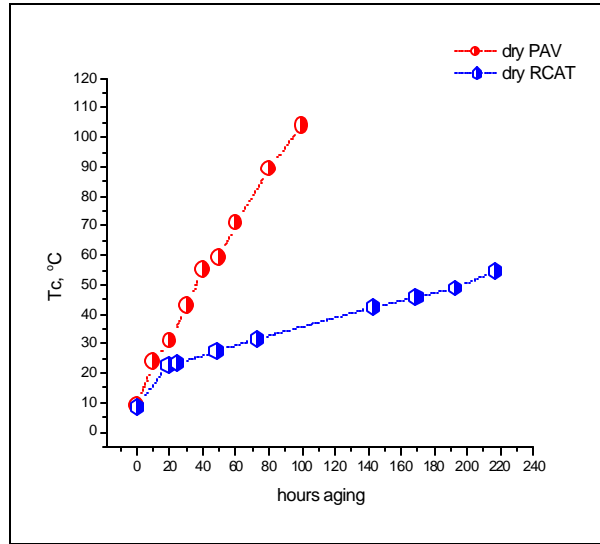


**Figure 5.1-6** Comparison between rheological parameter  $T_c$  of laboratory aged PMAC samples

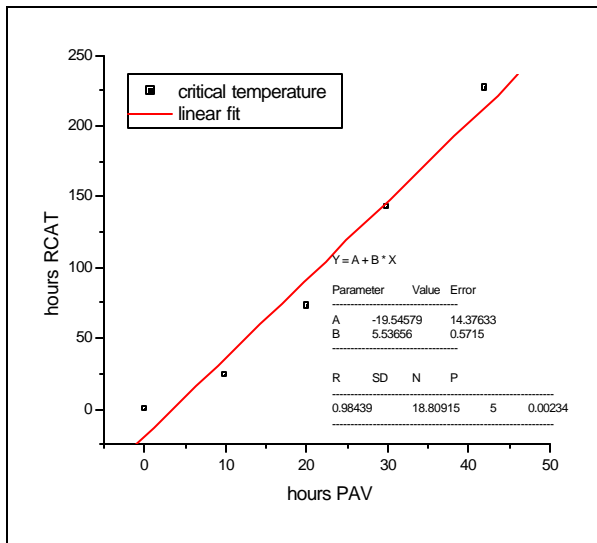


**Figure 5.1-7** Linear equivalence RCAT-PAV for  $T_c$  aged PMAC

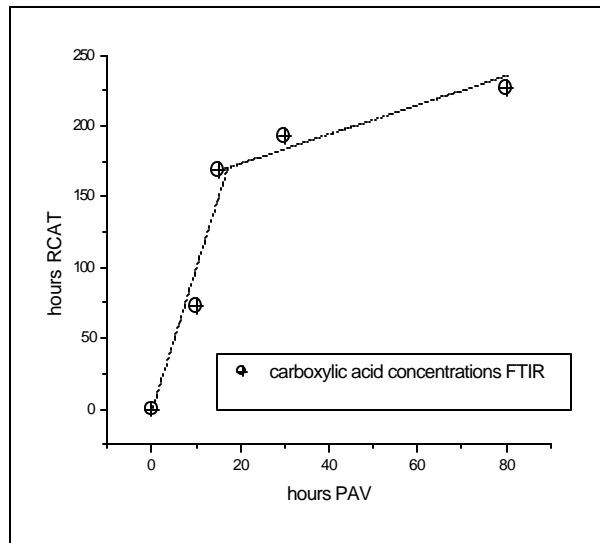


**Figure 5.1-8** Non-linear equivalence RCAT-PAV carboxylic acid concentrations for aged PMAC

## 5.2 REPEATED CREEP AND CREEP-RECOVERY TEST

Another important characteristic of the visco-elastic behavior of asphalt cement is the relaxation process estimate using the same DSR procedure in repeated creep and creep recovery test.

Asphalt binders are viscoelastic materials and, when subjected to a constant load, will deform at a constant rate until the load is removed. The deformation is a combination of elastic response and viscous flow. The magnitude of deformation, or mechanical response, is dependent on load magnitude, duration, and rate of application and the temperature state of the material. The deformation, however, will remain after the load is removed and the material will experience non-recoverable deformation.

Repeated creep and recovery test for binders (RCRT) was suggested by Bahia et al.<sup>42</sup> as a possible means to estimate the rate of accumulation of permanent deformation (strain) in asphalt binders (Figure 5.2-2). The RCRT test protocol consists of applying a creep load of 25 to 300 Pa for 1-second duration (loading time) followed by a 9-second recovery period (rest period) for 100 cycles. Also, the loading time can vary 1, 2 or 3 seconds, respectively. Accordingly, the recovery time should be 9, 18 or 27 seconds, respectively. Higher deformations were obtained for higher creep loads or longer loading times (Figure 5.2-1).

Asphalt deformation reflects the stiffness of the material that is dependent on temperature. Observing the same experimental conditions, the RCRT test is a valuable tool for monitoring the viscous response of asphalt binders as the material aged, as shown for repeated PAV-aging of PMAC (Figure 5.2-3).

Accumulated strain varies with temperature. The lowest temperature this test could be run at was the critical temperature (Figure 5.2-4); the asphalt was too brittle at a lower temperature. The

higher displacement is achieved at high temperature. Accumulated strain varies also with aging conditions. The differences are presented in Figure 5.2-5 for PMAC aged 10 hours in dry and wet conditions.

The water softened the samples with the result that more accumulated strain was shown by wet aged samples. The higher difference response between wet and dry aged samples was shown at the highest stress applied (300 Pa). During aging, the asphalt binder becomes stiffer which is why the older sample exhibited a lower accumulation in strain. Although oxidation of the asphalt components may be retarded by the presence of the water, age hardening continued to occur.

The asphalt suffered a large transformation between 0 and 20 hours PAV from a stiffness rheology point of view (Figure 5.2-6). These observations correlate with GPC analyses, where it was shown that polymer chains are broken in low molecular weight, inducing changings in the viscoelastic response of the binder.

Dry and wet samples exhibit an exponential growth in viscosity correlated with exponential decay of accumulated strain (Figure 5.2-7). The water “helped” the asphalt as was seen in previous tests also; aged PMAC in the presence of water is softer with lower viscosity. The accumulated strain and displacement for field samples also decreased 2.25 times in two years. Lab aged samples presented a decay of 6-7 times for every 10 hours PAV till 20 hours PAV when it reduced to 2.5 times. In the meantime, the viscosities increased 6-7 times. The binder extracted from the road samples (Figure 5.2-8) exhibited an almost linear displacement over 1000 cycles of repeated 25 Pa load and 70°C. In two years the binder aged in field lost almost half of its capability to recover. Deformation (strain) accumulated after 1000 cycles (1 second loading 25 Pa followed by 9 second recovery periods) at 70°C of laboratory aged binders and field-aged binders are compared in Table 5.2-1. The values of accumulated strain (displacement) for wet aged samples are slightly higher than dry aged samples for 10 hours PAV.



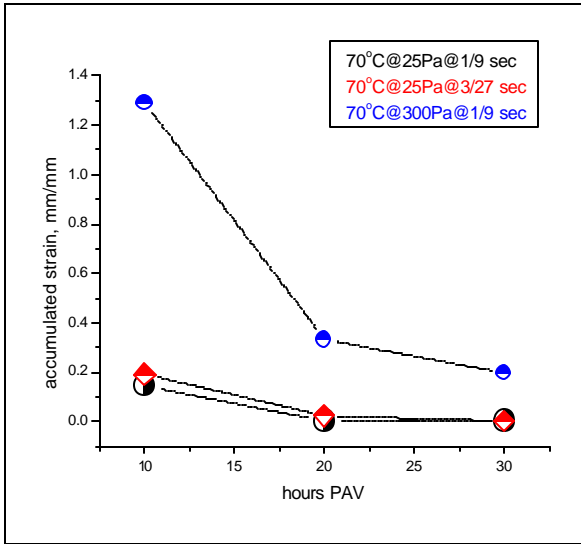


**Figure 5.2-1 Accumulated deformation (strain) of PMAC during RCRT test at different loads and loading times.**

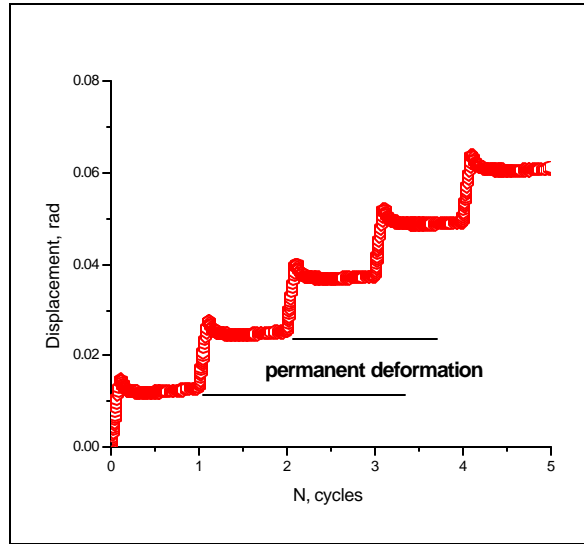


**Figure 5.2-2 Output for RCRT test (original PMAC)**

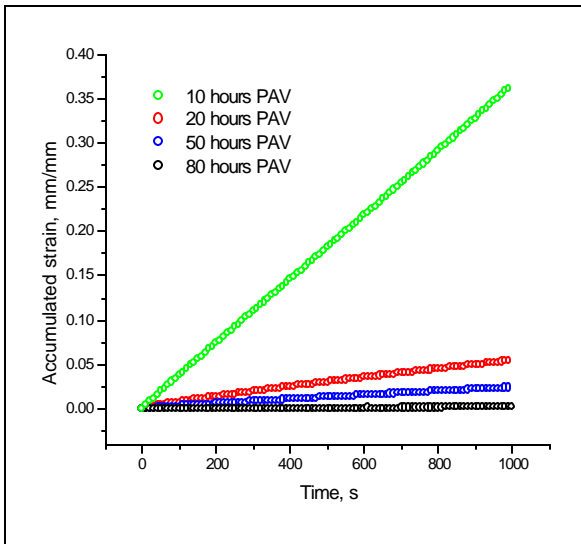


**Figure 5.2-3 Accumulated deformation (strain) of PAV-aged asphalt binder.**

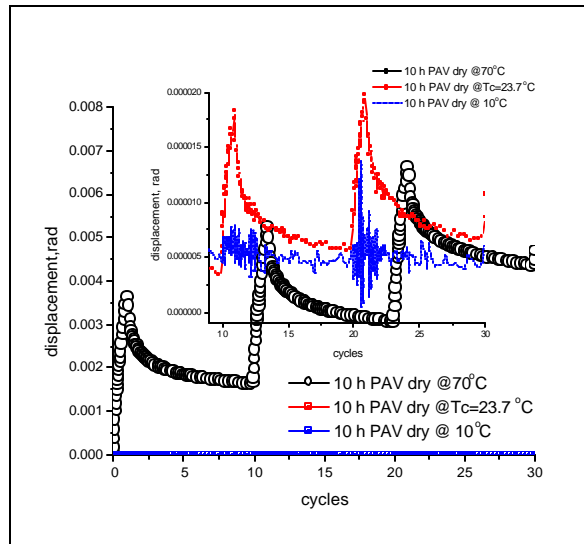


**Figure 5.2-4 Accumulated deformations PMAC 10 hours dry PAV aged for three temperatures**

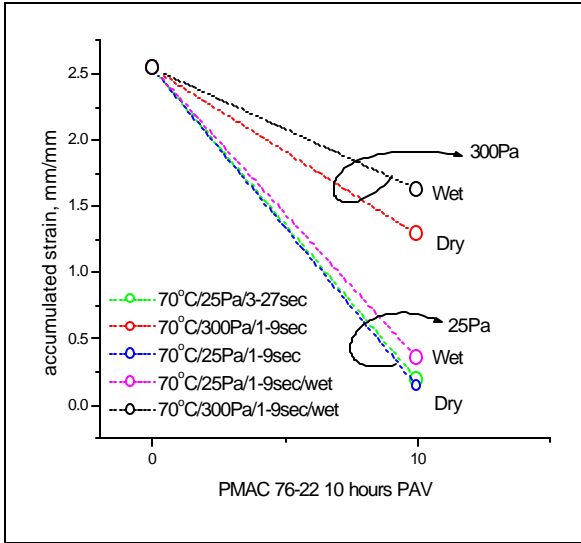


**Figure 5.2-5 Wet vs. dry aged samples in different condition test**

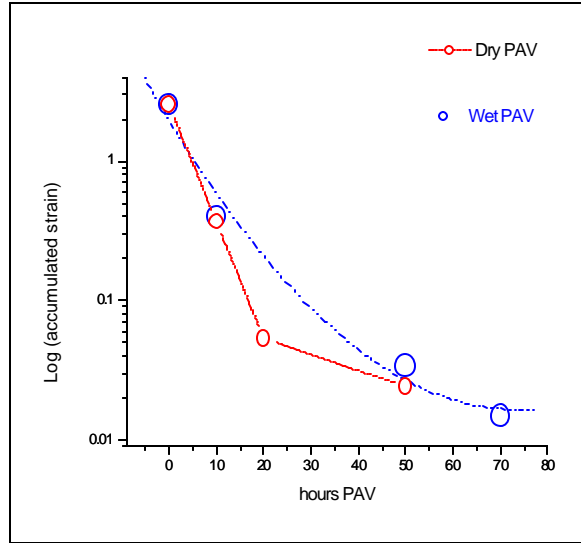


**Figure 5.2-6 Comparison accumulated strain for PMAC aged in wet and dry conditions**

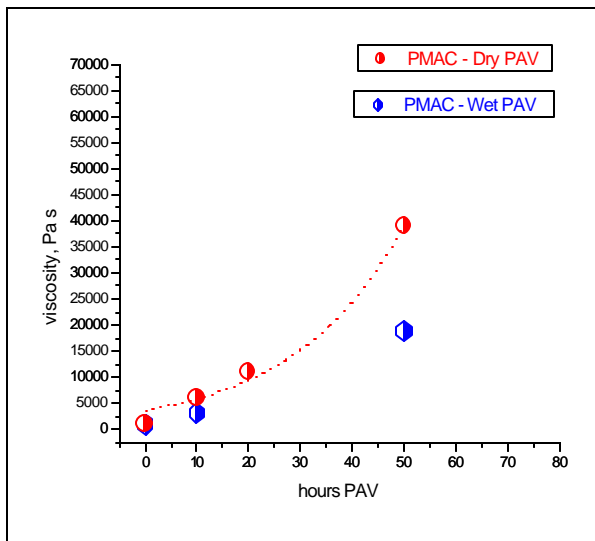


**Figure 5.2-7 The changes in viscosity for PMAC dry and wet PAV aged**

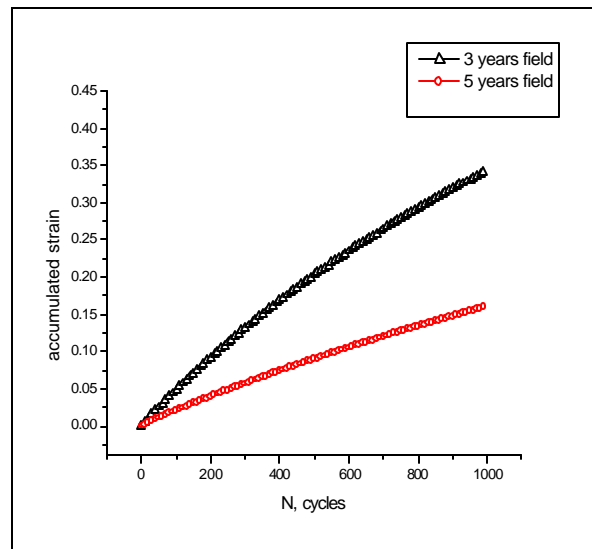


**Figure 5.2-8 RCRT- changes of accumulated strain for asphalt field-aged samples**

**Table 5.2-1 Data collection from creep-recovery test 1/9 25 Pa and 70°C**

Hours PAV	Acc.strain Dry	Acc. strain Wet	Displacement Dry	Displacement Wet	Viscosity Dry	Viscosity Wet	Years Field	Acc. strain	Displacement	Viscosity
	mm/mm		rad	rad	Pa s	Pa s		mm/mm	rad	Pa s
0	2.5324	2.5324	1.2671	1.2671	956	956				
10	0.3651	0.3942	0.1826	0.1926	6012	3159	3	0.3638	0.1819	4073
20	0.0531		0.0272		11160					
30							5	0.1605	0.0803	7019
50	0.0240	0.0336	0.0120	0.0168	39090	18840				
70		0.0148		0.0074		64620				

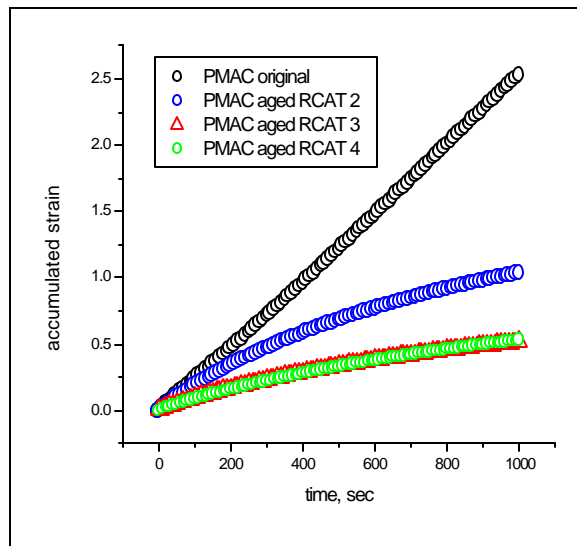


**Figure 5.2-9 RCRT for original PMAC and for RCAT aged PMAC**

After 50 hours, the wet aged samples show a noticeable increment in displacement (accumulated strain) relative to dry aged PMAC. Accumulated strain values for asphalt aged in the field situate 3-year-old close to 0.5 dry PAV aged PMAC, and 5-year-old between 0.5 and 1 PAV aged PMAC samples.

Deformation (strain) accumulated after 1000 cycles, 25 Pa at 70°C of laboratory- PAV- RCAT-and field-aged binders are compared in Figure 5.2-9 and Table 522. Perusing the data

listed in this table it can be concluded that there is no good match between dry PAV and RCAT samples. Around 200 hours under RCAT conditions produces a material similar to 15 hours PAV aged. PAV-aging for 10 hours or RCAT aging for >48 hours produced a material similar to the 3 year field-aged binder, while PAV-aging for >10 hours or RCAT aging for <73 hours produced a material similar to the 5 year field-aged binder.

**Table 5.2-2 Accumulated deformation of laboratory - and field aged binders after 1000 cycles (1 second loading 25 Pa followed by 9 second recovery periods) at 70°C.**

PAV	Accumulated	RCAT	Accumulated	Field	Accumulated
0	2.5324	6	1.0394		
10	0.3651	19	0.5139	3	0.3638
20	0.0531	24	0.5294	5	0.1605
50	0.0240	48	0.4070		
80	0.0014	73	0.1502		
		227	0.1005		

### 5.3 CONCLUSIONS

The asphalt architecture has been simulated with that of a gel. The cross-over temperature at which  $G''$  equals  $G'$  as temperature increases was considered as the critical temperature and chosen as a criterion to assess the advancement of hardening (aging). Critical temperature is dependent on frequency and therefore data have been compared at a frequency of 10 rad/s. Initially the SBS copolymer additive helped to disperse the asphaltenes. Breaking of C=C bonds shortened the B blocks and encouraged formation of an open gel structure. Upon aging, the copolymer crosslinked and contracted around the asphaltene aggregates. The combination of these effects with aggregation of asphaltenes led to an increase of the PMAC critical temperature. Water had a retarding effect on hardening. Critical temperatures of asphalts aged in presence of water were inferior to that of dry-aged PAV samples.

Critical temperature of the asphalt extracted from field 3-year-old sample correlated better with the laboratory wet PAV aged PMAC sample (between 0.5 and 1 wet PAV). Critical

temperature of the 5 years field-aged asphalt sample was intermediate between  $T_c$  of the dry 0.5 PAV and that of the dry 1.0 PAV laboratory aged PMAC samples.

The values of accumulated strain (displacement) strain for wet aged samples are slightly higher than dry aged samples for 10 hours PAV. After 50 hours, the wet aged samples show a noticeable increment in displacement (accumulated strain) relative to dry aged PMAC. The RCRT test provided equivalence for PAV-aged samples and field-aged samples similar to that indicated by critical temperature of binders. Longer RCAT aging times were required to produce materials of a similar RCRT response.

## CHAPTER 6

### SUMMARY AND CONCLUSIONS

Elastomeric polymer modified asphalt cements are complex compositions containing molecular species that answer differently to the orchestrated actions of aging agents. The aging intensity of elastic pavements is dictated among other factors by the climate, i.e., both the annual average temperature and humidity. As expected, the elastic characteristic of the polymer modified asphalt cement used in the present investigations was enhanced tremendously by SBS block copolymer over a large temperature domain. However, the butadiene blocks were the first to be sacrificed by oxidative aging of asphalt cements.

The extent of oxidation and changes in the molecular mass of the asphalt cement components of aged samples were estimated using Fourier Transform Infrared Spectroscopy (FTIR) data, Potentiometric Titrations (PT) and Gel Permeation Chromatography (GPC) analyses.

FTIR data have shown that multiple PAV aging introduced polar oxygen species derived mostly from carboxylic acid groups. Oxidative aging of PMAC subjected to multiple PAV and RCAT operations, as well as of 3-5 years field aged asphalt binders, were quantified from FTIR spectra; a calibration curve was developed to this aim by using un-aged asphalt cements containing various amounts of benzoic acid. It has been found – as one might expect – that the concentration of acid groups increased with the aging time. It was higher when the aging operation was carried out in the presence of water. Comparative infrared data have also shown that the concentration of carboxylic acid groups of the 3 yrs field-aged binder was similar to that of the PMAC sample dry-aged for 10 hrs in the PAV machine, and also to the PMAC binder sampled after 73 hrs of RCAT-aging. The FTIR acid equivalence of the extracted binder which

aged in the field for 5-yrs was similar to that observed for samples subjected to 20 hrs of PAV-aging and 193 hrs of RCAT-aging.

The non-aqueous potentiometric titration of binders identified the presence of strong acids in commercial PMACs, apparently sulfonic acids derived from the interaction of PMAC with sulfur used in preparing the blends. Comparison of PT acidity data with that obtained by FTIR analysis yielded a satisfactory correlation. Potentiometric titration also revealed that formation of carboxylic acid groups occurred primarily in the first 70 hours of aging under RCAT conditions.

Relative changes in molecular weight distribution of the asphalt components have been determined by GPC measurements. Laboratory aged asphalt samples were compared with field aged binders and the impact of water on the oxidative degradation was observed by shifting the GPC peaks to higher elution volumes (i.e., lower MW). Generally, the aging in the presence of water had the following effects: less asphaltene association in MMW region, less association for LMW asphalt species, and lower polymer concentration in HMW region. GPC traces showed also that, for extend PMAC oxidation in humid PAV conditions; the asphaltene association was lower compared to that observed when the water was absent. The GPC traces of binders extracted from MS I-55 pavements revealed a higher degradation of HMW polymer species for 5 years field –aged sample as compared to the 3-years one. At the same time, both extracts pointed to a higher concentration of species with molecular weight of ~ 10K (asphaltene associations), produced perhaps mainly on the expense of species with molecular weight of ~5K-3K. However, according to GPC analysis, the SBS polymer did not degrade significantly even after extensive RCAT aging times. By contrast, the polymer was rapidly crosslinked or degraded by PAV or field aging.

Since metals are present in catalytic amounts in asphalt binders, the oxidation mechanism of aging in the presence of metal ions catalysts was simulated in laboratory and the changes in

molecular weight distributions were monitored by GPC. The aging process of PMAC components has been mimicked using a cobalt naphthenate/cumene hydroperoxide redox system to generate free radicals. Under these conditions, it has been observed that the SBS copolymer served as a sacrificial antioxidant and protected the asphalt components from oxidation.

Viscoelastic properties of asphalts were determined from dynamic shear measurements over a large range of temperatures (25 – 70°C). The cross-over temperature at which  $G''$  equals  $G'$  as temperature increased was considered as a critical temperature and was chosen as the rheological criterion to assess the advancement of hardening (aging). The critical temperature of the 3 yrs field-aged binder was similar to that of <10 hrs PAV-aged or <19 hrs RCAT-aged PMAC samples. For the 5-yrs field-aged binder rheological equivalence was observed for >10 hrs PAV-aged and 48 hrs RCAT-aged samples. The wet atmosphere had a retarding effect on asphalt hardening. The  $T_c$  of binders subjected to PAV-aging in humid atmosphere was always less than that of binders aged for the same periods but in a dry environment. It has been concluded that the increase in oxygen content of aged binders (observed for samples aged in presence of water) does not necessarily determine an increase of the stiffness, because the actual aging of asphalt pavements is a concerted action of different stimuli, both chemical and physical.



## **CHAPTER 7**

### **RESEARCH IN PROGRESS AND FUTURE WORK**

A better understanding of the mechanism through which water affects the oxidative aging of polymer modified asphalt cements would be part of the future work. To this aim, extending the composition of binders, changing experimental conditions and using new methods of performance evaluation, additional investigations should be performed. Some of these are presented in the following.

The rotary cylinder type of aging instrument (RCAT) should be used in order to allow a greater variation of aging conditions (such as exposition to air or oxygen, water content, time and temperature of the process). FTIR measurements, along with titration methods and quantified GPC data, will help follow chemical changes occurring during laboratory aging. The catalytic influence of metal ions present in HMA will be better understood from asphalt binder samples exposed to a larger variety of redox pair concentrations. Rheological measurements will keep track of performance modifications induced by oxidative processes. Measurements on laboratory-aged mixtures (asphalt binder and fine aggregates) may simulate closer the field aging process.

It will be also the aim of a future work to continue the rheological tests presented below.

As the stress level of 300 Pa was too low for polymer-modified asphalts a new Standard Test Method for Multiple Stress Creep and Recovery (MSCR) of asphalt binder using a Dynamic Shear Rheometer will be soon implemented. This practice will cover the identification of elastomeric response of modified asphalt binders by means of percent recovery obtained in the MSCR test. The test will be conducted using the DSR instrument at the temperature

corresponding to the higher performance grade (PG Grade) temperature of the asphalt binder. It is intended for use with aged residue from Test Method D 2872 (RTFOT).

The percent recovery in the MSCR test of asphalt binders is affected by the type and amount of polymer used in the polymer modified asphalt binder. The percent recovery value is intended to provide a mean for determining if the polymer used in modification will provide an elastomeric response of the binder; however, it can not account for the type of elastomer used. According to proposed methodology, but using a lower temperature than that indicated by the test, our initial MSCR work collected data at the stress sweep of 25 to 25,600 Pa, a 1/9 seconds stress/recovery time, the temperature of 25°C, and 10 cycles per stress, using the same AR 2000 rheometer set-up in Dynamic Shear mode presented earlier in the text. This experiment should be continued for a larger set of samples at 25°C, at an intermediate temperature (40°C), and at a high temperature (set by the PG temperature of the binder).

Our results have shown, as one might expect, that both RTFOT and PAV aged PMAC samples had a lower ability to recover than that of the original sample (Figure 7.1). The proposed MSCR asks for a minimum 15 % recovery at 3,200 Pa at the PG temperature as a preliminary value for determining if the binder has suitable elastomeric properties to improve performance. We have extended the test to a much lower temperature (25°C) looking for a failure indication. The only sample which seemed to decay to the failure value of 15% average recovery for 3,200 Pa at 25°C was the original (i.e., un-aged) polymer-free asphalt cement PG 64-22 (Figure 7-2 and Table 7-1). However, the software for the MSCR procedure using the AR 2000 instrument needs to be updated for this type of test.

Other experiments have been performed in order to determine the failure point as an estimation of fatigue life under stress. The chosen stress level was 50,000 Pa. Results gathered

till now are for PMAC 76-22 original at low and intermediary temperatures (viz., 25 and 40°C).

A failure point has yet not to be reached, but an estimate can be extrapolated (Figure 7-3).

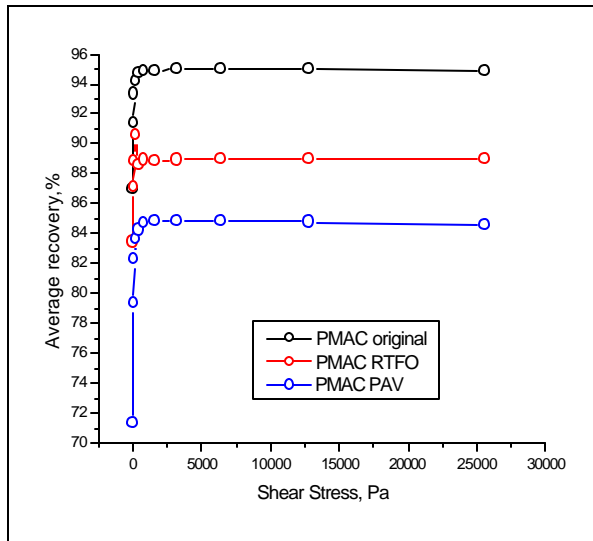


**Figure 7-1 MSCR results -PMAC average % recovery**

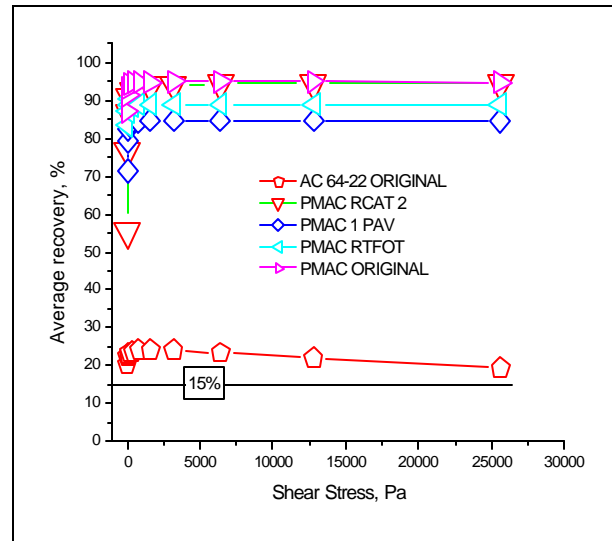


**Figure 7-2 MSCR results – average percent recovery for different asphalt binder samples**

**Table 7-1 MSCR average percent recovery at 25°C for various asphalt binder samples**

MSCR						
Shear Stress Pa	64-22 RTFOT	64-22 original	PMAC RCAT 2	76-22 1 PAV	76-22 RTFOT	76-22 original
25	60.48	20.20	55.49	71.35	83.45	87.02
50	58.48	22.46	76.72	79.34	87.07	91.34
100	61.23	22.92	86.44	82.33	88.88	93.33
200	62.32	23.42	90.77	83.66	90.54	94.21
400	61.72	23.72	92.64	84.25	88.60	94.71
800	62.14	24.00	93.67	84.75	88.93	94.86
1600	62.18	24.14	94.02	84.80	88.90	94.91
3200	62.24	24.22	94.27	84.88	88.93	94.99
6400	62.27	23.40	94.49	84.87	89.00	95.00
12800	62.24	22.07	94.44	84.79	88.95	95.00
25600	62.16	19.28	94.50	84.61	88.95	94.91

The estimate was computed using the equation  $[N \times G^*n / G^*o]$  (presented in details in Chapter 2).  $G^*n$  for the estimated points was computed by applying the average percentage

increment calculated from the tested points of  $G^*$ . The readings for  $G^*$  have been made at a constant time of 60 minutes each time. In this way was possible to estimate number of cycles (time x 1.592 cycles/s), and to compute possible values for  $G^*$ . The prognoses are presented in separated regions A and B.

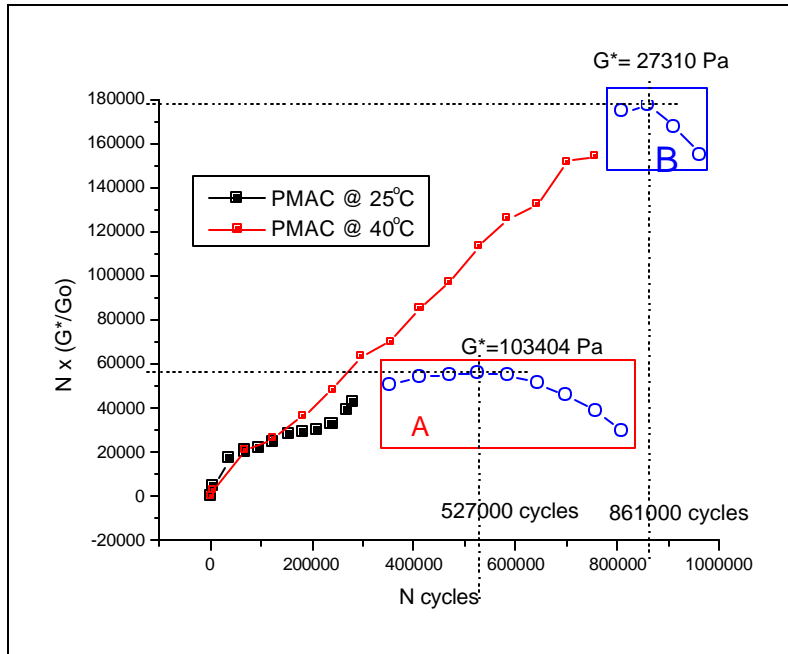


**Figure 7-3 Exercise for learning how to determine failure point for a certain stress level (The points of area A (for 25°C) and area B (for 40°C) are possible prognoses)**

## REFERENCES

1. Roberts, F.L., Kandhal, P.S., Brown, E.R., Lee, D-Y, Kennedy, T.W., *Hot Mix Asphalt Materials, Mixture design and Construction*, Text Book, NAPA Education Foundation Lanham Maryland, second edition, **1996**.
2. Mohammad, L.N., Negulescu, I.I., Wu, Z., Daranga, C., Daly, W.H., and Abadie, C., *Investigation of the Use of Recycled Polymer Modified Asphalt Binder in Asphalt Concrete Pavements*, *Journal of the Association of Asphalt Paving Technologist*, **2003**, 551-594.
3. Negulescu, I.I, Mohammad, L.N, Daly, W.H., Abadie, C., Cueto, R., Daranga, C., Glover, I., *Chemical and Rheological Characterization of Wet and Dry Aging of Polymer Modified Asphalt Cements: Field and Laboratory Evaluation*, *Journal of the Association of Asphalt Paving Technologies*, **2006**, 75.
4. "Differences between Concrete and Asphalt Pavement" presented in American Pavement Concrete Association [www.pavement.com](http://www.pavement.com) / Concrete Pavement /Technical/ Fundamentals/ Differences\_Between\_Concrete\_and\_Aspphalt.asp.
5. Klimisch, H.J., Andreae, M., Tillman, U., *Robust Summary of Information*, American Petroleum Institute December 9, **2003**.
6. Masson, J-F, Pelletier L., Collins P., *Rapid FTIR method for styrene-butadiene type copolymers in bitumen*, NRCCNRC, **2001**.
7. Branthaver, J.F., Petersen, J.C., Robertson, R.E., Duvall, J.J., Kim, S.S., Harsberger, P.M., Mill T., Ensley, E.K., Barbour, F.A., Schabron, J.F., *Binder Characterization and Evaluation Volume 2 Chemistry SHARP A-368*, Strategic Highway Research Program, National Research Council, Washington DC **1993**.
8. Gros, W.A., *Compatible asphalt-polymer blends*, United States Patent 5672642 published September **1997**.
9. Wen, G., Zhang, Y., Sun, K., Chen, Z., *Vulcanization characteristics of asphalt/SBS blends in the presence of sulfur*, *Journal Applied Polymer Science*, **2001**, 82, 989.
10. Hawkins, W. L., *Polymer Stabilization, Environmental Deterioration of Polymers*, Wiley Interscience, **1972**.
11. Wang, S.M., Chang, J.R., Tsiang, R.C., *Infrared studies of thermal oxidative degradation of polystyrene-block-polybutadiene-block-polystyrene thermoplastic elastomers*, *Polymer Degradation Stabilization*, **1996**, 52,51.

12. Munteanu, S.B., Brebu, M., Vasile, C., *Thermal and Thermo-oxidative behavior of butadiene-styrene copolymers with different architectures*, Polymer Degradation and Stability, **2005**,89,501-502.
13. Curtis, C.W., K. Ensley, K., Epps, J.A., *Fundamental Properties of Asphalt-Aggregate Interactions Including Adhesion and Absorption*, Final report SHRP A-341, Strategic Highway Research Program, National Research Council, Washington, D.C., **2001**.
14. Campbell, P.G, Wright, J.R., *The Effect of Temperature and Humidity on the Oxidation of Airblown Asphalts*. American Chemical Society, Division of Petroleum Chemistry. Preprints,**1962**, 7 (3), 123-125.
15. Chipperfield, E.H., Dutie, J.L., *Asphalt Characteristics in Relation to Road Performance*, Proceedings of Association of Asphalt Paving Technologists, 1970, 39, 79-88.
16. Kemp, G.R., Predoehl, N.H., *Comparison of Field and Laboratory Environments on Asphalt Durability*, Proceedings of Association of Asphalt Paving Technologists, **1981**, 50, 46-58.
17. Thomas, K., *Aging of Asphalt and Analytical Methods Developments*, FHWA Project Review, Washington, D.C., January 16, **2004**.
18. Daranga, C., *Characterization of Aged Polymer Modified Asphalt Cements for Recycling Purposes*, a Dissertation submitted in the Department of Chemistry, Louisiana State University, Baton Rouge, **2005**.
19. American Society for Testing and Materials, *Standard Test Method for Effect of Heat and Air on a Moving Film of Asphalt (Rolling Thin Film Oven Test)* Annual Book of ASTM Standards, D2872-88, Philadelphia PA **1991**,04.03
20. American Society for Testing and Materials, *Standard Test Method for Effect of Heat and Air on Asphaltic Materials (Thin-Film Oven Test)* Annual Book of ASTM Standards D 1754-87, Philadelphia PA **1991**,04.03
21. McGennis, R.B., Shuler, S., Bahia, H.U., *Background of SUPERPAVE Asphalt Binder Test Methods*, Final Report Publication No. FHWA-SA-94-069, NATC, July **1994**.
22. American Society for Testing and Materials, *Rubber, Natural and Synthetic-General Test Methods*, Annual Book of ASTM Standards, **1994**,04.04
23. Belgian Road Research Center, *Simulation of Field Ageing in Bituminous Binders – RCAT method*, Method of Measurement, ME 70/01, BRRC, Brussels, **2001**
24. Negulescu, I.I., Mohammad L.N., Daly, W.H, Abadie, C., Cooper, S., Cueto, R., Glover, I., *Comparison of RCAT versus PAV Aging Techniques for a Polymer Modified Asphalt Cement* manuscript submitted to AAPT, **2007**.
25. Petersen, J. C., Robertson, R.E., Branthaver, J.F., Hamsberger, P.M., Duvall, J.J., Kim,

- S.S., Anderson, D.A., Christiansen, D.W., Bahia, H.U., Dongre, R., Antle, C.E., Sharma, M.G., Button, J., and Glover, C.J., *Binder Characterization and Evaluation*. Strategic Highway Research Program, National Research Council: Washington, D.C., **1994**, 4.
26. Buell, B.E., *Differential Titration of Acids and Very Weak Acids in Petroleum with Tetrabutylammonium Hydroxide and Pyridine-Benzene Solvent*, *Analytical Chemistry*, **1967**, 39, 762-764.
27. Dutta, P.K., Holland, R.J., *Acid-Base Characteristics of Petroleum Asphaltenes as Studied by Non-Aqueous Potentiometric Titrations*, *Fuel*, **1984**, 63, 197-201.
28. Robertson R.E. and collaborators, *Fundamental Properties of Asphalt and Modified Asphalt*, Western Research Institute, October **2001**, 2.
29. Harman, T.P., *G\* Complex Shear Modulus A Detailed Review*, Federal Highway Administration, Office of Technology Application, Demonstration Projects Program HTA-21, August **1993**.
30. [Washington.edu/wsdot/modules/03\\_materials/03-3\\_body.htm](http://Washington.edu/wsdot/modules/03_materials/03-3_body.htm)
31. D'Angelo J.A., Dongre, R., Reinke, G., *Creep and Recovery*, Public Roads, Federal Highway Administration, **2007**, 70.
32. Martono, W., Bahia, H., Massad, E., D'Angelo, J., *Validation of Binder Fatigue Test & Potential Surrogate Test*, The 6th Int. Symposium on Binder Rheology and Pavement Performance, Tampa Bay Florida, April 2/3, **2007**.
33. Petersen, J. C., *Chemical Composition of Asphalt as Related to Asphalt Durability: State of the Art*, Transportation Research Record, **1984**, 999, 13-30.
34. Xiaohu, L.; Isacson, U., *Fuel*, **1998**, 77, 961-972.
35. Green, J., Yu, S., Pearson, C., Reynolds, J., *Analysis of Sulfur Compounds Types in Asphalt*, National Institute for Petroleum and Energy Research, Bartlesvill, OK, SHRP-A-667, **1993**.
36. Negulescu, I.I, Mohammad, L.N, Daly, W.H., Abadie, C., Cueto, R., Daranga, C., Glover, I., *Chemical and Rheological Characterization of Wet and Dry Aging of Polymer Modified Asphalt Cements: Field and Laboratory Evaluation*, 42<sup>nd</sup> Petersen Asphalt Research Conference; Cheyenne, WY, June 21-24, **2005**.
37. Petersen, J. C., *Chemical Composition of Asphalt as Related to Asphalt Durability: State of the Art*, Transportation Research Board, **1984**, **999**, 13-30.
38. McGennis, R.B., Shuler, S., Bahia, H.U., *Background of SUPERPAVE Asphalt Binder Test Methods*, Final Report Publication No. FHWA-SA-94-069, NATC, July **1994**.

39. Partl, M.N., Gubler, R., Poulikakos, L.D., Sokolov, K., *Innovations in testing of Bituminous Pavement Materials*, 5th International Symposium on Binder Rheology and Pavement Performance, Baltimore, MD, 4-5 October, **2004**.
40. Oft, W.P.V., *Durability of Asphalt: Its Aging in the Dark*, Industrial and Engineering Chemistry, **1956**, 48(7), 6-15.
41. Verhasselt, A., *Laboratory Simulation of Bituminous Binder Ageing. A New Realistic Method for Long-Term RCAT (Rotating Cylinder Ageing Test)*, WRI Website published Presentation made at the P3 Symposium on Aging of Pavement Asphalts, WRI, Laramie, WY, July 16-18, **2003**.
42. Bahia, H.U., Hanson, D.I., Zeng, M., Zhai, H., Khatri, M.A., Anderson, R.M., *Characterization of Modified Asphalt Binders in SUPERPAVE Mix Design*, NCHRP Report 459, Transportation Research Board, National Research Council, National Academic Press, Washington D.C., **2001**.



## APPENDIX A: ADDITIONAL TABLES

**Table A-1 Required SUPERPAVE specification for the asphalts PG 64-22 and Pg 76-22**

Performance Grade	PG 64-	PG 76-											
Average 7-days maximum pavement design temperature, °C	<64	<76											
Minimum pavement design temperature, °C, >	<table border="1" style="display: inline-table; border-collapse: collapse;"> <tr> <td style="width: 20px; text-align: center;">-10</td> <td style="width: 20px; text-align: center;">-16</td> <td style="width: 20px; text-align: center;">-22</td> <td style="width: 20px; text-align: center;">-28</td> <td style="width: 20px; text-align: center;">-34</td> <td style="width: 20px; text-align: center;">-40</td> </tr> </table>	-10	-16	-22	-28	-34	-40	<table border="1" style="display: inline-table; border-collapse: collapse;"> <tr> <td style="width: 20px; text-align: center;">-10</td> <td style="width: 20px; text-align: center;">-16</td> <td style="width: 20px; text-align: center;">-22</td> <td style="width: 20px; text-align: center;">-28</td> <td style="width: 20px; text-align: center;">-34</td> </tr> </table>	-10	-16	-22	-28	-34
-10	-16	-22	-28	-34	-40								
-10	-16	-22	-28	-34									
<b>ORIGINAL BINDER</b>													
Flash point minimum, °C	230	230											
Viscosity, maximum 3 Pa at test temperature	135	135											
Dynamic shear G*/sin δ minimum 1.00 kPa, test temperature@ 10 rad/s	64	76											
<b>ROLLING THIN FILM OVEN RESIDUE</b>													
Mass loss, maximum percentage	1.00	1.00											
Dynamic shear G*/sin δ minimum 2.20 KPa, test temperature@ 10 rad/s	64	76											
<b>PRESSURE AGING VESSEL RESIDUE</b>													
PAV temperature, °C	100	100(110)											
Dynamic shear G*/sin δ maximum 5000 kPa test temperature@ 10 rad/s	<table border="1" style="display: inline-table; border-collapse: collapse;"> <tr> <td style="width: 20px; text-align: center;">31</td> <td style="width: 20px; text-align: center;">28</td> <td style="width: 20px; text-align: center;">25</td> <td style="width: 20px; text-align: center;">22</td> <td style="width: 20px; text-align: center;">19</td> <td style="width: 20px; text-align: center;">16</td> </tr> </table>	31	28	25	22	19	16	<table border="1" style="display: inline-table; border-collapse: collapse;"> <tr> <td style="width: 20px; text-align: center;">37</td> <td style="width: 20px; text-align: center;">34</td> <td style="width: 20px; text-align: center;">31</td> <td style="width: 20px; text-align: center;">28</td> <td style="width: 20px; text-align: center;">25</td> </tr> </table>	37	34	31	28	25
31	28	25	22	19	16								
37	34	31	28	25									
<b>Physical hardening</b>													
Creep stiffness S maximum 300 MPa and m-value minimum 0.300 test temperature@ 60s, °C	<table border="1" style="display: inline-table; border-collapse: collapse;"> <tr> <td style="width: 20px; text-align: center;">0</td> <td style="width: 20px; text-align: center;">-6</td> <td style="width: 20px; text-align: center;">-12</td> <td style="width: 20px; text-align: center;">-18</td> <td style="width: 20px; text-align: center;">-24</td> <td style="width: 20px; text-align: center;">-30</td> </tr> </table>	0	-6	-12	-18	-24	-30	<table border="1" style="display: inline-table; border-collapse: collapse;"> <tr> <td style="width: 20px; text-align: center;">0</td> <td style="width: 20px; text-align: center;">-6</td> <td style="width: 20px; text-align: center;">-12</td> <td style="width: 20px; text-align: center;">-18</td> <td style="width: 20px; text-align: center;">-24</td> </tr> </table>	0	-6	-12	-18	-24
0	-6	-12	-18	-24	-30								
0	-6	-12	-18	-24									
Direct tension failure strain minimum 1.0% test temperature@ 1.0 mm/mm, °C	<table border="1" style="display: inline-table; border-collapse: collapse;"> <tr> <td style="width: 20px; text-align: center;">0</td> <td style="width: 20px; text-align: center;">-6</td> <td style="width: 20px; text-align: center;">-12</td> <td style="width: 20px; text-align: center;">-18</td> <td style="width: 20px; text-align: center;">-24</td> <td style="width: 20px; text-align: center;">-30</td> </tr> </table>	0	-6	-12	-18	-24	-30	<table border="1" style="display: inline-table; border-collapse: collapse;"> <tr> <td style="width: 20px; text-align: center;">0</td> <td style="width: 20px; text-align: center;">-6</td> <td style="width: 20px; text-align: center;">-12</td> <td style="width: 20px; text-align: center;">-18</td> <td style="width: 20px; text-align: center;">-24</td> </tr> </table>	0	-6	-12	-18	-24
0	-6	-12	-18	-24	-30								
0	-6	-12	-18	-24									
Louisiana extra requirements Force ratio @ 4°C, 30 cm, minimum Force ductility @4°C,30 cm minimum RTFOT material – elastic recovery @ 25°C, minimum	<p style="margin: 0;">0.3</p> <p style="margin: 0;">0.5 Lb</p>	<p style="margin: 0;">0.3</p> <p style="margin: 0;">0.5 Lb</p> <p style="margin: 0;">60%</p>											

**Table A-2 Equations for G\* computation**

$t_{\max} = \frac{2T}{pr^3}$		$g_{\max} = \frac{q r}{h}$		$G^* = \frac{t_{\max}}{g_{\max}}$		$d = \text{time lag}$
$t_{\max}$	maximum applied shear stress, Pa					
T	maximum applied torque, N					
r	radius of binder specimen (either 12.5 or 4 mm)					
$g_{\max}$	maximum resulting shear strain					
$\theta$	deflection (rotation) angle					
h	specimen height (either 1 or 2 mm)					
$G^*$	complex shear modulus, Pa					
d	phase angle. This is the time lag (expressed in radians) between the maximum applied shear stress and the maximum resulting shear strain					

## APPENDIX B: LETTER OF PERMISSION

**From:** AAPT [aapt@qwest.net](mailto:aapt@qwest.net)  
**Sent:** Wednesday, October 10, 2007 2:18:09 PM  
**To:** "Ionela Glover" [ichiparus2001@yahoo.com](mailto:ichiparus2001@yahoo.com)  
**Subject:** Re: Request for release to use published research data in dissertation - Ionela Glover

Dear Ms. Glover-

You have the permission of the Association of Asphalt Technologists to use all or part of both of the papers that you mentioned below.

If you have any questions, please let us know.

Sincerely-

Eugene L. Skok  
AAPT Secretary-Treasurer

-----Original Message-----

From: Ionela Glover [<mailto:ichiparus2001@yahoo.com>]  
Sent: Wednesday, October 10, 2007 10:55 AM  
To: [aapt@qwest.net](mailto:aapt@qwest.net)  
Subject: Request for release to use published research data in dissertation - Ionela Glover

Hello,

I am a co-author of a paper which has been published in the "Journal of the Association of Asphalt Paving Technologists" and another paper which has been submitted and approved. The data and analysis used in these papers are essential elements of my PhD dissertation at Louisiana State University and I am writing to request permission to use significant elements of those two papers in my dissertation. The relevant identifying information for the two papers is presented below:

“Comparison of RCAT versus PAV Aging Techniques for a Polymer Modified Asphalt Cement”, Ioan Negulescu, Louay Mohammad, William Daly, Chris Abadie, Sam Cooper, Rafael Cueto, and Ionela Glover; forwarded to the Journal of the Association of Asphalt Paving Technologies, approved 2007.

“Chemical and Rheological Characterization of Wet and Dry Aging of SBS Copolymer Modified Asphalts: Laboratory and Field Evaluation”, Ioan I. Negulescu, Louay N. Mohammad,

William Daly, Christopher Abadie, Rafael Cueto, Codrin Daranga and Ionela Glover; Journal of the Association of Asphalt Paving Technologies, Volume 75, 2006.

I look forward to hearing from you and I would like to thank you in advance for your consideration.

Ionela Glover  
PhD Candidate  
Department of Chemistry  
Louisiana State University  
Baton Rouge, LA 70803

## VITA

Ionela Chiparus Glover was born in Romania in Piatra Neamt city. She is the daughter of Vasile and Veronica Chiparus. Ionela is married to Donald G Glover Jr., and has a two-year-old son, Christopher Jonathan.

Ionela graduated in 1989 from the Technical University “Gheorghe Asachi” from Iasi, Romania, with a Bachelor of Science degree in chemical engineering with a concentration in the technology of macromolecular compounds. Her favorite topic as an undergraduate student was computer modeling of chemical processes, under guidelines of Professor Simioan Petrovan, her thesis advisor.

Ionela was accepted in 2002 by the LSU Graduate School as a doctoral student in the School of Human Ecology and transferred in 2003 to the graduate program from the Department of Chemistry where she joined Professor William Daly’s and Professor Ioan Negulescu’s groups. Her investigations were focused on the characterization of polymer modified asphalt cements using a variety of techniques. During this period she became familiar with the concepts of civil engineering related to the design and construction of asphalt pavements, having access to the invaluable guidance of Professor Louay N. Mohammad from the Department of Civil and Environmental Engineering. As a graduate student Ionela worked for the past four years as a teaching assistant in the Department of Chemistry. Ionela is looking forward to graduating from Louisiana State University in December 2007 with a Doctor of Philosophy degree in chemistry.